

Lecture Notes in Civil Engineering

Srinivas Pulugurtha
Indrajit Ghosh
Sabyasachi Biswas *Editors*

Advances in Transportation Engineering

Select Proceedings of TRACE 2018

 Springer

Lecture Notes in Civil Engineering

Volume 34

Series Editors

Marco di Prisco, Politecnico di Milano, Milano, Italy

Sheng-Hong Chen, School of Water Resources and Hydropower Engineering,
Wuhan University, Wuhan, China

Ioannis Vayas, Institute of Steel Structures, National Technical University of
Athens, Greece

Sanjay Kumar Shukla, School of Engineering, Edith Cowan University, Joondalup,
WA, Australia

Anuj Sharma, Iowa State University, Ames, IA, USA

Nagesh Kumar, Department of Civil Engineering, Indian Institute of Science
Bangalore, Karnataka, India

Chien Ming Wang, School of Civil Engineering, The University of Queensland,
Brisbane, QLD, Australia

Indexed by Scopus

Lecture Notes in Civil Engineering (LNCE) publishes the latest developments in Civil Engineering—quickly, informally and in top quality. Though original research reported in proceedings and post-proceedings represents the core of LNCE, edited volumes of exceptionally high quality and interest may also be considered for publication. Volumes published in LNCE embrace all aspects and subfields of, as well as new challenges in, Civil Engineering. Topics in the series include:

- Construction and Structural Mechanics
- Building Materials
- Geotechnical Engineering
- Earthquake Engineering
- Coastal Engineering
- Hydraulics, Hydrology and Water Resources Engineering
- Structural Health and Monitoring
- Surveying and Geographical Information Systems
- Heating, Ventilation and Air Conditioning (HVAC)
- Transportation and Traffic
- Risk Analysis
- Safety and Security

To submit a proposal or request further information, please contact the appropriate Springer Editor:

- Mr. Pierpaolo Riva at pierpaolo.riva@springer.com (Europe and Americas);
- Ms. Swati Meherishi at swati.meherishi@springer.com (India);
- Ms. Li Shen at li.shen@springer.com (China);
- Dr. Loyola D’Silva at loyola.dsilva@springer.com (Southeast Asia and Australia/NZ).

More information about this series at <http://www.springer.com/series/15087>

Srinivas Pulugurtha · Indrajit Ghosh ·
Sabyasachi Biswas
Editors

Advances in Transportation Engineering

Select Proceedings of TRACE 2018

 Springer

Editors

Srinivas Pulugurtha
University of North Carolina
Charlotte, NC, USA

Indrajit Ghosh
Indian Institute of Technology Roorkee
Roorkee, India

Sabyasachi Biswas
National Institute of Technology Jamshedpur
Jamshedpur, India

ISSN 2366-2557 ISSN 2366-2565 (electronic)
Lecture Notes in Civil Engineering
ISBN 978-981-13-7161-5 ISBN 978-981-13-7162-2 (eBook)
<https://doi.org/10.1007/978-981-13-7162-2>

Library of Congress Control Number: 2019934359

© Springer Nature Singapore Pte Ltd. 2019

This work is subject to copyright. All rights are reserved by the Publisher, whether the whole or part of the material is concerned, specifically the rights of translation, reprinting, reuse of illustrations, recitation, broadcasting, reproduction on microfilms or in any other physical way, and transmission or information storage and retrieval, electronic adaptation, computer software, or by similar or dissimilar methodology now known or hereafter developed.

The use of general descriptive names, registered names, trademarks, service marks, etc. in this publication does not imply, even in the absence of a specific statement, that such names are exempt from the relevant protective laws and regulations and therefore free for general use.

The publisher, the authors and the editors are safe to assume that the advice and information in this book are believed to be true and accurate at the date of publication. Neither the publisher nor the authors or the editors give a warranty, expressed or implied, with respect to the material contained herein or for any errors or omissions that may have been made. The publisher remains neutral with regard to jurisdictional claims in published maps and institutional affiliations.

This Springer imprint is published by the registered company Springer Nature Singapore Pte Ltd. The registered company address is: 152 Beach Road, #21-01/04 Gateway East, Singapore 189721, Singapore

TRACE 2018 Committees

General Chair

Dr. R. K. Tomar, Head, Civil Engineering Department, ASET, AUUP, Noida

Organizing Secretaries

Dr. Sabyasachi Biswas, NIT Jamshedpur

Dr. Ankur Mehta, ASET, AUUP, Noida

Academic and Industrial Collaboration Committee

Prof. (Dr.) J. Bhattacharjee, ASET, AUUP, Noida

Dr. Madhuri Kumari, ASET, AUUP, Noida

Advisory Committee

International

- Dr. Srinivas Pulugurtha, Professor and Director of Infrastructure, Design, Environment and Sustainability, University of North Carolina, Charlotte, USA
- Dr. J. S. J Van Deventer, Honorary Professional Fellow, University of Melbourne, Parkville, Australia
- Dr. Sondipon Adhikari, Professor, Swansea University, Wales, UK
- Dr. Abhijeet Mukherjee, Professor, Curtin University, Perth, Australia

- Dr. Costas Georgopoulos, Professor of Structural Engineering Practice and Head of the Department of Civil Engineering
- Dr. Michael Riley, Professor, Liverpool John Moores University, UK
- Dr. Rafid Al Khaddar, Professor, Liverpool John Moores University, UK
- Dr. Guoqiang Zhang, Professor, Hunan University, China
- Dr. S. K. Shukla, Professor, Edith Cowan University, Perth, Australia
- Dr. Jit Sharma, Professor, Lassonde School of Engineering, York University, Canada
- Dr. Sung-Chi Hsu, Professor, Chaoyang University of Technology, Taichung, Taiwan
- Dr. Ashish Sharma, Professor, University of New South Wales, Sydney, Australia
- Dr. Ram Karan Singh, Professor, King Khalid University, Saudi Arabia
- Prof. Dato' Ir. Dr. Abdul Wahab Mohammad, Dean, Universiti Kebangsaan Malaysia

National

- Dr. Satish Chandra, Director, CRRI, Delhi, and Professor, IIT Roorkee, India
- Dr. Rafat Siddique, Senior Professor, Thapar University, India
- Dr. Manoranjan Parida, Professor, Indian Institute of Technology Roorkee
- Dr. Parveen Kumar, Professor, Indian Institute of Technology Roorkee, India
- Dr. Sudip Kr. Roy, Professor, Indian Institute of Engineering Science and Technology, Shibpur
- Dr. Rajan Choudhary, Associate Professor, Indian Institute of Technology Guwahati
- Dr. Akhilesh Kr. Maurya, Associate Professor, Indian Institute of Technology Guwahati

Industry

- Dr. P. K. Sikdar, Director, ICT Pvt. Ltd
- Mr. Arvind Arora, IDSE, Former Director General (MESMOD), President, DIPM
- Mr. Pradeep Aggarwal, IDSE, Director (MES/MOD), CEO, DIPM
- Dr. P. R. Swarup, Director General, CIDC
- Dr. N. Gopalakrishnan, Director, CSIR-CBRI
- Dr. Chandan Ghosh, Professor and Head, NIDM
- Dr. Atul Nanda, Former Chairman, IGS (Delhi), and Head (Technology), EIL
- Dr. Altaf Usmani, Honorary Secretary, IGS (Delhi Chapter), Manager, EIL
- Mr. K. B. Rajoria, Advisor, IBC, and Former E-In-C, PWD, Delhi
- Mr. Abhay Sinha, DG, CPWD, President, IBC
- Prof. Mahesh Tandon, MD, Tandon Consultants Pvt. Ltd
- Ms. Sangeeta Wij, Former President, WISE (India)

- Dr. Vasant G. Havanagi, Senior Principal Scientist and Professor, CRRI, and Chairman IGS Delhi Satish Sehta, National Manager—Business Development, Institution of Civil Engineers
- Mr. Manoj Mittal, President, IAStructE
- Mr. Alok Bhowmick, Honorary Secretary, IAStructE

Preface

India is on the threshold of a major forward thrust in the field of transportation infrastructure. Mixed traffic has in recent years increased manifold in both urban and rural areas. There is also a general increase in awareness of mobility and safety. These factors, we believe, constitute a recipe for fast development in the area of transportation.

The need for the professionals with specialization in transportation engineering and infrastructure, equipped with the knowledge of modern as well as traditional techniques, is bound to grow over the next few years. Therefore, this book, we believe, not only fills this gap, but also presents the area of transportation engineering in a manner that will prepare professionals to tackle real-life problems. Further, the book entitled *Advances in Transportation Engineering*, is basically a systematic outcome of research works conducted by the many professionals in this field.

In the other way, transportation engineering and infrastructure development, transportation planning, and ITS technologies are of critical importance to the modern-day life including businesses, government, education, science, and economy. Trends and Recent Advances in Civil Engineering, TRACE 2018, provides a forum for researchers and practitioners from civil engineering in order to address recent research issues and to present and discuss the ideas, theories, technologies, systems, and practical issues related to transportation engineering and infrastructures.

TRACE 2018 received more than 300 papers from the authors representing many continents and countries. The papers were submitted to different tracks, wherein each track has a separate technical program committee.

We express our sincere thanks to all advisers for their valuable support. We are also indebted to local organizing committee for their work in the local arrangements and support. We are very grateful to all the reviewers for their great support and providing us with extensive reviews and constructive criticism of the research papers.

Many thanks also go to all the authors who have submitted their research work to the conference. Without their contributions, we would not have been able to put together such a strong and interesting technical program.

Jamshedpur, India

Dr. Sabyasachi Biswas
Assistant Professor

Contents

Exploring Rural Road Impacts Using Fuzzy Multi-criteria Approach	1
Makrand Wagale, Ajit Pratap Singh and A. K. Sarkar	
Assessment of Accessibility for Mixed Land Use Neighborhoods Through Travel Behavior Pattern	13
Jayesh Juremalani and Krupesh A. Chauhan	
Assessing Travel Time Reliability of Public Transport in Kolkata: A Case Study	21
Saptarshi Sen, Tarun Chowdhury, Ayan Mitra and Sudip Kumar Roy	
Estimation of PCU and Saturation Flow at Signalised Intersection	35
Sabyasachi Biswas, Harjeet Prasad, Amit Jaiswal and Aditya Raj Gehlot	
Travel Behavior of Agartala City, India Using Panel Data	47
Amitabha Acharjee and Partha Pratim Sarkar	
Effect of Natural Rubber, Carbon Black, and Copper Slag as Construction Materials in Flexible Pavement: A Review	59
S. Asvitha Valli and Sreevalsa Kolathayar	
Finite Element Modelling of Built-Up CFS Channel Columns Under Axial Load	65
Krishanu Roy, Tina Chui Huon Ting, Hieng Ho Lau and James B. P. Lim	
Experimental Investigation into the Behaviour of CFS Built-Up Channels Subjected to Axial Compression	89
Krishanu Roy, Tina Chui Huon Ting, Hieng Ho Lau and James B. P. Lim	
Development of Speed Prediction Model for Mixed Traffic Conditions: Case Study of Urban Streets	107
Satyajit Mondal, Vijai Kumar Arya and Ankit Gupta	

**Safety Assessment at Unsignalized Intersections
Using Post-Encroachment Time’s Threshold—A Sustainable
Solution for Developing Countries** 117
Madhumita Paul

**Effect of Stratification on Underground Opening:
A Numerical Approach** 133
Mudassir Ali Khan, Mohd. Rehan Sadique and Mohammad Zaid

About the Editors

Dr. Srinivas Pulugurtha is currently working as Professor & Graduate Program Director of the Department of Civil and Environmental Engineering at The University of North Carolina at Charlotte (UNC Charlotte). He also directs the Infrastructure, Design, Environment and Sustainability (IDEAS) Center on UNC Charlotte campus. He has experience working in diverse fields of transportation including transportation safety, Intelligent Transportation Systems (ITS), transportation system planning, Geographic Information Systems (GIS) applications, internet applications, traffic operations, and, artificial intelligence (AI) techniques and operations research applications. During his 24-year tenure as a researcher, Dr. Pulugurtha has led and completed 70 sponsored projects as Principal Investigator or co-Principal Investigator. He has authored/co-authored over 220 publications which include 57 journal papers. Furthermore, he has advised and mentored 13 Ph.D. students, over 50 M.S. students, and several undergraduate students. He was recognized with the UNC Charlotte College of Engineering Graduate Teaching Award in 2010 for his accomplishments as a mentor, adviser and teacher. Dr. Pulugurtha is a registered Civil Engineer in the State of North Carolina.

Dr. Indrajit Ghosh is currently an Assistant Professor in the Department of Civil Engineering at Indian Institute of Technology (IIT) Roorkee, India. He received his Ph.D. in Civil Engineering from Wayne State University, Detroit, Michigan. He did his M.S. in transportation engineering also from Wayne State University, and M.E. in highway engineering from the Indian Institute of Engineering, Science and Technology, Shibpur (IEST, Shibpur). He is academically and professionally active in the areas of traffic flow modelling, driver behaviour, road safety audit and accident analysis, traffic data collection and analysis studies. He has published more than 50 technical papers in international journals and conferences. Dr. Ghosh received the Institute of Transportation Engineers (ITE) Michigan Section Education-Scholarship award in the year 2008. He also received the prestigious Thomas C. Rumble Fellowship for exceptional academic performance from the College of Engineering at Wayne State University for the year 2007–2008.

Dr. Sabyasachi Biswas is currently working as Assistant Professor & Faculty Adviser of undergraduate student in the Department of Civil Engineering at the National Institute of Technology (NIT) Jamshedpur, India. He did his B.E. in Civil Engineering from IEST Shibpur, and obtained his Masters in Transportation System Engineering from IIT Guwahati in 2012. He completed his Ph.D. (Civil Engineering) from IIT Roorkee in 2017. He has published several technical papers in reputed international and national journals. His research interests include traffic engineering, ITS, traffic planning, traffic modelling, road safety, statistical modelling and analysis. Dr. Biswas has worked as a Project Scientist in DST, Ministry of Science and Technology. In 2015, he was selected for the prestigious IIT Roorkee Heritage Foundation Award for his research contribution. Further, he received “The IIT Roorkee Alumni fund” to participate in the 96th Annual Meeting of Transportation Research Board 2017, held in Washington, DC, USA.

Exploring Rural Road Impacts Using Fuzzy Multi-criteria Approach



Makrand Wagale , Ajit Pratap Singh  and A. K. Sarkar

Abstract The purpose of this article is to develop a novel strategy to explore the impacts of rural road construction on quality of neighborhood (social environment). There has been broad consensus that rural roads assist in change in socioeconomic status of rural regions and have been justified by traditional methods. However, conventional assessment techniques lag in incorporating uncertainties and singularities associated with evaluation process of impacts. These limitations enable researchers to rely on more perceptible techniques. Fuzzy multi-criteria framework is one such approach which can deal effectively with such qualitative and quantitative assessment. It handles uncertainties and vagueness with ease. The present study proposes fuzzy Preference Ranking Organization Method for Enrichment Evaluation (F-PROMETHEE) technique for assessing the impacts of rural road construction on quality of neighborhood. Efficacy of proposed technique is illustrated by employing a case study for the habitations connected in Jhunjhunu district of Rajasthan state, India. The habitations are connected under Pradhan Mantri Gram Sadak Yojna (PMGSY) scheme. The results indicate a significant change in factors contributing to quality of neighborhood and provide essential information to the decision and policy-makers to take necessary initiatives for sustainable rural development.

Keywords Rural (PMGSY) roads · Fuzzy multi-criteria framework · Quality of neighborhood · Fuzzy PROMETHEE · Rural development

1 Introduction

Rural roads significantly influence social and economic status of rural inhabitants. They instigate growth and development of rural community. Rural road infrastructure plays significant role in poverty alleviation and assists in enhancing socioeconomic development of the rural communities [1]. They play vital role in distribution of

M. Wagale (✉) · A. P. Singh · A. K. Sarkar
Department of Civil Engineering, BITS, Pilani 333031, India
e-mail: p2014005@pilani.bits-pilani.ac.in

© Springer Nature Singapore Pte Ltd. 2019
S. Pulugurtha et al. (eds.), *Advances in Transportation Engineering*,
Lecture Notes in Civil Engineering 34,
https://doi.org/10.1007/978-981-13-7162-2_1

services to rural habitations. Improvised road infrastructure in developing countries can have a significant impact on the target population and bring out economic growth with poverty alleviation [2, 3]. Change in socioeconomic status of rural habitations is dependent on the conditions or circumstances of access and travel, to certain extent [4]. Rural roads enhance mobility and access to social services [5, 6].

Conventionally, transportation projects have been justified on the basis of their economic efficiency. They have been assessed in consideration with cost–benefit analysis. In recent decade, a few attempts have been made to assess transportation projects in consideration to social and economic impacts attributed by road infrastructure [7, 8]. Lombard and Coetzer [9] assessed numerous techniques for quantifying socioeconomic impacts due to the improvement in rural roads. Nirban et al. [10] stated the need to identify the variables which are capable in quantifying socioeconomic benefits incurred by the rural households in efficient manner.

Most of the studies in context with socioeconomic impact assessment instigated by the deliverance of road infrastructure are of singular nature. They have been focused prominently on assessing socioeconomic impacts incurred. This creates a need to assess the impacts on quality of neighborhood (social environment) along with other impacts. Quality of neighborhood is significant aspect which depicts the rural development in the form of living status of rural inhabitants. Assessment of impacts induced by road infrastructure comprises both quantitative and qualitative methods. Conventionally, a number of quantitative methods such as double differences, reflexive comparisons randomization, etc. have been employed to assess the socioeconomic impacts. These methods are able to impart better understanding about impacts incurred when sufficient data are available and are advantageous in terms of cost, time as well as can be employed for assessing the impacts after the deliverance of road infrastructure. Among impact evaluation methodologies randomization method is considered to be the most efficient and flexible [11].

The one important disadvantage of quantitative methods is that they reach to generalized conclusions and require expertise with specialized skills. In comparison with quantitative methods, qualitative approaches provide profound insight into the impacts incurred. They are more perceptible and are based on focus group (community) surveys which involve the target population as decision-makers. Such group decision-making can be well handled by employing several methods, most popular being multi-criteria decision-making (MCDM) techniques [12]. These techniques are capable of incorporating judgments provided by stakeholders involved in the decision-making process in efficient manner. Several qualitative studies have been performed by employing MCDM techniques such as Elimination Et Choice Translating Reality I (ELECTRE) [13], Technique of Order Preference by Similarity to Ideal Solution (TOPSIS) [14], Analytic Hierarchy Process (AHP) [15], Vise Kriterijumska Optimizacija kompromisno Resenja (VIKOR) [16], and Preference Ranking Organization Method for Enrichment Evaluations (PROMETHEE) [17].

Although traditional MCDM techniques are capable of handling qualitative assessments efficiently, they have one limitation. They are unable to capture the inconsistency and vagueness associated with group decision-making. These uncer-

tainties and impression can be effectively handled by employing fuzzy set theory. Therefore, when traditional MCDM techniques are integrated with the fuzzy set theory, it overcomes the risks and inconsistency associated with participative assessments. They also overcome the fuzziness associated with opinions of decision-makers [18, 19]. Even though different fuzzy MCDM techniques are available, fuzzy PROMETHEE technique is most flexible and efficient. The main advantage of F-PROMETHEE is its user-friendliness and simplicity. It also has ability to deal with tangible and intangible factors with ease.

The present study proposes a holistic approach to assess the impacts of rural road construction on quality of neighborhood of rural inhabitants. The key objective of this research is twofold: (a) to explore and exploit the capabilities of F-PROMETHEE and (b) to identify the quality of neighborhood attributes that impacted the most, on basis of their relative importance, thereby assisting the decision- and policy-makers in understanding the impacts instigated, and formulating necessary schemes and policies for overall sustainable rural development. The effectiveness of methodology is presented by employing a case study for 27 habitations connected through rural (PMGSY) roads constructed in the year 2013–14 in Jhunjhunu district of Rajasthan state, India. A total of five attributes have been considered for assessing the impacts of rural roads on quality of neighborhood.

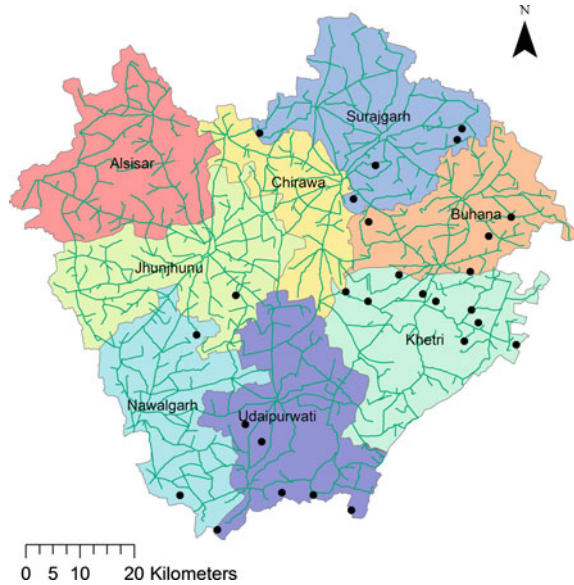
2 Materials and Methods

The uncertainties and imprecision associated with impact assessment studies which are of qualitative and quantitative in nature can be effectively dealt by incorporating fuzzy multi-criteria decision-making techniques (F-MCDM) [20]. In the present research, F-PROMETHEE has been applied to identify impacts induced by the construction of rural roads on attributes contributing to quality of neighborhood (social environment) of the rural habitations. The methodology follows seven steps: (a) determination attributes, criteria and decision-makers, (b) defining perception of decision-makers in linguistic terms, followed by application of corresponding fuzzy number, (c) aggregation of decision-makers' judgments, (d) computation and construction fuzzy decision matrix, (e) construction of fuzzy preference function, (f) deciding valued outranking relation by defining multi-criteria preference index, and (g) calculation of the flow to rank the attributes.

2.1 Study Area and Quality of Neighborhood Attributes

The study employs a case study for connectivities constructed under PMGSY scheme in Jhunjhunu district, Rajasthan, India. It accounts a total of 27 new connectivities constructed in the year 2013–14. These connectivities are distributed in six different blocks, viz., Buhana, Jhunjhunun, Khetri, Surajgarh, Nawalgarh, and Udaipurwati

Fig. 1 Divisional blocks of Jhunjhunu district along with habitations location for study and through routes



of Jhunjhunu district. The study follows ex-post approach, and the connectivities are selected on the basis of the year of construction. The population served by these connectivities ranges between 350 and 390 persons. Divisional blocks of Jhunjhunu district along with habitations location and through routes are shown in Fig. 1. The study takes into account five attributes, namely, livability (Q_L), involvement in social gathering within the village (Q_{SGIV}), involvement in social gathering outside the village (Q_{SGOV}), ownership of television (Q_{TVO}), and ownership of personal phone (Q_{PPO}).

These attributes defining the status of quality of neighborhood have been identified based upon preliminary survey, literature available, and experts (individuals belonging to government organizations, research and education institutes, etc.) opinions. The study is mainly focused on status of social environment and its improvement. It does not account impacts of rural roads on income, health, and education.

2.2 Data Collection

Data for the study is collected through focus group discussions consisting of 14 individuals. The population size of the habitations is in the range of 350–390 individuals, which is small. This makes it difficult to have group discussion and develop models separately based upon age and gender. Moreover, the percentage difference in age and gender varies differently for each habitation. Considering this fact and to have uniformity in the group discussion process, the focus groups are chosen in

such a way that it involves participants belonging to different genders, age groups, and livelihoods. The focus group discussions have been conducted during (April and May 2016). Preliminary informal discussions have been conducted to overcome the risks associated with data collection and to have necessary knowledge. The questionnaire for the survey is designed to collect data of both qualitative and quantitative in nature; it also considers the inputs from preliminary informal discussions conducted.

The questionnaire is designed in such way that it focuses on all the attributes contributing to quality of neighborhood with open-ended questions. The questionnaire is formulated to gauge necessary information in terms of categorical manner. Satisfaction level of each of the attributes defining quality of neighborhood is also assessed using a qualitative scale which represents perceptions of habitants toward the change. An attempt has been to reduce indulgence of error in the data collection process by facilitating feedback at the end of the questionnaire.

2.3 Fuzzy Preference Ranking Organization Method for Enrichment Evaluation

Fuzzy PROMETHEE technique of MCDM is more flexible outranking technique. The steps followed in implementing the method are elaborated as below:

Step 1: The first step in implementing F-PROMETHEE involves identification of attributes, criteria, and decision-makers. The present study employs five attributes and two criteria, viz., conditions before construction (C_1) and after construction (C_2) of the rural (PMGSY) roads and 27 focus groups/decision-makers.

Step 2: Further, the perceptions of focus group in linguistic terms are defined as fuzzy numbers. This study adopts 11 linguistic variables, namely, “ultimate low”, “absolutely low”, “very low”, “low”, “moderately low”, “fair”, “moderately high”, “high”, “very high”, “absolutely high”, and “ultimate high”, and are expressed as triangular fuzzy numbers, to assess the impact weights of attributes as shown in Table 1. The triangular fuzzy scale adopted for the study is depicted in Fig. 2.

Step 3: This step follows aggregation of perceptions of the focus group judgments into mean priority weights. The mean priority weight (\tilde{w}_i) of the attributes is computed as illustrated in Eq. (1):

$$\tilde{w}_i = \frac{1}{N} \left[\sum_{k=1}^N \tilde{w}_i^k \right] = \frac{1}{N} \left[\tilde{w}_i^1 + \tilde{w}_i^2 + \dots + \tilde{w}_i^N \right] \quad (1)$$

Step 4: In this step, fuzzy decision matrix is constructed by employing computed the average fuzzy weight.

Step 5: This step follows construction of fuzzy preference function. The preference function shows how much an attribute is preferred over the another.

Table 1 Definition of fuzzy numbers

Fuzzy numbers	Definition	Symbol
(0.9, 1, 1)	Ultimate high	UH
(0.8, 0.9, 1)	Absolutely high	AH
(0.75, 0.8, 0.9)	Very high	VH
(0.67, 0.75, 0.8)	High	H
(0.5, 0.67, 0.75)	Moderate high	MH
(0.4, 0.5, 0.67)	Fair	F
(0.33, 0.4, 0.5)	Moderate low	ML
(0.25, 0.33, 0.4)	Low	L
(0.1, 0.25, 0.33)	Very low	VL
(0, 0.1, 0.25)	Absolutely low	AL
(0, 0, 0.1)	Ultimate low	UL

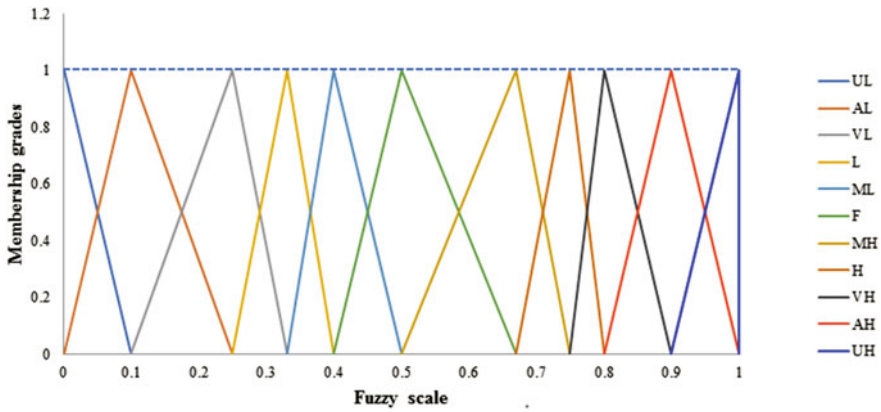


Fig. 2 Triangular fuzzy scale

Consider set S with attributes a and b, and the fuzzy preference function $\tilde{P}_i(a, b)$ is defined as in Eq. (2). It depicts superiority of a with respect to b.

$$\tilde{P}_i(a, b) = \begin{cases} 0, & \tilde{X}_{ai} \leq \tilde{X}_{bi} \\ \tilde{X}_{ai} - \tilde{X}_{bi}, & \tilde{X}_{ai} > \tilde{X}_{bi} \end{cases} \quad (2)$$

where, $i = 1, 2, \dots, m$.

Furthermore, outranking relation for attributes is constructed as given in Eq. (3):

$$\begin{cases} \tilde{X}_{ai} \leq \tilde{X}_{bi} \Leftrightarrow aPb(a \text{ out ranks } b) \\ \tilde{X}_{ai} = \tilde{X}_{bi} \Leftrightarrow aIb(a \text{ is indifference to } b) \end{cases} \quad (3)$$

Step 6: This step follows the evaluation of multi-criteria preference index by the aggregation of preference function to determine valued outranking relation. The multi-criteria preference index ($\tilde{\Pi}(a, b)$) for criterion (C_i) is given in Eq. (4):

$$\tilde{\Pi}(a, b) = \frac{1}{m} \sum_{i=1}^m \tilde{P}_i(a, b) \quad (4)$$

where $i = 1, 2, \dots, m$.

Further, the fuzzy multi-criteria preference index is defuzzified into crisp value as shown in Eq. (5)

$$A(l, \mu, u) = \frac{(l + \mu + u)}{3} \quad (5)$$

where l and u are the lower and upper bounds of the fuzzy value.

Step 7: This step follows the calculation of outranking flow and net outranking flow. The outranking flows are defined as positive outranking and negative outranking flows. The positive outranking flow is also defined as outgoing/leaving flow and is given below in Eq. (6):

$$\phi^+(a) = \sum_{b \neq a} \tilde{\Pi}(a, b) \quad (6)$$

where $\phi^+(a)$ indicates superiority of attribute a with respect to the other attributes, the higher the $\phi^+(a)$, the better is the attribute a .

The negative outranking flow is also defined as incoming/entering flow and is given in Eq. (7):

$$\phi^-(a) = \sum_{b \neq a} \tilde{\Pi}(a, b) \quad (7)$$

where $\phi^-(a)$ indicates the superiority of other attributes with respect to attribute a , the lower the $\phi^-(a)$, the better is the attribute a .

Finally, the net outranking flow is given in Eq. (8):

$$\phi(a) = \phi^+(a) - \phi^-(a) \quad (8)$$

3 Results and Discussion

The study develops a model to evaluate the impacts of rural (PMGSY) road construction on social environment of rural habitations. The model assesses the impacts in terms of relative importance of the attributes contributing to the quality of

neighborhood. A total of five attributes, viz., livability (Q_L), involvement in social gathering within the village (Q_{SGIV}), involvement in social gathering outside the village (Q_{SGOV}), ownership of television (Q_{TVO}), and ownership of personal phone (Q_{PPO}), have been considered for the assessment. These attributes are evaluated on the basis of their relative importance by taking into account the perceptions of rural inhabitants. These attributes depict the change in social status of the inhabitants after the construction of rural (PMGSY) roads in comparison with their status before. The perceptions gathered through focus group discussion have been converted to triangular fuzzy scale as given in Table 1.

According to Eq. (1), the mean fuzzy weights for the attributes in correspondence to the criteria are evaluated as depicted in Table 2.

The multi-criteria preference index for all the attributes is evaluated by employing Eq. (4) and are shown in Table 3. The multi-criteria preference index is evaluated to assess the outranking relation of the attributes. These assign the preference to the attributes over each other.

Furthermore, the outgoing, entering, and net flows are evaluated by employing Eqs. 6–8 to order the attributes accordingly. Table 4 depicts the outgoing, entering, and net flows for the attributes.

From Table 4, it is observed that the livability condition of the inhabitants is improved after the deliverance of rural (PMGSY) roads as compared to their condition before. It also illustrates that the livability status of marginal groups (especially women and children) has changed significantly, and also can be put forth that they are able to have better access to social services. Furthermore, it can also be observed that the inhabitants are able to involve themselves in social gathering outside their habitations which was found difficult before the deliverance of roads. This is also reflected by the change in the values of Q_{TVO} and Q_{SGIV} . The inhabitants are able to have facilities for their recreations purpose as well as they are able to get involved in various activities within their community. The attribute Q_{PPO} shows least impact; the reason for this is that the inhabitants are less perceptive over the change in comparison with other attributes.

Moreover, on the basis of the ranking obtained, it can be inferred that though there is significant improvement with respect to livability condition and involvement in social gathering outside village of residents, there is still enough scope for improvement with respect to remaining other three attributes. Thus, policy-makers

Table 2 Mean fuzzy weights of attributes with respect to criteria

Attributes	Before the construction (C_1)			After the construction (C_2)		
	Q_{PPO}	0.652	0.759	0.814	0.857	0.957
Q_{TVO}	0.550	0.660	0.731	0.727	0.827	0.860
Q_L	0.338	0.448	0.563	0.696	0.815	0.857
Q_{SGIV}	0.656	0.784	0.832	0.731	0.827	0.865
Q_{SGOV}	0.481	0.586	0.676	0.651	0.753	0.817

Table 3 Multi-criteria preference index of the attributes

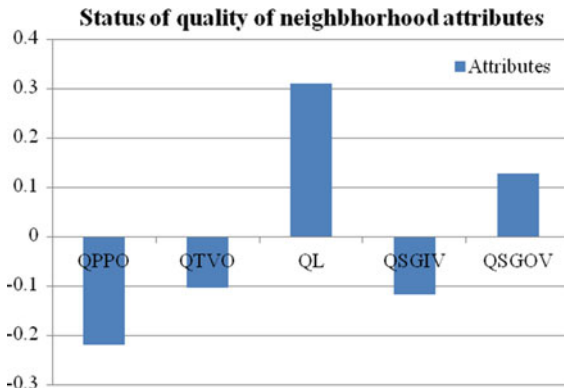
a	b	$\Pi(a, b)$
Q _{PP0}	Q _{TVO}	0.1082
	Q _L	0.2147
	Q _{SGIV}	0.0516
	Q _{SGOV}	0.1734
Q _{TVO}	Q _{PP0}	-0.1082
	Q _L	0.6065
	Q _{SGIV}	-0.0566
	Q _{SGOV}	0.0651
Q _L	Q _{PP0}	-0.2147
	Q _{TVO}	-0.1065
	Q _{SGIV}	-0.1631
	Q _{SGOV}	-0.0414
Q _{SGIV}	Q _{PP0}	-0.0516
	Q _{TVO}	0.0566
	Q _L	0.1631
	Q _{SGOV}	0.1217
Q _{SGOV}	Q _{PP0}	-0.1734
	Q _{TVO}	-0.0651
	Q _L	0.0414
	Q _{SGIV}	-0.1217

Table 4 Outgoing, entering, and net flows for the attributes

Attributes	Q _{PP0}	Q _{TVO}	Q _L	Q _{SGIV}	Q _{SGOV}	ϕ^+	ϕ
Q _{PP0}	0.0000	-0.1082	-0.2147	-0.0516	-0.1734	-0.1096	-0.2192
Q _{TVO}	0.1082	0.0000	-0.1065	0.0566	-0.0651	-0.0014	-0.1027
Q _L	0.2147	0.6065	0.0000	0.1631	0.0414	0.2051	0.3102
Q _{SGIV}	0.0516	-0.0566	-0.1631	0.0000	-0.1217	-0.0579	-0.1159
Q _{SGOV}	0.1734	0.0651	-0.0414	0.1217	0.0000	0.0638	0.1275
ϕ^-	0.1096	0.1014	-0.1051	0.0579	-0.0638	0.1096	

are requiring drafting schemes that will help to benefit the target population and assist in overall rural development. The proposed method also suggests the shortcomings of conventional approaches. Figure 3 illustrates the status of attributes contributing to quality of neighborhood (social environment) in a comprehensive way.

Fig. 3 Status of attributes contributing to quality of neighborhood



4 Conclusion

Assessment of impacts instigated by rural road construction on quality of neighborhood (social environment) is one of the significant aspects of rural development. They are to be accounted along with other socioeconomic impacts. They put forth the living status of inhabitants and assist the policy-makers in implementing schemes and policies, to attend the indented goal of overall sustainable rural development. Quality of neighborhood is defined by the attributes which are both qualitative and quantitative in nature and can be well handled with application of fuzzy MCDM methods. This study proposes application of F-PROMETHEE to assess the impacts incurred on social environment by deliverance of rural roads. Application of F-PROMETHEE has proved to be significant decision-making tool. The main advantage of the proposed methodology is that it takes into account the imprecision and uncertainty associated with the data, which is based upon group decision-making process. The methodology is simple and can be handled with ease. The proposed F-PROMETHEE model can effectively deal by providing a good scope of assessing qualitative data set.

The model is flexible and robust in nature as it takes into account the perceptions of focus group (rural inhabitants) which are imprecise in nature. Considering this fact, the technique applied in the study can be utilized for assessment of road infrastructure development at global level rather than region specific. Moreover, from practical application viewpoint, the developed model can enable the policy- and decision-makers to investigate the status of social environment so that it can assist to take necessary actions by intensifying their efforts for improving rural life in a sustainable manner. It also takes into account temporal and spatial variations, making it a significant tool in assessing the overall rural development. From future scope and limitations point of view, there is need to focus more on the change on the status of marginal groups (women and children) specifically, after the deliverance of rural roads.

References

1. Oraboune S (2008) Infrastructure (rural road) development and poverty alleviation in Lao PDR. International infrastructure development in East Asia—towards balanced regional development and integration. ERIA Research Project Report 2, Jakarta
2. Banister D, Berechman Y (2001) Transport investment and the promotion of economic growth. *J Transp Geogr* 9:209–218. [https://doi.org/10.1016/s0966-6923\(01\)00013-8](https://doi.org/10.1016/s0966-6923(01)00013-8)
3. Khandker SR, Bakht Z, Koolwal GB (2009) The poverty impact of rural roads: evidence from Bangladesh. *Econ Dev Cult Change* 57(4):685–722. <https://doi.org/10.1086/598765>
4. Kanuganti, S., Sarkar, A.K., Singh, A.P.: Evaluation of access to health care in rural areas using enhanced two-step floating catchment area (E2SFCA) method. *J. Transp. Geogr.* 56:45–52 (2016)
5. Freeman PN (2009) Ten years of World Bank action in transport: evaluation. *J. Infrastruct Syst* 15:297–304
6. Porter G (2012) Reflections on a century of road transport developments in West Africa and their (gendered) impacts on the rural poor. *EchoGéo* 20. <https://doi.org/10.4000/echogeo.13116>
7. Aderamo AJ, Magaji SA (2010) Rural transportation and the distribution of public facilities in Nigeria: a case of Edu local government area of Kwara State. *J Hum Ecol* 29:171–179. <https://doi.org/10.1080/09709274.2010.11906260>
8. Grootaert C, Calvo CM (2002) Socioeconomic impact assessment of rural roads: methodology and questionnaires. Impact Evaluation report, INFTD, World Bank, Washington, DC, United States
9. Lombard P, Coetzer L (2007) The estimation of the impact of rural road investments on socio-economic development. In: International seminar on sustainable road financing & investment, Arusha, Tanzania, p 14
10. Nirban VS, Metri BA, Singh AP, Sarkar AK (2003) Socioeconomic benefits of PMGSY projects: perceptions of rural community. In: Proceedings of a seminar on integrated development of rural and arterial road network for socio-economic growth, New Delhi, India, pp 166–173
11. Barnow BS, King CT (2000) Improving the odds: increasing the effectiveness of publicly funded training. The Urban Institute Press, Washington, DC
12. Srinivas R, Singh AP (2018) Application of fuzzy multi-criteria approach to assess the water quality of river Ganges. In: Pant M, Ray K, Sharma T, Rawat S, Bandyopadhyay A (eds) *Soft computing: theories and applications. Advances in intelligent systems and computing*, vol 583, pp 513–522. Springer, Singapore. https://doi.org/10.1007/978-981-10-5687-1_46
13. Raj A (1995) Multicriteria methods in river basin planning—a case study. *Water Sci Technol* 31(8):261–272
14. Yazdani M, Payam AF (2015) A comparative study on material selection of microelectromechanical systems electrostatic actuators using Ashby, VIKOR and TOPSIS. *Mater Des* 65:328–334. <https://doi.org/10.1016/j.matdes.2014.09.004>
15. Minatour Y, Khazaei J, Ataei M (2012) Earth dam site selection using the analytic hierarchy process (AHP): a case study in the west of Iran. *Arab J Geosci* <https://doi.org/10.1007/s12517-012-0602-x>
16. Liu HC, Mao LX, Zhang ZY, Li P (2013) Induced aggregation operators in the VIKOR method and its application in material selection. *Appl Math Model* 37:6325–6338
17. Singh AP, Shrivastava P, Vidyarthi AK (2018) Potential impacts of climate change on water resources in semi-arid region of Chittoargarh, India. In: Singh V, Yadav S, Yadava R (eds) *Climate change impacts. Water Science and Technology Library*, vol 82, pp 201–211. Springer, Singapore. https://doi.org/10.1007/978-981-10-5714-4_17
18. Singh AP, Vidyarthi AK (2008) Optimal allocation of landfill disposal site: a fuzzy multi-criteria approach. *Iranian J Environ Health Sci Eng* 5:25–34
19. Hsu YL, Lee CH, Kreng VB (2010) The application of Fuzzy Delphi method and Fuzzy AHP in lubricant regenerative technology selection. *Expert Syst Appl* 37:419–425. <https://doi.org/10.1016/j.eswa.2009.05.068>

20. Wagale M, Singh AP, Sarkar AK (2018) Assessment of socio-economic impacts of PMGSY roads using fuzzy multi-criteria decision making tool. In: Singh UP, Sivakumar Babu GL (eds) Urbanization challenges in emerging economies: resilience and sustainability of infrastructure, Proceedings of ASCE india conference, 12–14 December 2017. ASCE, pp 71–79. <https://doi.org/10.1061/9780784482032.008>

Assessment of Accessibility for Mixed Land Use Neighborhoods Through Travel Behavior Pattern



Jayesh Juremalani  and Krupesh A. Chauhan

Abstract In general, accessibility shows the ease of reaching destinations and the interaction between the land use and the transportation systems. In this paper, attempt is made to assess the accessibility through commuters' travel behavior pattern for working trip only. The effects of trip characteristics like trip length, trip time, and trip cost and socioeconomic characteristics like gender, age, income, occupation, and vehicle ownership on travel behavior and mode choice are studied for work trips for different mixed land use neighborhoods (wards) of Vadodara city. Four types of modes are considered, namely, car, bus, shared auto, and two wheelers. Accessibility index is prepared for different neighborhoods. It is found that the change in the land use mix affects the commuters' travel behavior and mode choice selection.

Keywords Accessibility · Public transportation · Land use · Trip behavior · Mode choice

1 Introduction

Accessibility refers to a measure of the ease of reaching destination or activities distributed in space, e.g., around a city or country. Accessibility is generally associated with a place of origin. A place with “high accessibility” is one from which many destinations can be reached, or destinations can be reached with relative ease. “Low accessibility” implies that relatively few destinations can be reached for a given amount of time/effort/cost or that reaching destinations is more difficult or costly from that place. Travel behavior may be explained as what people do over space, and how people use transport. Travel behavior in current time is considered to be influ-

J. Juremalani (✉) · K. A. Chauhan
Civil Engineering Department, Sardar Vallabhbhai National Institute of Technology,
Surat 395007, Gujarat, India
e-mail: jayesh1575@gmail.com

K. A. Chauhan
e-mail: kac@ced.svnit.ac.in

© Springer Nature Singapore Pte Ltd. 2019
S. Pulugurtha et al. (eds.), *Advances in Transportation Engineering*,
Lecture Notes in Civil Engineering 34,
https://doi.org/10.1007/978-981-13-7162-2_2

enced by several determinants such as changing land use, changing demographics, socioeconomical changes, state-of-the-art transportation infrastructure, technological advancements, pricing of services, and policy interventions. Mode choice analysis allows the modeler to determine what mode of transport will be used, and what modal share results.

Modeling of mode choice is done by means of discrete choice model; the different available alternatives in a discrete choice experiment are mutually exclusive and collectively exhaustive. Discrete model is based on selecting the alternative that provides highest utility to the choice maker.

2 Introduction of Study Area

Vadodara is located on the banks of the Vishwamitri River. As per census 2011, the population of Vadodara is 16,70,806, of which male and female are 8,69,647 and 8,01,159, respectively. Figure 1 shows location and map of the Vadodara city.

3 Socioeconomic Background of the Commuters

The Vadodara city has 19 election wards as per census, so 19 wards were considered as 19 parts of the study area. A questionnaire was prepared, and a total of 1394 responded were asked to fill up the form from all the 19 wards. After removing

Location of the study area-“Vadodara” (Gujarat)

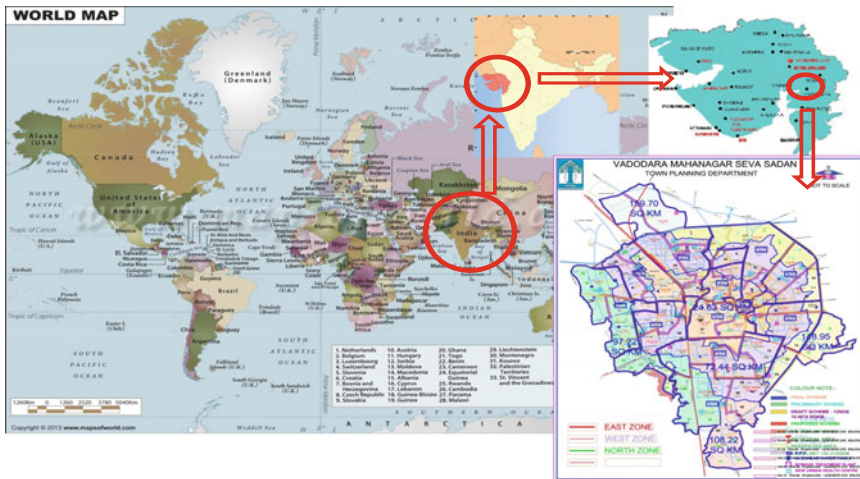


Image source: VMSS

Fig. 1 Location and the map of Vadodara city

outliers, a total of 1358 forms were selected for analysis. There were total of 983 male and 375 female respondents. The information on various social and economic variables like age, income, gender, occupation, and vehicle ownership were collected and analyzed. For example, ward numbers 7 and 14 has younger respondent having age below 35 years as high as 77.67 and 72.97%, respectively, and ward numbers 8 and 15 has lower percentage of younger respondent whose age is below 35 years 39.32 and 40.62%, respectively (Table 1).

Table 2 shows the occupation of the respondents. The average percentage of government employee, private sector employee, service industry employee, businessmen, and housewife are 8.7%, 20.91%, 17.54%, 26.32%, and 26.53%, respectively. So it is clear from the analysis that more number of shopping trips are made by business class people and housewife.

The segregation of respondents based on income is shown in Table 3. The maximum respondents fall under the income group of 20,000–30,000 and 30,000–40,000. Total 53.21% of respondents have their income between Rs. 20,000 and Rs. 40,000.

Table 1 Statistical analysis of age of respondents

Ward no.	16–25 years	26–35 years	36–45 years	46–55 years	55 years above	Total respondents
1	25	24	13	8	4	74
2	34	30	13	14	10	101
3	11	36	17	9	12	85
4	12	36	19	10	6	83
5	4	26	23	10	1	64
6	4	22	14	10	0	50
7	49	31	16	4	3	103
8	10	25	15	32	7	89
9	6	18	11	5	3	43
10	2	16	14	4	4	40
11	2	15	15	4	2	38
12	30	29	22	14	5	100
13	12	21	22	10	5	70
14	16	38	12	7	1	74
15	6	20	15	8	15	64
16	10	34	23	14	3	84
17	12	19	22	11	3	67
18	13	36	15	9	4	77
19	12	17	12	9	2	52
	270	493	313	192	90	1358

Table 2 Statistical analysis of occupation of respondents

Ward	Government employee	Private sector	Service industry	Businessman	Housewife	Total
1	8	27	20	14	5	74
2	16	28	27	20	10	101
3	10	30	12	16	17	85
4	7	23	18	21	14	83
5	6	5	5	15	33	64
6	5	6	9	2	28	50
7	6	24	24	41	8	103
8	11	18	16	20	24	89
9	1	11	5	20	6	43
10	1	1	3	11	24	40
11	0	1	4	13	20	38
12	16	32	25	23	4	100
13	17	19	13	12	9	70
14	2	17	12	34	9	74
15	9	15	10	14	16	64
16	10	14	14	17	29	84
17	0	4	0	29	34	67
18	4	19	26	22	6	77
19	1	12	11	10	18	52

Table 3 Statistical analysis of income of respondents

Ward	Less than 5000	5000–10,000	10,000–20,000	20,000–30,000	30,000–40,000	40,000–50,000	50,000–100,000	Above 100,000	Total
1	1	7	19	19	15	8	5	0	74
2	1	3	21	16	21	17	10	12	101
3	1	2	7	26	31	14	4	0	85
4	1	9	15	22	25	8	2	1	83
5	0	3	9	17	15	17	2	1	64
6	0		5	12	9	10	13	1	50
7	5	16	10	58	14	0	0	0	103
8	1	2	16	29	25	10	4	2	89
9	5	1	12	6	14	5	0	0	43
10	1	2	3	4	22	5	3	0	40
11	0	1	2	3	10	16	3	3	38

(continued)

Table 3 (continued)

Ward	Less than 5000	5000–10,000	10,000–20,000	20,000–30,000	30,000–40,000	40,000–50,000	50,000–100,000	Above 100,000	Total
12	0	3	15	18	29	19	13	3	100
13	3	5	11	14	17	11	5	4	70
14	4	6	13	36	15	0	0	0	74
15	1	7	12	22	17	5	0	0	64
16	1	2	13	22	26	15	4	1	84
17	1	1	6	10	22	24	3	0	67
18	4	5	7	23	25	8	4	1	77
19	3	3	11	8	17	7	3	0	52
	33	78	207	365	369	199	78	29	1358

Only 6% of respondents have income between Rs. 50,000 and Rs. 1,00,000, and merely 2% are having monthly income of more than 1 lakh.

4 Analysis of Accessibility

Generally, people select the mode which gives them maximum utility value. Here, utility value is nothing but the advantages one gets from the particular mode. The equations for the utility function are generated using SPSS software. Analysis for ward number 1 is shown in Table 4. For example, utility for car can be found, $U_{car} = 3.659 - 0.03 * \text{Distance} - 0.082 * \text{Travel time} - 0.022 * \text{Travel Cost} = 1.61$. Here, mean value is taken for distance, time, and cost. Similarly, all the utility values are found. After finding utility values, they are converted into log values and summation of all gives the accessibility of the ward for working trips.

The accessibility for all the wards along with their population and area and density is shown in Table 5. Density is found by dividing population with area.

Chart 1 shows the mode share and working trip distance relationship. It can be seen from Chart 1 that after 12 km use of public transport like bus, shared auto

Table 4 Calculation of accessibility score for ward number 1

Ward 1	Modes	Coefficients	Utility function	Log utility	Sum log U
Car	(Constant)	3.659	1.61	0.48	3.30
	Distance for car	-0.03			
	Travel time for car	-0.082			
	Travel cost for car	-0.022			

(continued)

Table 4 (continued)

Ward 1	Modes	Coefficients	Utility function	Log utility	Sum log U
Share auto	(Constant)	3.53			
	Distance for auto	-0.155	1.73	0.55	
	Travel time for auto	-0.06			
	Travel cost for auto	-0.035			
Bus	(Constant)	3.427	3.16	1.15	
	Distance for bus	-0.007			
	Travel time for bus	-0.004			
	Travel cost bus	-0.018			
Two wheelers	(Constant)	2.829	3.07	1.12	
	Distance TW	-0.043			
	Travel time for TW	0.048			
	Travel cost for TW	0.016			

Table 5 Accessibility index

Rank	Accessibility index	Name	Ward	Area in SQ KM	Population above 18 as per census 2011	Density
1	4.07	Waghodia Ajwa area	5	5.34	68,216	12774.53
2	4.01	Makarpura area	18	8.09	69,908	8641.29
3	3.72	Atladra area	12	3.27	69,004	21102.14
4	3.63	Sardar estate	4	11.5	57,669	5014.70
5	3.41	Harni airport	3	5.98	68,124	11391.97
6	3.30	Chhani area	1	9.49	64,860	6834.56
7	3.21	Gorwa	8	16.14	69,640	4314.75
8	3.19	Mandvi CBD area	14	6.78	63,618	9383.19
9	2.99	Pratapnagar	16	10.15	62,888	6195.86
10	2.76	Tarsali	17	5.34	62,101	11629.40
11	2.66	Gotri Talav	9	6.6	70,092	10620.00
12	2.59	Nizampura	2	9.17	73,258	7988.88
13	2.56	Kothi Raopura	13	7.38	57,493	7790.38

(continued)

Table 5 (continued)

Rank	Accessibility index	Name	Ward	Area in SQ KM	Population above 18 as per census 2011	Density
14	2.26	Manjalpur	15	4.43	75,990	17153.50
15	2.22	Warsia Sangam area	6	5.18	67,050	12944.02
16	2.22	Maneja area	19	20.58	62,556	3039.65
17	1.36	Akota area	11	6.84	73,779	10786.40
18	0.86	Vasna Tandalja	10	7.08	66,099	9336.02
19	0.13	Fatehgunj area	7	9.3	67,553	7263.76

increases drastically. This is a very useful finding. While making land use planning, this finding should be kept in mind.

5 Conclusion

From the analysis, it may be concluded that the ward numbers 5, 18, 12, 4, and 3 are more accessible for working trips than their other counterparts. Similarly, ward numbers 7, 10, 11, and 19 are less accessible for the work trips.

From Chart 1, it can be concluded that the use of bus and shared auto increases as distance between home and workplace increases. Especially, after 12–15 km, use of public transport increases drastically. For promoting use of public transportation, this finding is very useful. In other words, if land use planning should be made in

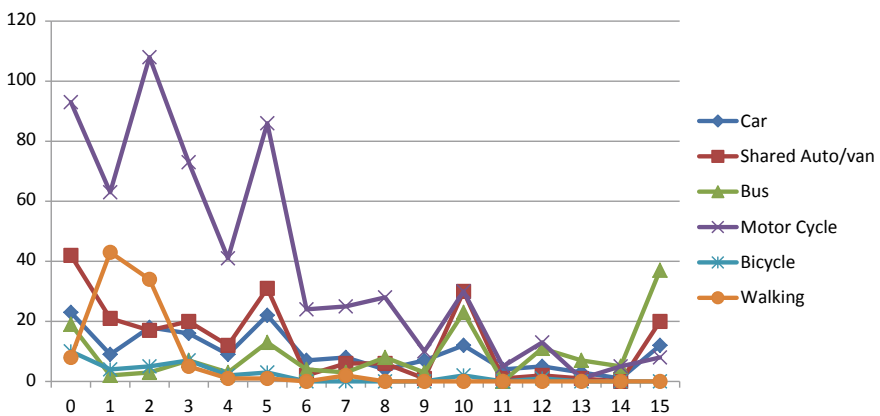



Chart 1 Mode choice and working trip distance

such a way that distance between working destination and home is more than 12 km, then people would prefer public transportation over private vehicles.

Assessing Travel Time Reliability of Public Transport in Kolkata: A Case Study



Saptarshi Sen , Tarun Chowdhury, Ayan Mitra and Sudip Kumar Roy

Abstract Punctuality of a trip maker directly depends on the on-time performance of the whole transportation system and specifically on the travel time reliability of the preferred mode of transport. As a matter of this fact, daily commuters prefer a reliable mode of transport which adheres to its schedule and is frequently available. Thus, the present study aims to find only the travel time reliability of the different public transport modes in a particular route of Kolkata Metropolitan Area. The route from Bansdroni Bazar Area to Park Street Area was chosen as the case study area. The in-vehicle travel time reliability of the state government bus, private bus and minibus were estimated using the method proposed by Liu and Sinha [15] and the results compared with that of the metro railway. The result of the analysis shows that the travel time reliability of all bus types ranges from 45 to 65% of the reliability of the metro railway. The parameters prescribed by FHWA, such as Buffer Time (T_B), Buffer Index (B_i), Planning Time (P_t) and Planning Time Index (P_i), were also estimated which provides valuable information about the reliability of the buses plying on the route under study. Delay parameters in transit contribute a lot to the travel time which was also observed to indicate the reliability of buses from delay perspective. The effects of some other relevant traffic parameters such as the congestion delay and waiting time delay on reliability have also been discussed as well.

Keywords Public transport · Reliability · Travel time · Buffer time · Buffer index · Planning time

S. Sen (✉) · T. Chowdhury · S. K. Roy
Civil Engineering Department, IEST, Shibpur, Howrah, India
e-mail: sen.saptarshi91@gmail.com

T. Chowdhury
e-mail: tarun19devcon@gmail.com

S. K. Roy
e-mail: royksudip@gmail.com

A. Mitra
Development Consultants Pvt. Ltd, Kolkata, India
e-mail: ayan_mitra18@yahoo.co.in

© Springer Nature Singapore Pte Ltd. 2019
S. Pulugurtha et al. (eds.), *Advances in Transportation Engineering*,
Lecture Notes in Civil Engineering 34,
https://doi.org/10.1007/978-981-13-7162-2_3

1 Introduction

Commuters all over the world try to minimise their overall journey time. This gives rise to the need for reliable services of transportation system, especially the public transport system. Reliability for various systems can be defined in various forms. Reliability can be defined as the operational consistency of a facility over an extended period of time. Ebeling [8] defined reliability as the probability that a system will perform a required function for a given period of time. In transportation engineering, reliability can be defined as the level of variability between the commuters' expectation and the actual experience. Kolkata is a densely populated city and according to a study by the Union Ministry of Urban Development in 2013, about 54% of daily commuters avails bus for any trips. Hence, reliability of the bus system in Kolkata is highly desirable. In a city where majority of the trip makers are of captive characteristic, the unreliable public bus system would force the commuters to either opt for para-transit system or shift towards personal vehicles. In most of the cases, the personal vehicles will be of motorised two wheelers and four wheelers and also the para-transit modes are mostly three-wheeled auto-rickshaws along with taxis and application-driven cabs such as Uber/Ola, etc. Increase of these smaller size modes of traffic in the same right of way along with the bigger size vehicles will not only cause increase in congestion but will also have a bad impact on environmental pollution. Therefore, it is necessary to operate the public transport system at desired level of reliability. The present study mainly focuses on the in-vehicle travel time reliability of the buses and the delays incurred during the bus trips in Kolkata. The objectives of the study can be stated as follows:

- To estimate the travel time reliability of the public transport modes plying along the specific study corridor.
- To compare the travel time reliability of different category of buses with that of the metro railway.
- To estimate the buffer time and planning time required for the trip makers choosing the public mode of transport system, especially buses as their mode of transport.
- To identify the delays in a trip and its effect on the travel time reliability.

The previous works and journals related to public transport reliability literature have been summarised in the next section.

2 Literature Review

The concept of reliability in travel time has been introduced in the late twentieth century, though in Indian context the applications have been in limited quantity. Some of the recent works have been studied, and the relevant points have been discussed here.

In 2013, Tony [17] identified the public transit priority features and the method to enhance the operational characteristics of public transit in Munich, Germany and

Zurich, Switzerland. Diab and El-Geneidy [6], in the same year, tried to understand the impacts of various improvement strategies on transit service reliability. Chien and Liu [5] measured the travel time variability and reliability with floating car data. Diana [7] showed that satisfaction measures of trip makers can be exploited to gain insights on the relationships between personal attitudes, transit use and urban context. Cantwell et al. [2] examined the level of stress caused by commuting into Dublin city centre. It revealed that the commuters who spend long time for waiting for public transport service tend to be more stressed. This occurs when the reliability of the bus service is poor. Route length, headway, distance from stop to original terminal and the use of exclusive bus lanes affect the service reliability as found by Chen et al. [4]. Lyman and Bertini [16] tried to improve regional transportation planning and operations using travel time reliability measures. Liu and Sinha [15] estimated some of the measures to assess reliability of an urban bus network using microsimulation model framework. It was observed that with increasing congestion and passenger demand, reliability is reduced. Reduction in per passenger boarding time proves to be an effective measure in improving reliability. Iseki et al. [11] studied the effects of out-of-vehicle time on travel behaviour, and the findings were used to improve the travel connectivity at the transit transfer points. Laura [13] and Lin et al. [14] used new techniques, such as AVL and APC techniques, to collect data and measured reliability, cause of unreliability and application of strategies to improve the service. During early twenty-first century, Kimpel [12] analysed transit service reliability and estimated passenger demand.

The reliability measure of a corridor is important for the operational efficiency of a road. In the Indian context, it is important to enhance and maintain accessible, reliable and affordable public transport services as mentioned by Badani and Haider [1] in their work. The travel time reliability of urban arterial corridor in Delhi road network was studied by Gopi et al. [10]. They used the reliability measures developed by Federal Highway Administration (FHWA Report 2006) [9] to measure the reliability of the arterial corridor at a different time of the day. Higher Planning Time Index (PTI) and Buffer Index (BI) values during the morning peak hour of non-working days as compared to morning peak hour of working days were obtained from their analysis. Chalumuri et al. [3] also used the FHWA measures for estimating reliability of an urban corridor and further used the microsimulation to determine the travel time reliability. They also found out the influence of the demand side factors (such as traffic flow, speed distribution vehicle composition, driver characteristics, etc.) and supply-side factors (such as reserved lane for bus, lane closure, etc.) on the reliability value (Reviewer 2).

In most of the previous literature, it is found that travel time reliability has been considered to be the key indicator for the performance and health of a region's transportation system. Thus, in this article, the performance of the public transport (especially buses) has been analysed using the methods of travel time reliability measures. In the following sections, the methodology and the case study area has been described. The reliability of the buses has been compared with that of the most reliable mode of public transport in the same route, i.e. metro railway.

3 Methodology

The metro railway is considered as the benchmark for the travel time reliability. The estimated travel time reliability for all the modes is compared with that of the metro railway. The comparison reveals the current situation of travel time reliability of all the modes with respect to the metro railway.

The data collected from the on-board survey (the process is described in ‘Data collection and Survey’ section later) was analysed in three categories. Initially, the travel time reliability was estimated for each of the modes considering the method used by Liu and Sinha [15]. They defined travel time reliability as the ratio of the mean travel time to the standard deviation. The formula can be written as follows:

$$RT = \frac{\mu}{\sigma} \quad (1)$$

where

- μ is the mean travel time and
- σ is the standard deviation of travel time.

The data collection and the calculations are easy for this method and hence have been used in this study to estimate the reliability (Reviewer 1).

Second, the five standard measures developed by Federal Highway Administration (FHWA Report 2006) [9] to determine the travel time reliability are also used here. It is used in this study as it is a well-established method and has been used by many researchers for estimating the route reliability (Reviewer 1). The parameters are mentioned below.

95th Percentile Travel Time (T_{95}). It denotes the travel time which is less than or equal to 95% of sample travel times. Higher T_{95} means the variation in travel time of the bus is high. This indicates less reliability.

Buffer Time (T_B). The difference between the 95th percentile travel time and the mean travel time (μ_t) is called the buffer time. This represents the extra time needed to compensate for unexpected delays. The higher the buffer time for a passenger, the less reliable is the mode of travel for that passenger.

$$T_B = T_{95} - \mu_t \quad (2)$$

Buffer Index (B_i). It is the ratio of buffer time to the mean travel time expressed in terms of percentage. This indicates the extra percentage of time a trip maker should add to his/her expected mean travel time to ensure on-time or earlier arrival to the destination. The more the buffer index, the lower is the reliability.

$$B_i = \frac{T_B}{\mu_t} \times 100\% \quad (3)$$

Planning Time Index (P_i). It is the ratio of the 95th percentile travel time to the free-flow travel time expressed in terms of percentage. It compares the longest travel

time against a travel time incurred by free-flow traffic. The higher the P_i , the less reliable is the mode of travel. In the present study, free-flow travel time was obtained by observing the travel time taken by a car to reach the destination from the origin via the same route in the early morning hours. The free-flow speed is observed to be 1380 s for this present study.

$$P_i = \frac{T_{95}}{T_F} \times 100\% \quad (4)$$

Planning Time (P_t). It is the summation of average/mean travel time and buffer time. The higher the buffer time, the more will be the planning time and lesser there liability of the mode.

$$P_t = \mu_t + T_B \quad (5)$$

Finally, the reliability is also indicated with the help of the delay caused by travelling in public buses. The more the delay, the less is the reliability. The different types of delay focussed in this present study are as follows:

- **Signal Delay:** The vehicle stopping within a distance of 100 m from the 'stop' line under the influence of signal which incurs the delay in the travel time is termed as signal delay.
- **Bus Stop Delay:** These delays are attributed to boarding and alighting of individual passengers at specified bus stops only.
- **Waiting Delay:** This includes any extra delay occurred due to unnecessary halt at empty stoppages.
- **Congestion Delay:** Any delay caused by the congestion created due to the huge volume of traffic during the peak hours.

Since the bus routes are the same, the number of signalised intersection encountered in a single trip is the same for all modes. So, in addition to congestion delay, the travel time delay is dependent mostly on the bus stop delay and the waiting time delay which will negatively affect the travel time reliability. A sensitivity analysis is included in this study to understand and identify the delay that affects the travel time reliability of a public bus.

4 Study Area

Kolkata is the third largest metropolitan city in India and the capital city of West Bengal state. It has a huge population, mostly residing in the suburban regions. Bansdronei Bazaar area is one such region in the southern part of Kolkata that generates a significant amount of work trips to Park Street, a well-known commercial area in the central part of Kolkata. Out of the various corridors connecting Bansdronei Bazaar with Park Street, one corridor of about 10.5 km long is selected as the case study due to the presence of metro railway all along the corridor (Fig. 1) in addition to the

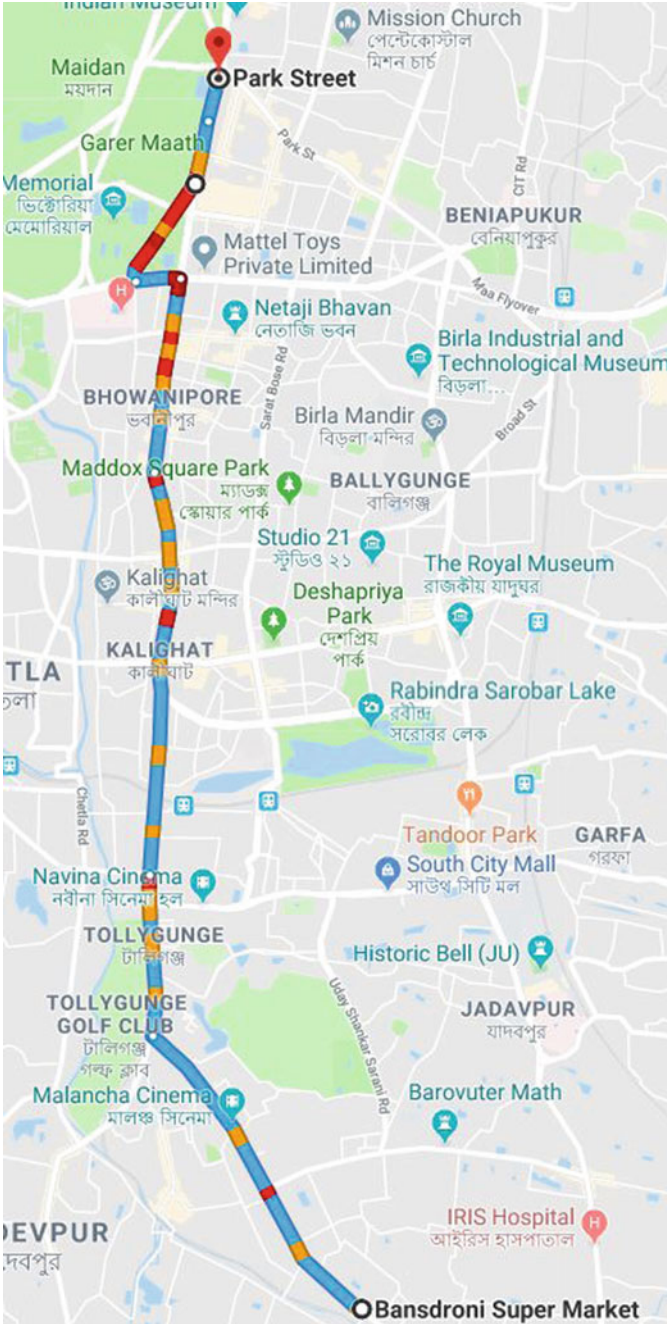


Fig. 1 Map showing the case study route from Bansdrone Bazaar to Park Street. *Source* Google Map

Table 1 Bus route characteristics under study

Bus route	Bus operator	Origin	Destination	Route segment under study
A	State Govt.	Garia bus stand	Howrah station	Bansdronei bazar to Park street
B	State Govt.	Garia bus stand	Howrah station	Bansdronei bazar to Park street
C	Private	Bansdronei bazar	Howrah station	Bansdronei bazar to Park street
D	Private (minibus)	Naktala bus stand	Howrah station	Bansdronei bazar to Park street

different public modes of transport. This corridor consists of four busiest roads of Kolkata. They are Netaji Subhash Chandra Bose Road, Shyama Prasad Mukherjee Road, Ashutosh Mukherjee Road and Jawaharlal Nehru Road. These roads are having all types of modes of transport plying on Kolkata streets, namely, regular private and government buses, private minibuses, three-wheeled auto-rickshaw, taxi/cabs and private cars and motorised two wheelers along with other non-motorised modes.

A number of bus routes of various characteristics and different routes are plying on the study corridor. Out of them, four bus routes have been considered for this study as these four bus routes have a common segment in their route from Bansdronei Bazar to Park Street. The other routes do not have such a long common route segment. Moreover, these four types of buses (i.e. Govt. AC, Govt. Non-AC, Ordinary Private Non-AC and Private Minibus) mostly ply in the urban streets of Kolkata and represents the public bus system of Kolkata (Reviewer 2).

A brief description of these bus routes is provided in Table 1. The survey procedure and the data collected for analysis are discussed in the next section.

5 Data Collection and Survey

In this study, two state government buses (Route A and Route B), one private bus (Route C), one mini private bus (Route D) and metro railway were selected. To calculate the reliability measures (as mentioned in the 'Methodology' section), the time taken by the buses of the aforesaid bus routes to travel from Bansdronei Bazar to Park Street along the route (mentioned in 'Study Area') was observed. This travel time is nothing but the running time of the buses between two consecutive bus stops whose summation gives the total running time. Along with the travel time, different delays such as signal delay, bus stop delay, waiting delay and congestion delay were also noted using a stopwatch. AVL data [14] was not available to obtain these data, hence, on-board technique was adopted. In this technique, an enumerator travelled from Bansdronei Bazar to Park Street in a bus of the study routes and the different

delay and travel time are noted down using a stopwatch. Since the study focuses on the reliability of buses for work trips only, the morning peak hour was selected for conducting the survey. Three buses of each bus route travelling between 9 and 10 am each day were randomly selected on any seven weekdays of a month. The same procedure was carried out for metro railway as well. Free-flow travel time was obtained by observing the time taken by a standard car to reach Park Street from Bansdroni Bazar via the same route at 6 am for three consecutive weekdays and the average is calculated. This is considered as the datum for free-flow travel time. There is difference in the operational characteristics of car and bus but the free-flow travel time cannot be extracted accurately from a bus because the drivers of the public buses drive according to their own will and may not drive at a free-flow speed even if a free-flow condition prevail in the road segment. Due to this reason mainly, free-flow travel time was obtained by observing the travel time taken by a car to travel the road segment under study during the early morning hours at a speed not more than 30 kmph to replicate the free-flow driving characteristics of a bus (Reviewer 2).

6 Results

6.1 *Travel Time Reliability (RT) and Comparison of Reliabilities of Bus with Metro Railway*

The travel time reliability of the different modes is estimated using the expression mentioned in Eq. 1. The expression indicated the variation of the travel time of public buses from the average travel time of the bus. The higher the variation, the less will be the RT value and vice versa. Thus in this context, the higher the RT value, the more reliable is the mode. The RT value of the metro railway service has been set as the benchmark and is compared with the other modes, i.e. the different buses under study. The comparison of the reliability of different modes with that of the metro railway is done by estimating the ratio of the RT of different modes to that of the metro railway expressed in percentage. The average travel time and its deviation from the average are also tabulated in Table 2 along with the RT values. This provides an overview of the present condition of the public buses of the Kolkata region.

Table 2 shows that the average travel time of state government buses ranges from 40 to 45 min with a deviation of 6 to 7 min, which is comparable to the private minibus (Route D) which has an average travel time of 47 min with a deviation of 9 min. But the travel time of private bus (Route C) is maximum with a mean of 64 min and a deviation of 12 min. These are compared with the metro railway which has an average travel time of 23 min and a deviation of just 2 min. It is a typical characteristic of the government-run buses that it will maintain the travel time with minimum deviation from the average travel time. This increases the RT value and makes it more reliable. On the other hand, private buses because of their operating characteristics have a tendency to maximise the revenue earned from the passenger.

Table 2 Comparison of travel time reliability of different buses with that of the metro railway

Bus route	Average travel time, μ (min) ^a	Standard deviation, σ (min) ^a	Travel time reliability (RT)	Comparison of reliability of the studied bus routes w.r.t reliability of metro railway (in %)
Route A	44	6	7.33	63.8
Route B	42	7	6.00	52.2
Route C	64	12	5.33	46.4
Route D	47	9	5.20	45.4
Metro railway	23	2	11.50	100 ^b

^aThe values are rounded off to the next minute

^bThe RT value of metro railway is considered as benchmark and is assumed a value of 100%

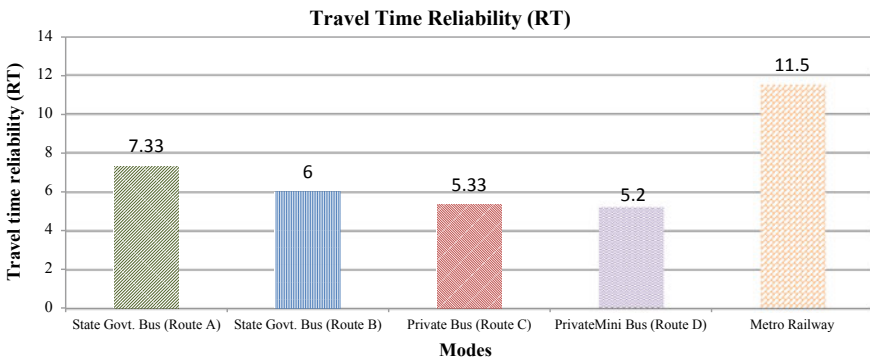


Fig. 2 Travel time reliability comparison among different modes

Due to this reason, the deviation from the average travel time is higher and the RT value decreases. Comparing the above results with the travel time reliability of the metro railway wherein it is found that the value of travel time reliability of Route A and Route B buses is more than 50% of the value of metro railway travel time reliability, whereas the same for Route C and Route D buses are less than 50%. The Travel Time Reliability (RT) values of the different modes have been demonstrated graphically in Fig. 2.

6.2 Travel Time Reliability Measure According to FHWA

The Federal Highway Administration developed some factors to measure the reliability of a particular mode in FHWA Report 2006. The results obtained by using Eqs. 2–5 are tabulated below. The 95th percentile travel time for each of the modes are obtained from cumulative frequency curves.

Table 3 Measure of travel time reliability parameters of different modes (by FHWA)

Mode	95th percentile travel time, $T_{95\%}$ (min)	Buffer time, T_B (min)	Buffer time index, B_i (%)	Planning time index, P_i (in %)	Planning time, P_t (min)
Route A	52	9	20.45	226.1	52
Route B	49	7	16.66	213.04	49
Route C	81	17	26.56	352.17	81
Route D	60	13	27.66	260.87	60
Metro railway	24	2	8.70	104.35	24

*Free-flow speed is observed to be 23 min

From Table 3, it is evident that the 95th percentile travel time of the government buses is around 50 min, whereas it is as high as 81 min for Route C which is the highest with respect to all other modes. The buffer time is the extra time which a commuter should include in his/her journey time so as to compensate any unexpected delay. A mode is said to be reliable if the buffer time is less. In this context, it is evident from Table 3 that the state government buses have a buffer time within 10 min, whereas the buffer time of 17 min for the Route C buses is quite high. The higher the value of planning time index indicates unreliable mode of transport, as a commuter has to include these extra time while planning their journey time. Once the journey time of passenger increases which finally forces the passengers to shift their mode, from this analysis, it is evident that buses of Route C are the most unreliable in nature and of Route B have the highest reliability.

6.3 Delay Measurement

Apart from these two types of measure of reliability, delay measurement can also be used to estimate the reliability. Deviations from the scheduled departure time and the delay in transit are the two broad categories in which the total delay can be classified. The in-transit delay can be classified as signal delay, bus stop delay, congestion delay and waiting delay. Referring to Table 4, it is clearly evident that the Route A has the maximum starting time delay which is followed by Route C. On the other hand, the delay in transit is maximum for Route C which is followed by the Route B. If the in-transit delay is compared to the total travel time of the different modes, it is observed that the transit delay of 29 and 15 min make up 30–45% of the total travel time for Route C, whereas the government buses have a transit delay within 20 min which comprises 25–40% of the total travel time.

The delays in transit are separately shown in the bar chart which compares the different delays for the different buses. The figure is shown (Fig. 3).

Due to heavy traffic movement during the peak hours, congestion on the road network in Kolkata is a major issue that deviates the actual travel time from the

Table 4 Comparison of the delays

Type of delays	Route A		Route B		Route C		Route D	
	min	%	min	%	min	%	min	%
Starting time delay from scheduled time	15	–	7	–	13	–	10	–
<i>Delay in transit</i>								
Signal delay	5	47	7	45	8	28	6	43
Bus stop delay	2	17	4	21	6	19	4	25
Congestion delay	3	28	5	28	11	39	4	26
Waiting delay	1	8	1	6	4	14	1	6
Total delay in transit and its share in total transit time	11	25	17	41	29	45	15	32

scheduled travel time. These congestions sometimes are created by the bus drivers himself due to unnecessarily waiting for the passengers not only at the scheduled stoppages but also in between the scheduled stoppages and sometimes the bus drivers willingly get on the congested side of the road. This driving behaviour is persistent in private buses of Route C more than the other buses. These influence the travel time to a great extent. The graph in Fig. 3 shows that all the delays for buses of Route A are less than all other buses in that route. On the other hand, buses of Route C have the maximum delays in transit among all the modes. Among all the types of delay, signal delay has the maximum share in all the modes which is followed by congestion delay. Observing all the results, it can be clearly stated that private buses of Route C have the least reliability among all the modes. The state government buses show better reliability among the buses.

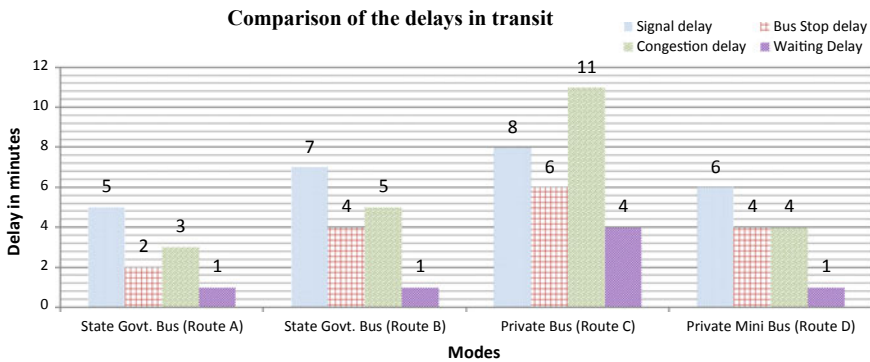


Fig. 3 Comparison of the delays in transit

6.4 Sensitivity Analysis

The analysis shows that the most reliable mode of public transport in this route is the metro railways. The buses have a very low reliability as compared to that of the metro railways. As metro railway has a separate right of way, the in-transit delay is negligible, whereas the buses face delay during the transit as it travels through a heterogeneous traffic stream. A sensitivity analysis was carried out to determine the effect of congestion delay and the waiting delay of the buses on its travel time reliability. Table 5 shows the RT using modified average travel time and standard deviation of buses if there was no congestion or waiting delay, i.e. zero minutes of congestion delay and waiting delay. The RT is compared with that of the metro railway.

Table 5 shows that the reliability of buses can be improved if the congestion and waiting delay can be minimised. The modified RT value of state government buses (RT of buses of Route A: 9.75 and RT of buses of Route B: 7.60) increased by one-third of the actual value. Buses of Route C have the maximum improvement of 66% which may be attributed to the fact that the delay of buses of Route C mostly comprises congestion delay and waiting delay and has a high impact on the overall travel time reliability. In case of Route D buses, the modified value increased to 6.83 which shows an improvement of 31% from the actual RT. In comparison to the metro railway, the RT of buses of Route B and Route C increased by almost 15%. On the other hand, buses of Route A increased by 21% and the maximum improvement of 30% occurred in buses of Route C.

Table 5 Effect of congestion and waiting delay on RT

Mode	Modified average travel time, μ (min)	Modified standard deviation, σ (min)	Travel time reliability (RT)			Comparison of RT of all the different modes under study with RT of metro railway (in %)		
			Actual	Modified	Improvement (%)	Actual	Modified	Improvement (%)
Route A	39	4	7.33	9.75	33	63.8	84.8	21
Route B	38	5	6.00	7.60	27	52.2	66	13.8
Route C	53	6	5.33	8.83	66	46.4	76.8	30.4
Route D	41	6	5.20	6.83	31	45.4	60	14.6
Metro railway			11.50			-		

7 Conclusion and Discussion

The present study is focused on the travel time reliability of public transport in Kolkata. The public transports included in this study are two state government buses, private bus, private minibus and metro railway all running along the same route. The reliability of all these modes is estimated using the method proposed by Liu and Sinha [15]. As per Liu and Sinha, the higher the RT value, the more reliable is the mode. The analysis showed that the RT value ranges from 5 to 7.5 which is low as compared to the RT of metro railway (11.50) as mentioned in Table 2.

The parameters developed by FHWA in the FHWA Report 2006 to measure the reliability were also used here to determine important reliability parameters like buffer time, buffer time index, planning time index and planning time (Table 3). A buffer time of more than 14 min was estimated for private bus and minibus and below 10 min for state government buses are quite high as compared to 2 min buffer time of metro railway. All these results showed that the public buses, especially the private bus (Route C), are having the least reliable service.

Finally, the delay measurement shows that the buses face a high signal and congestion delay during the peak hour. Figure 3 reveals the comparison of delay in transit for all the buses under study. From the figure, it is shown that all the types of delay are high for private bus (Route C). Sometimes, these delays are incurred intentionally by some bus drivers which is a common behaviour of many of the bus drivers. This delay increases the travel time of the buses which ultimately reveals the poor service reliability of the buses in Kolkata. The high unreliability of buses, in terms of travel time, is pushing commuters to choose private vehicles as their mode of transport which increases traffic volume and congestion on the road.

The sensitivity analysis shows that if the in-transit delay can be minimised when the reliability of the buses improves by more than 30% on an average with the private bus (Route C) having the maximum improvement (Table 5). It is of utmost importance to improve the reliability of the buses in order to restrict the shift of the mode choice to private vehicles. This will not only minimise the environmental degradation but also help to control and manage the traffic flow on the roadway networks more efficiently.

In this study, the main focus is on the public buses, but the metro railway is set as benchmark for comparison. Further research can be done by including other modes of transport like para-transit, etc. Moreover, only one route is selected as the case study route. This may be applied to other significant routes of Kolkata as well and compared with the present study.

References

1. Badani MG, Haider M (2007) An analysis of public bus transit performance in Indian cities. *Transp Res Part A* 961–981
2. Cantwell M, Caulfield B, OMahony M (2009) Examining the factors that impact public transport commuting satisfaction. *J Public Trans* 12(2)

3. Chalumuri RS, Errampalli M, Gangopadhyay S (2013) Analysis of travel time reliability of an urban corridor using micro simulation techniques. *Curr Sci* 105(3):2013
4. Chen X, Lei Yu, Zhang Y, Guo J (2009) Analysing urban bus service reliability at the stop, route and network levels. *Transp Res Part A* 43:722–734
5. Chien S, Liu X (2012) An investigation of measurement for travel time variability. In: Rahim AA (ed) *Intelligent transportation system*, In Tech. ISBN 978-953-51-0347-9
6. Diab E, El-Genedy AM (2013) Variation in bus transit service understanding the impacts of various improvement strategies on transit service reliability. *Public Trans Plann Oper* 4(3):209–231
7. Diana M (2012) Measuring the satisfaction of multimodal travellers for local transit services in different urban contexts. *Transp Res Part A* 46:1–11
8. Ebeling CE (1997) *An introduction to reliability and maintainability engineering*. McGraw-Hill
9. FHWA. Travel time reliability: making it there on time, all the time. www.ops.fhwa.dot.gov/publications/tt_reliability/TTR_Report.htm. Accessed 14 July 2007
10. Gopi P, Sachdeva SN, Bharati AK (2014) Evaluation of travel time reliability on urban arterial. *Int J Eng Res Technol*. 3(6). ISSN 2278-0181
11. Iseki H, Taylor BD, Miller M (2006) The effects of out-of vehicle on travel behaviour: implications for transit transfers. Institute of Transportation Studies
12. Kimpel TJ (2001) Time point-level analysis of transit service reliability and passenger demand. Portland State University
13. Laura CC (2006) Understanding bus service reliability: a practical frame work using AVL/APC data. Massachusetts Institute of Technology
14. Lin J, Peng W, Darold TB (2007) A quality control framework for bus schedule reliability. *Trans Res Part E*
15. Liu R, Sinha S (2007) Modelling urban bus service and passenger reliability. Institute for Transport Studies, University of Leeds, Leeds, UK
16. Lyman K, Bertini RL (2008) Using travel time reliability measures to improve regional transportation planning and operations. In: 87th annual meeting of the transportation research board, 13–17 January
17. Tony M (2013) Prioritizing public transit for speed, reliability and rider satisfaction. The German Marshall fund of the United States

Estimation of PCU and Saturation Flow at Signalised Intersection



Sabyasachi Biswas, Harjeet Prasad, Amit Jaiswal and Aditya Raj Gehlot

Abstract In homogeneous form of traffic, the vehicles in traffic are not so versatile and the vehicles move in dedicated lanes, whereas in countries such as India, the form of traffic is heterogeneous in nature where the traffic is very versatile with many combinations of vehicles which rarely move in dedicated lanes. The combinations make it harder to calculate the headway, PCU, etc. because every vehicle possesses a different shape and size. The lack of use of dedicated lanes makes it very tough to check which vehicle belongs to which queue and how it will move or accelerate. Hence, the methodology used for homogeneous traffic condition fails drastically when used in heterogeneous traffic conditions. The recent researches based on heterogeneous form of traffic do not present us with a reliable methodology to compute or calculate the saturation flow in heterogeneous traffic condition. This makes it difficult to design and plan the working of intersections because the traffic almost always tends to move differently than the calculated outcome. The current research is primarily focused on the development of a reliable methodology which can present us with a more accurate saturation flow traffic data, i.e. intersection capacity in heterogeneous traffic conditions. In the clearance method, different factors such as effective turning radius, projected area of the vehicles, etc. are required for the calculation of saturation flow. In velocity method, during a traffic jam all the vehicles are almost at the same speed so the PCU deviates from its actual value making all PCU values of different vehicles almost the same. In India, we have heterogeneous type of conditions not homogeneous and also the lane discipline is not followed. In this clearance method,

S. Biswas (✉)
NIT Jamshedpur, Jamshedpur, India
e-mail: sabyasachibiswas01@gmail.com

H. Prasad · A. Jaiswal · A. R. Gehlot
Amity University, Noida, India
e-mail: prasadharjeet52@gmail.com

A. Jaiswal
e-mail: aditya.raj.gehlot@gmail.com

A. R. Gehlot
e-mail: amit.jaiswal1995@gmail.com

the study considers only a particular type of vehicle at an instance and we have to determine the clearance time it requires, i.e. the time it takes from curb line to front curb line.

Keywords Saturation flow · PCU · Homogeneous traffic · Clearance time method

1 Introduction

Intersection is an area defined as a cross section where two or more junctions of roads meet. Intersection can be signalised or manually controlled depending upon the density of traffic. The conflicts arising from movements of traffic flow or the saturation flow from different orders are managed by time-sharing rule (i.e. fixed time and automated time). There are two main types of intersection of roads, namely, grade-separated intersections and at-grade intersections.

Main function of the intersection is to guide vehicles to their respective directions with safe traffic environment (i.e. avoid number of conflicts). Traffic intersections can be in complex locations on any highway. Overall traffic flow depends on the performance in terms of level of service (LOS) and the saturation flow of the intersections. Therefore, quantification of the saturation flow is a vital aspect for the traffic engineers especially in the case of heterogeneous traffic scenario. It is one of the most important features in evaluating the capacity of a signalised intersection. Saturation flow will be affected by several geometric, traffic, operating and other parameters. There are several methods available in literature to estimate saturation flow (SF) of an intersection. Among them, the U.S. [1] and U.K. [2] methods are the most popular. Indian code of practice (IRC:SP 41, 1994) [3] advocates use of U.K. method to determine saturation flow at a signal control intersection. In addition, several researchers [4–6] have reported that SF is influenced by many factors of geometry, traffic and control. The extent of influence depends on the driving culture and hence is different in different countries. It will be worthwhile to study the effect of individual or a group of parameters on saturation flow for Indian conditions. In the circumstance, the current research was taken up with the following objectives to evaluate Passenger Car Unit (PCU) for various categories of vehicles at signalised intersections and thereby to observe the influence of intersection geometry on PCU factors and saturation flow. Further, this study identifies the effect of proportion of heavy vehicles on saturation flow of through movements.

2 Methodology

This portion of the study explains the methodology that has been adopted to collect and extract the data in the present study. The method of analysing the data is also given here.

Identification of the study areas and intersections was very important before starting the field study. Study area should be located in urban or suburban area and signalised intersections must be available there. The requirement criteria were considered to select an intersection based on the suggestions by previous researchers [7–9].

2.1 Data Collection and Extraction

This study comprises two categories of data: geometric data and traffic data. The geometric data of the intersections were collected manually. The traffic data were collected using videography from a reasonable height so as to cover all arms of an intersection in a single frame or at least two mutually perpendicular legs of the intersection.

Four intersections locations are selected as per the criteria, and data were collected by using videography. All the four intersections had four arms with varying approach width and right turning is allowed at all the approaches in all intersections.

2.1.1 Layouts of the Intersections

Details of the selected intersections are given below.

Four intersections are located between Sector-16 and 18, 4 and 9; 19 and 20 of Noida and Lodhi road. Figure 1 shows the layout of the four-lag intersections with geometric details.

The field data were collected for about 2 h during peak period, and the recorded video was played on a monitor in traffic engineering laboratory by using video player. A simple software to display to stopwatch on the screen was used. The stopwatch has an accuracy of 0.01 s which was very useful to record the accurate clearing time of the vehicle (t_i , t_c). The following information were extracted from the recorded films of the intersections.

1. Total period of saturation flow in a green phase for the movement under consideration.
2. Classified volume count of vehicles discharging from the approach in the intersection during the saturated period of green.
3. Clearance time taken by individual vehicle to move from stop line to stop line (i.e. clearing time of a vehicle).

For the further analysis, all vehicles were categorised into seven groups as shown in Table 1. Out of four intersections, cycle rickshaws and bicycles were found in considerable proportion at the intersection 1 only. At remaining four intersections, the non-motorised traffic was very marginal and therefore was not considered for the analysis at these intersections.

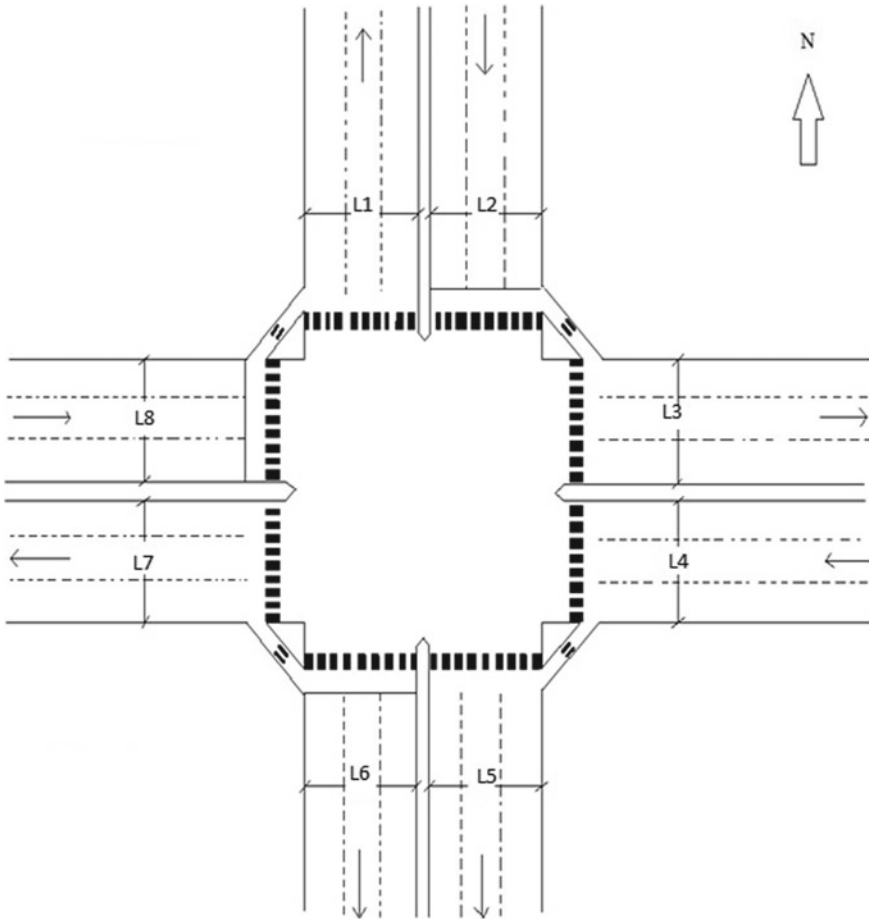


Fig. 1 Layout of four-lag intersections

Table 1 Detailed description of classification of vehicles in Indian road condition [10]

Vehicle type	Notation	Projected length (m)	Projected width (m)	Projected rectangular area (m ²)
Small car	C	3.61	1.44	5.20
Big car	BC	4.48	1.80	8.06
Three wheeler	3W	3.2	1.40	4.48
Motorcycle	2W	1.87	0.64	1.20
Bus	HV	10.1	2.43	24.54

2.2 Method for Calculation of Passenger Car Unit (PCU)

Under the heterogeneous traffic circumstances, Passenger Car Equivalent (PCE) or Passenger Car Unit (PCU) is the most commonly used factor for converting heterogeneous traffic into its equivalent homogeneous.

PCU of a vehicle type is an traffic equivalent factor that depends on geometric factors of the intersection approach, traffic and operating factors of a stream. PCU of a vehicle type has been calculated in the present study by using Eq. 1 [11]

$$PCU_i = \frac{V_c / V_i}{A_c / A_i} = \frac{t_i / t_c}{A_c / A_i} \quad (1)$$

where

PCU_i Passenger car unit of i-type of vehicle,
 V_c intersection clearing speed of standard car,
 V_i intersection clearing speed of vehicle type-i,
 t_c intersection clearing time for standard car,
 t_i intersection clearing time for i-type of vehicle and
 A_c, A_i projected area of standard car and i-type of vehicle, respectively.

In India, most of the road users do not bother about lane discipline; therefore, most of the drivers do not move in designated lanes. Although the lanes are marked for cars and buses, these lanes can conveniently accommodate more than one small-sized vehicle at a time. Consequently, unoccupied lateral lane width is generally used by two wheelers, three wheelers and other small-sized vehicles. So Eq. 1 is used to estimate the PCU of a respective vehicle category as it considers the total static area of the vehicle, and not length alone.

2.3 Estimation of Saturation Flow

Saturation flow of a signalised controlled intersection is measured as the total number of vehicles that would cross the stop line by utilising the green signal time (i.e. all the vehicles are effectively utilised the green time allotted to them). It is expressed in terms of vehicles per hour of green [1]. Saturation flow rate for each approach had been computed by using Eq. 2 [5, 9, 12]:

$$SF = \left[\sum n_i PCU_i \right] \frac{3600}{g_s} \quad (2)$$

where

SF saturation flow (pcuphg),
 n_i number of classified vehicle, i.e. i-type of vehicles,

PCU_i PCU value of individual vehicle category, i.e. i-type, and
 g_s effectively utilised green time, i.e. saturated green period at a signalised intersection.

3 Results and Discussion

3.1 Estimation of PCU Factors

PCU factors for each category of vehicles as given in Table 2 were determined using Eq. 1. Since PCU for a vehicle depends on clearing speed of the vehicles, these factors were determined for through and right-turning movements separately. Clearing time of a vehicle type was noted in each cycle during saturation flow, and PCU values were calculated. Tables 2 and 3 provide average PCU values for various categories of vehicles at different intersections for through and right-turning movements, respectively.

It is observed that the PCU values vary from one approach to another. It is due to the variation in effective width of the approach for through traffic and variation in turning radius for right-turning movements.

Table 2 PCU factors for through movements

Intersection number	Name of the intersection	Approach considered	Effective approach width	No. of cycles	Average PCU value			
					Big car	Three wheeler	Two wheeler	Heavy vehicle
I 3	Noida intersection-3	NB	4.50	22	1.478	0.946	0.221	4.920
I 3	Noida intersection-3	SB	5.20	20	1.492	0.820	0.193	5.126
I 4	Lodhi road	NB	6.10	29	1.480	0.929	0.217	4.677
I 4	Lodhi road	SB	6.50	29	1.495	0.920	0.224	4.815
I 1	Noida intersection-1	NB	7.70	22	1.566	0.969	0.205	5.631
I 2	Noida intersection-2	SB	8.90	23	1.555	0.941	0.238	5.900
I 3	Noida intersection-3	EB	9.00	23	1.542	1.003	0.241	6.366
I 3	Noida intersection-3	WB	9.00	20	1.570	0.923	0.225	5.620
I 4	Zakir chowk	EB	9.00	29	1.574	0.919	0.241	5.049
I 1	Noida intersection-1	SB	9.70	23	1.550	1.050	0.231	5.692

Table 3 PCU factors for right-turning vehicles

Intersection number	Name of the intersection	Approach considered	Effective approach width (m)	Radius of right turn (m)	Number of cycles	Average PCU value			
						Big car	Three wheeler	Two wheeler	Heavy vehicle
I 3	Noida intersection-3	SB	3.56	13.89	21	1.558	0.810	0.183	6.850
I 3	Noida intersection-3	EB	7.5	15.01	19	1.472	0.816	0.178	5.795
I 1	Noida intersection-1	WB	4.46	16.11	18	1.533	0.812	0.212	6.051
I 1	Noida intersection-1	NB	2.5	18.23	16	1.500	0.843	0.204	7.011
I 4	Lodhi road	WB	5.12	18.39	18	1.620	0.817	0.178	6.741
I 1	Noida intersection-1	EB	2.5	25.80	18	1.833	0.821	0.212	-
I 4	Lodhi road	NB	3.19	29.51	20	1.792	0.825	0.214	7.150

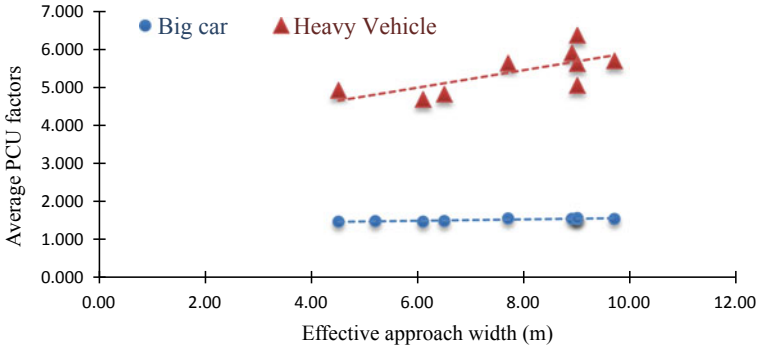


Fig. 2 Variation of average PCU factors with approach width for big car and heavy vehicle

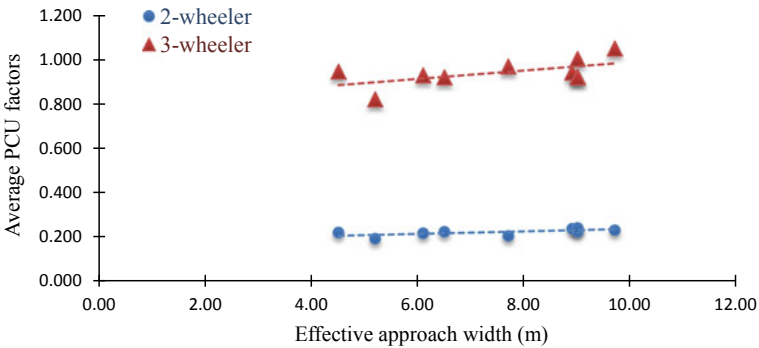


Fig. 3 Variation of average PCU factors with approach width for two wheelers and three wheelers

Figures 2 and 3 show the influence of approach width on PCUs for through moving vehicles. Further, it is observed that PCU value of the vehicles increases linearly with approach width. It is due to the availability of more freedom to drivers on wider approach road. Figures 4 and 5 show the impact of turning radius on PCU values of right-turning vehicles. PCU of a right-turning vehicle increases linearly with turning radius. This trend is expected as the radius of right turn increases, and ease of movement becomes more. It results in more speed differential among vehicles, and therefore, PCU for a vehicle type increases.

3.2 Analysis of Saturation Flow for Through Movement

The PCU values yielded for each type of vehicle in every cycle of saturation flow were used to transform the mixed traffic flow into equivalent number of PCUs, and then flow was converted to hourly saturation flow values. Average saturation flow of all cycles in an approach was calculated. The effective approach width for through

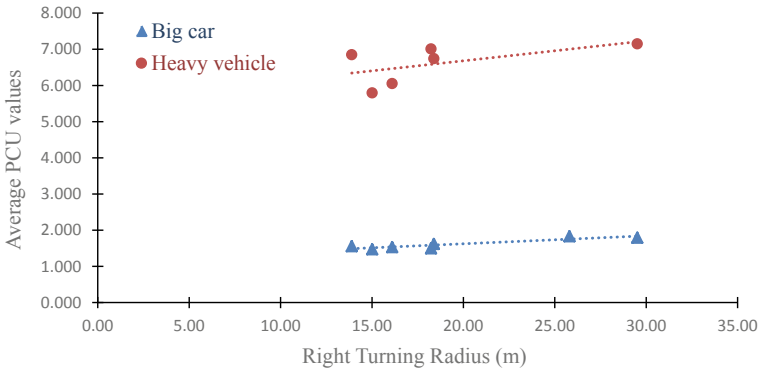


Fig. 4 Variation of average PCU factors with turning radius for big car and heavy vehicle

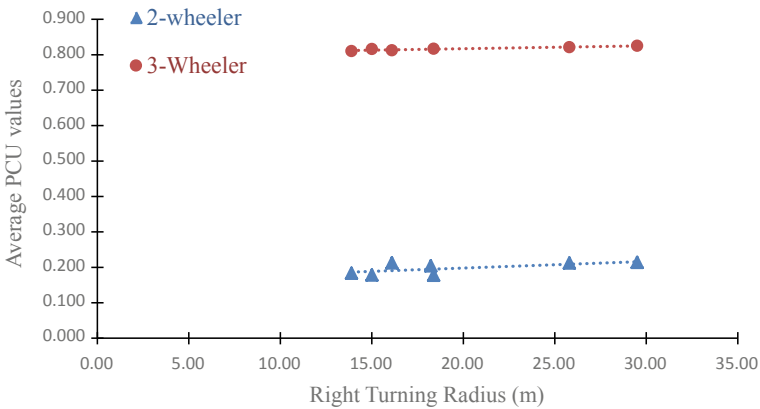


Fig. 5 Variation of average PCU factors with turning radius for three wheelers and two wheelers

traffic was taken in the same ratio as the proportion of through traffic in the approach. Results are given in Table 4. Plot between saturation flow and effective approach width is shown in Fig. 6. Second-degree polynomial curve was found as the best fit for the data points and the expression is given below:

$$\text{Saturation flow, } SF = 51.357 * W^2 - 139.11 * W + 2224.2 \text{ PCU/h of green} \quad (R^2 = 0.79) \tag{3}$$

where W is the effective approach width for through movement in metres. The average saturation flow per lane width of all intersection approaches was 1960 PCU/h of green, and it is around 3.16% higher than 1900 PCUs per hour of green proposed in HCM 2010. It might be due to heterogeneity in the traffic, poor lane discipline followed by the vehicle users and small car being taken as standard vehicle for calculating PCUs of remaining categories of vehicles.

Table 4 Variation in saturation flow of different approaches with approach width

Intersection no.	Intersection name	Approach considered	Approach volume (vph)	Effective through width (m)	Saturation flow pcuphg
3	Noida intersection-3	NB	930	4.50	2960
3	Noida intersection-3	SB	936	5.20	2697
4	Lodhi road	NB	720	6.10	2975
4	Lodhi road	SB	734	6.50	3078
1	Noida intersection-1	NB	2110	7.70	5098
2	Noida intersection-2	SB	3290	8.90	6015
3	Noida intersection-3	EB	1858	9.00	4610
3	Noida intersection-3	WB	1416	9.00	4473
4	Lodhi road	EB	2668	9.00	5006
1	Noida intersection-1	SB	2728	9.70	5753

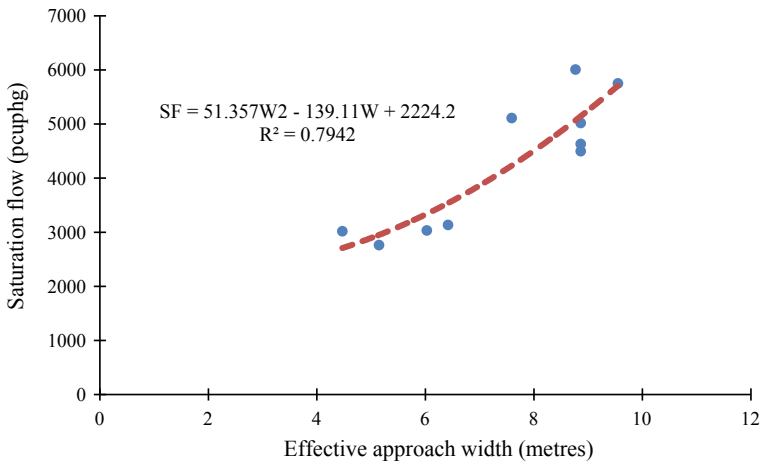


Fig. 6 Variation of saturation flow with effective approach width

4 Conclusion

Traffic data were collected at four intersections having different approach widths. Saturation flow was estimated for through movements and right-turning movements separately, and results are presented and discussed in the paper. Present study proposed a new method to yield the saturation values at signalised intersection by clearance method. The proposed method minimises the variance in the saturation flow for each cycle at a signalised intersection. PCU values were determined for each type of vehicles separately. PCU values obtained from this method were found comparatively better than the PCU values obtained from other methods. This study later

estimated saturation flow values in most of the approaches, whose estimate has been carried out based on all PCU values by clearance method. It was observed that PCU values for through moving vehicles increase linearly with effective approach width and PCU values for right-turning vehicles increase linearly with the radius of right turn. Further, the saturation flow of an approach increases with its effective approach width, and a model is proposed to measure the effect of approach width on saturation flow. In addition, saturation flow for through movements is found to increase with the presence of heavy vehicles in the approach.

References

1. TRB (2010) Highway capacity manual, 5th edn. Transportation research record. Transportation Research Board, National Academy, D.C.
2. Transport and Road Research Laboratory (1963) A method of measuring saturation flow at traffic signals. London, U.K
3. Indian Roads Congress (1994) Guidelines for the design of at grade intersections in rural and urban areas. IRC Code Pract. SP41
4. Hossain M (2001) Estimation of saturation flow at signalised intersections of developing cities: a micro-simulation modelling approach. *Transp Res Part A Policy Pract* 35:123–141. [https://doi.org/10.1016/s0965-8564\(99\)00050-6](https://doi.org/10.1016/s0965-8564(99)00050-6)
5. Hadiuzzaman M, Rahman M, Karim MA (2008) Saturation flow model at signalized intersection for non-lane based traffic. *Can J Transp* 2
6. Rahman M, Nur-Ud-Deen S, Hassan T (2005) Comparison of saturation flow rate at signalized intersections in Yokohama and Dhaka. *Proc East Asia Soc Transp Stud* 5:959–966
7. Bonneson J, Nevers B, Zegeer J, et al (2005) Guidelines for quantifying the influence of area type and other factors on saturation flow rate. Texas
8. Gates TJ, Noyce D (2010) Dilemma zone driver behavior as a function of vehicle type, time of day, and platooning. *Transp Res Rec J Transp Res Board* 2149:84–93. <https://doi.org/10.3141/2149-10>
9. Biswas S, Chakraborty S, Ghosh I, Chandra S (2018) Saturation flow model for signalized intersection under mixed traffic condition. *Transp Res Rec* 0361198118777407. <https://doi.org/10.1177/0361198118777407>
10. Biswas S, Ghosh I (2018) Modeling of the drivers' decision-making behavior during yellow phase. <https://doi.org/10.1007/s12205-018-0666-6>
11. Chandra S, Kumar U (2003) Effect of lane width on capacity under mixed traffic conditions in India. *J Transp Eng* 129:155–160. [https://doi.org/10.1061/\(asce\)0733-947x\(2003\)129:2\(155\)](https://doi.org/10.1061/(asce)0733-947x(2003)129:2(155))
12. Biswas S, Ghosh I, Chandra S (2017) Influence of signal countdown timer on efficiency and safety at signalized intersections. *Can J Civ Eng* 44:308–318. <https://doi.org/10.1139/cjce-2016-0267>

Travel Behavior of Agartala City, India Using Panel Data



Amitabha Acharjee and Partha Pratim Sarkar

Abstract This study analyzes the change in mobility pattern and their psychological effect on dynamic travel behavior. 3,416 respondents' data have been collected from the Agartala city randomly to understand the travel behavior of two different panels. More specifically, from the data, it can be observed that motorized two wheelers (MTW) ownership, car ownership, and nonmotorized transport were increasing from the last 5 years. The influences of attitudes along with socioeconomic parameters such as monthly cluster income, motorized two wheeler ownerships (MTW), non-motorized ownerships (NMT), employment type were used for modeling. Structural equation modeling has been used to analyze the travel behavior. Results show that the change of travel decision varies with income. From the analysis of latent variables such as comfort, flexibility, reliability, and safety associated with modes such as car, motorized two wheeler, nonmotorized transport was found to be significant with cluster income over the change of time. Also from the data, it can be seen that there was an increase in the use of NMT modes even when infrastructure was not favorable; and with improvement in infrastructure, there is a good probability to increase the mode share of NMT modes across all income level.

Keywords Psychological · Habit · Car ownership · Two wheeler ownership (MTW) · Bicycle ownership (NMT) · Flexibility · Safety · Comfort · Reliability

1 Introduction

Rapid urbanization, shifting behavior of vehicle especially nonmotorized to motorization, and the change of economy are leading to decline urban transportation systems substantial in many developing countries like in South Asia [18]. Because of limited resource, the restricted and imperfect way of implementing system capacity and the inequality between demand and supply is increasing further [19]. As a result,

A. Acharjee (✉) · P. P. Sarkar
Department of Civil Engineering, National Institute of Technology, Agartala, Tripura, India
e-mail: amitabhaacharjee1990@gmail.com

© Springer Nature Singapore Pte Ltd. 2019
S. Pulugurtha et al. (eds.), *Advances in Transportation Engineering*,
Lecture Notes in Civil Engineering 34,
https://doi.org/10.1007/978-981-13-7162-2_5

many cities are facing problems of increased suburbanization and congestion and also decrease the safety of human mobility [19].

Because of these changes, the specific human mobility characteristics need to be studied broadly [14]. For making a good urban planning strategy, it is essential to study the dynamic travel behavior in developing countries. This paper carried out an extensive study of human behavior on mobility characteristics of two panels in Agartala city, India. Mode choice behavior generally consists of individual's attitudes, subjective norms, and perception of travel behavior [4]. Psychological effect on the choice of different modes is an important factor which was considered in this study. A person who uses the bus for work trip may not reflect the habits of bus choice for the very next day. Choice of mode of the past and the present panel of data may not depend on their habits but also on their socioeconomic factors [2, 5, 6]. But it is true that past behavior could contribute to the predictions of present behavior. The hypotheses proposed on social norms [15], anticipated regret [20], and self-identity [7, 8] were found to affect the travel behavior. Some authors [8–10, 12, 13] carried out a longitudinal study to investigate the effect of new bus service among the college students in Germany. They observed that attitude and subjective norms are important factors for the choice of bus mode.

To test the habit and psychological factors, we studied some frequency performance parameters to analyze the variation of travel behavior. The parameters were generally used to identify travel behavior on mode choice based on number of trips per person per day, travel time per trip, travel distance per trip, and passenger kilometers of travel (PKT) [11, 26, 27]. Temporal variabilities of car use and the car ownership were also important factors for understanding the habit process in mode choice [21]. Attitudes and perceptions of different modes were also reported to affect travel behavior [16, 25, 28]. Some of the author [17] adopted Markov models to analyze the changes in the activity and travel patterns over time in the Puget sound transportation panel. One-way analysis of variance ANOVA was carried out to investigate the three different panel data like stayers, dropouts, and refresher. The same panel data were used by Sunkanapalli et al. [26] and carried out a dynamic analysis of traveler's attitudes and perceptions. They found that bus mode was declining more than the automobile mode. This outlined the use of association rules to identify patterns in activity [14].

2 Study Area Description

Data have been collected in Agartala city to understand the effect of dynamic travel behavior. Agartala city is the second largest city based on population and municipality area in northeastern part of India, after Guwahati. Municipality area is divided into 49 wards (Fig. 1).

According to census data 2011, the population of Agartala was 5,22,613 with male population of 2,66,103 and female population of 2,56,864 and having a total municipal area of 76.51 km² [3, 22, 23].

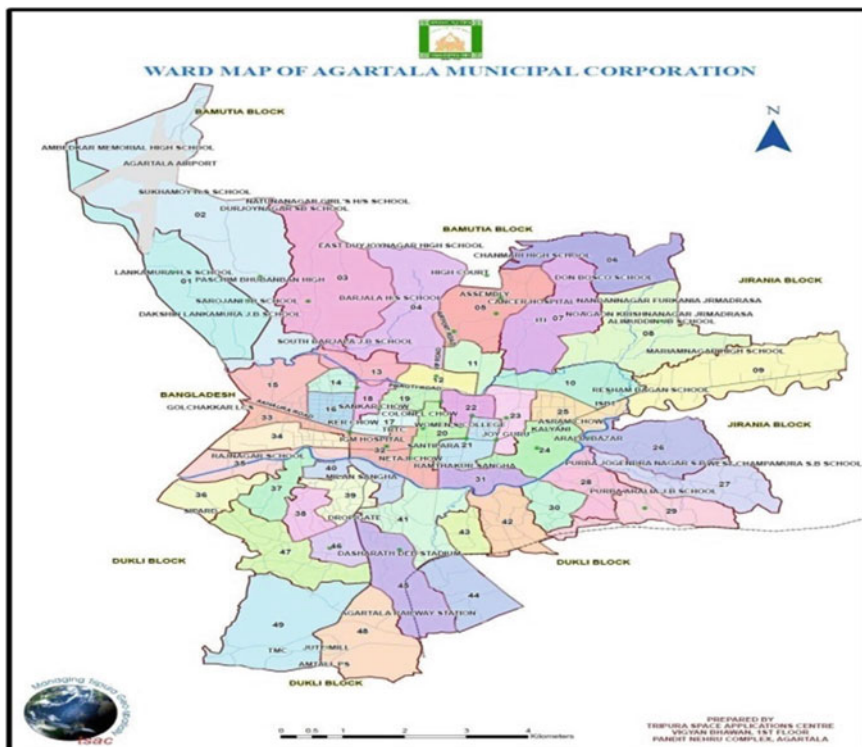


Fig. 1 Location of the study area (Agartala)

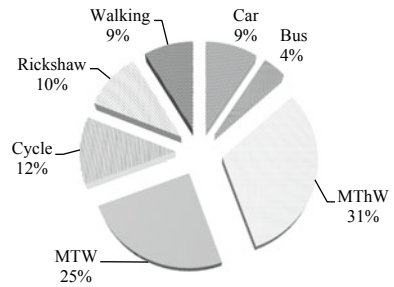
Table 1 shows different percentages of vehicle ownership between two panel data, in which one panel is retrospective in nature. It is observed that motorized vehicle increased very abruptly compared to the nonmotorized vehicle. Data indicate that a number of students slightly reduced in current scenario. Data were categorized into three education qualifications such as graduate, higher secondary level, and secondary school certificate (SSC) level. It is observed that the large percentages of people are educated up to SSC level. In work-related trips, 75% of people traveled between 0 and 1 km at the last end of the panel data in 2012.

People are more interest to walk compared to motorized and nonmotorized vehicle when the travel distance is less. Apart from walking, people use more NMT and motorized three wheeler (MThW) vehicle. Figure 2 shows the mode used for work trips. It can observe that MThW use is 31% and MTW is 25%. Mode shares of buses and car are less commute mode compared to the other modes. The share of bicycle and walking are almost equal.

Table 1 Comparison of two panel data

	At present (value in percentage)	5 years back (value in percentage)
<i>Vehicle ownership</i>		
Car ownership	11	7
Motorized two wheeler	43	28
Nonmotorized mode	20	7
<i>License driver in a family</i>		
Four wheeler vehicle	7	4
Two wheeler vehicle	35	25
Both four and two wheeler vehicles	6	3
No vehicle	56	40
<i>Education qualification</i>		
Up to SSC	79	48
Class 12	8	4
Graduate	50	35
<i>Distance of work trip (km)</i>		
0–1	75	65
2–5	40	30
6–10	30	25
11–20	22	12
Above 20	10	7

Fig. 2 Mode use for work trip



In Table 2, the statistics of socioeconomic characteristics like age, gender, household income, vehicle ownership, and driving license status of commuter are presented. These data are useful in examining the variability of socioeconomic information, which could be useful in the formulation of the Dynamic model.

Table 2 Summary of socioeconomic data acquired for the study

Socioeconomic characteristic	Value in percentage
<i>Gender</i>	
Male	73.38
Female	26.62
<i>% of individual age</i>	
Up to 19	3.95
20–29	17.69
30–39	18.53
40–49	24.08
50–59	22.77
>60	12.98
License	49.5
Not having license	50.5
<i>% of individuals (years of education)</i>	
0	0.19
1–5	4.05
5–8	9.13
8–10	20.51
11–12	15.62
16–18	17.31
19–21	0.00
More	0.19
Car ownership	13.83
MTW ownership	44.21
<i>Household income (monthly)</i>	
0–2000	0.03
2001–10,000	30.86
10,000–20,000	25.55
20,000–50,000	31.37
>50,000	12.15

3 Methodology

More precisely, structural equation modeling (SEM) is a general modeling framework that integrated a number of different multivariate techniques into the overall framework. It is a framework which draws on a number of different disciplines. In this study, structural equation modeling has been applied to reveal the causal relationship between sociodemographics and latent attitudinal factors of the two different waves. Confirmatory factor analysis was one of the suitable processes to understand

Table 3 Average perception rating for different modes

Statement of attribute	Car	Bus	MTW	NMT
Comfortable journey	4.06	3.80	3.72	2.48
Comfortable seats	3.76	3.98	3.68	2.6
Very easy accessibility	3.69	2.90	3.89	2.71
Quickly accessible mode	3.91	2.78	3.89	2.49
Travel time prior to trip is known	3.89	3.22	3.91	2.29
Safety (accident)	3.83	4.20	3.22	2.14
Safety (theft)	3.91	3.70	3.68	1.97
Safety (weather)	3.88	4.00	2.2	1.8
Ability to make more trips	3.85	2.90	3.68	3.85
Can travel in a same vehicle	3.94	2.70	3.92	3.95

the travel analysis. Confirmatory factor analysis is a process by which judgment regarding the structure and content of the factors was applied and then the statistical results for these established factors were estimated. Confirmatory factor analysis (CFA) produces many goodness-of-fit measures to evaluate the model. Therefore, CFA using AMOS was carried out in this study area.

A general SEM model can be written as

$$Y = \alpha + \beta y + \Gamma x + \xi \quad (1)$$

where “X” represent the independent variables, “Y” represent the dependent variables, “ α ” is a intercept term, “ β ” is a square matrix of the direct relationship between the dependent variables, “ Γ ” is a square matrix of coefficients from independent to dependent variables, and “ ξ ” is a column vector of errors.

Table 3 gives the mean perception rating of different modes. From Table 3, it can be seen that people generally prefer car for their comfort as well as safety. In case of flexibility, people experience MTW to be more flexible mode compared to the other modes.

4 Model Formation and Result

The study has verified the hypothesis that perception of individuals influences mode choice with respect to the level of income. The contribution of this study with respect to 5 years back responses about income in the consideration of heterogeneity in individual choice, especially comparing the attributes of individual mode choice characteristic. This study also highlights the reason for shifting of mode for 5 years back to the current scenarios. Table 4 is estimated using all two waves of the panel data carried out in Agartala city. Statistically, significance of latent variable is included in

the model. Structural equation model is used to correlate the 5-year socioeconomic panel along with their cluster income. From the model, it is clearly observed that motorized and nonmotorized transportation mode increased from the last 5 years and also observed the shifting behavior of the mode from last 5 years. Model also suggests that high-income person are likely to use a car, and low-income person are likely to use bicycle (NMT) mode. The reason behind the use of car is comfort, flexible, reliable, and safe. All the three alternative comforts are measured in terms of journey, reliability measured in terms of easy to access, flexibility measured in terms of ability of trip, and safety is measured with accident. The latent factor of MTW ownership such as comfort of MTW, reliability of MTW, safety of MTW, and flexibility of MTW modes are correlated with medium-income person. Flexibility, comfort, and reliability of motorized two wheeler ownerships are positively correlated but the safety of MTW is negatively correlated. It seems that the causes of accident by MTW vehicles are more comparing to other two modes. Similarly, the four latent variables such as flexibility, comfort, reliability, and safety are correlated with NMT with respect to low income. Low-income people are feeling that motorized vehicles have the ability to make more trips in a short time. Estimated results show good model fit. The values of RMSEA and GFI values are 0.015 and 0.97, respectively, which is in the range of good model fit [1] (Fig. 3).

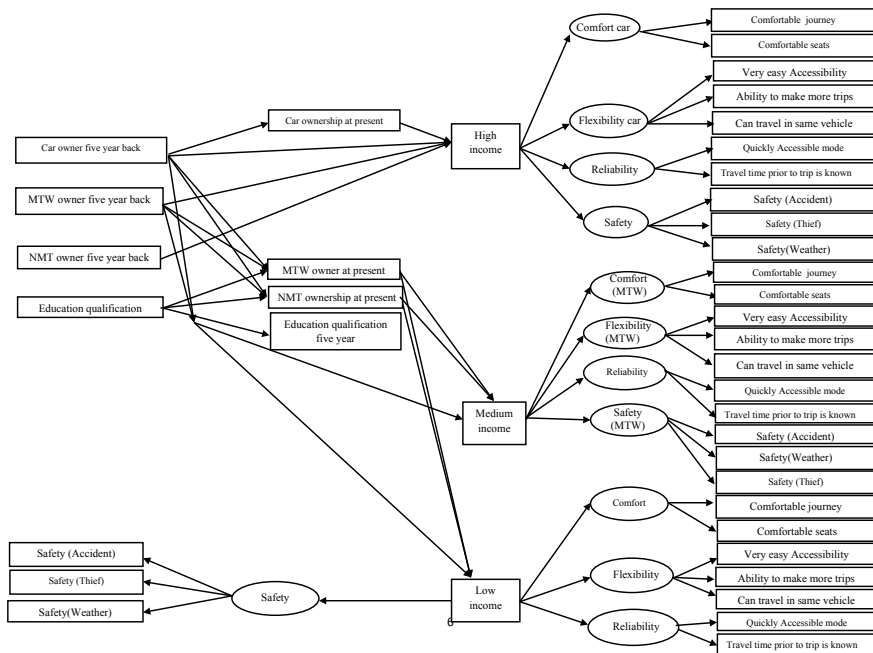


Fig. 3 Schematic diagram

Table 4 Results of two panels of car, MTW, and NMT travel mode

Latent construct	Path		Estimate	P-value
Education qualification	←	Education qualification five	1.192	0.001
NMT ownership	←	NMT 5 years	1.776	0.001
Car ownership	←	Car ownership 5 years	1.14	0.002
MTW ownership	←	MTW 5 years back	1.49	0.01
NMT ownership	←	MTW 5 years back	2.054	0.01
NMT ownership	←	Car ownership 5 years	1.102	0.01
MTW ownership	←	Car ownership 5 years	2.193	0.01
NMT ownership	←	Education qualification	-1.3	0.003
Car ownership	←	Education qualification	2.002	0.05
MTW ownership	←	Education qualification	2.02	0.01
High income	←	Car ownership	1.97	0.03
Low income	←	MTW ownership	-1.18	0.04
Medium income	←	MTW ownership	2.639	0.05
High income	←	MTW ownership	2.009	0.02
Medium income	←	NMT ownership	-1.15	0.01
Low income	←	Car ownership 5 years	-1.05	0.01
High income	←	Car ownership 5 years	1.002	0.01
Medium income	←	Car ownership 5 years	-1.27	0.03
Low income	←	MTW 5 years back	-3.086	0.04
Medium income	←	MTW 5 years back	3.05	0.01
High income	←	MTW 5 years back	2.01	0.00
Low income	←	NMT 5 years	1.172	0.01
Medium income	←	NMT 5 years	2.069	0.01
High income	←	NMT 5 years	-1.07	0.00
High income	←	NMT ownership	-3.08	0.002
Medium income	←	Car ownership	1.51	0.06
Low income	←	NMT ownership	1.13	0.07
License 5 years	←	Car ownership	1.248	0.05
Comfort (MTW)	←	MTW 5 years back	-1.03	0.02
Comfort (NMT)	←	Low income	2.383	0.04
Reliability (NMT)	←	Low income	1.184	0.03
Flexibility (NMT)	←	Low income	2.214	0.05
Safety (NMT)	←	Low income	1.002	0.02
Safety (MTW)	←	Medium income	-2.14	0.02
Comfort (MTW)	←	Medium income	1.319	0.03
Reliability (NMT)	←	Medium income	2.066	0.01
Flexibility (MTW)	←	Medium income	1.124	0.02
Flexibility (NMT)	←	High income	-2.24	0.01

(continued)

Table 4 (continued)

Latent construct	Path		Estimate	P-value
Comfort car ownership	←	High income	1.046	0.04
Safety car ownership	←	High income	1.071	0.04
Reliability car ownership	←	High income	2.061	0.01
Comfortable in journey (MTW)	←	Comfort (MTW)	1	
Very easy accessibility (MTW)	←	Reliability (MTW)	1	
Can exactly travel time prior to trip is known (MTW)	←	Reliability (MTW)	1.986	0.05
Very easy accessibility (MTW)	←	Flexibility (MTW)	1	
Can travel in a same vehicle (MTW)	←	Flexibility (MTW)	2.844	0.04
Ability to make more trips (MTW)	←	Flexibility (MTW)	3.499	0.01
Safety (weather) (MTW)	←	Safety (MTW)	1	
Safety (theft) (MTW)	←	Safety (MTW)	2.381	0.03
Safety (accident) (MTW)	←	Safety (MTW)	1.855	0.08
Comfortable seats (car)	←	Comfort (car)	1	
Comfortable in journey (car)	←	Comfort (car)	1.699	0.01
Can exactly travel time prior to trip is known (car)	←	Reliability (car)	1	
Very easy accessibility (car)	←	Reliability (car)	2.225	0.00
Very easy accessibility (car)	←	Flexibility (car)	1	
Can travel in a same vehicle (car)	←	Flexibility (car)	-1.06	0.04
Ability to make more trips (car)	←	Flexibility (car)	-1.29	0.05
Safety (weather) (car)	←	Safety (car)	1	
Safety (theft) (car)	←	Safety (car)	-1.54	0.04
Safety (accident) (car)	←	Safety (car)	1.73	0.09
Comfortable seats (NMT)	←	Comfort (NMT)	1	
Comfortable in journey (NMT)	←	Comfort (NMT)	1.676	0.03
Can exactly travel time prior to trip is known (NMT)	←	Reliability (NMT)	1	
Very easy accessibility (NMT)	←	Reliability (NMT)	1.86	0.05
Very easy accessibility (NMT)	←	Flexibility (NMT)	1	
Can travel in the same vehicle (NMT)	←	Flexibility (NMT)	-1.64	0.03
Ability to make more trips (NMT)	←	Flexibility (NMT)	-1.87	0.06
Safety (weather) (NMT)	←	Safety (NMT)	1	
Safety (accident) (NMT)	←	Safety (NMT)	2.637	0.03
Goodness of model fit		RMSEA	0.015	
		GFI	0.97	

5 Conclusion

In this paper, we have explored several latent variables related to the physiological parameter along with the socioeconomic and demographic parameters of two panel waves. From the analysis of latent variables such as comfort, flexibility, reliability, and safety associated with modes such as car, MTW and NMT are significant with income. It is observed that higher income people are choosing a car as it provides comfort, safety, reliability, and flexibility. In case of medium income, people are choosing MTW for comfort, reliability, and flexibility but not as a safe mode. If we talk about the NMT mode, lower income persons are choosing NMT mode as a comfortable, reliable, and safe mode but not as a flexible mode. It is observed from the two waves (2007 and 2012) of the similar household data that Agartala city with its thousands of nonmotorized users has a huge potential to become a state with major share of nonmotorized user in India. From the structural equation model, ownership of a car and motorized vehicle also increased from the last 5 years. It is noteworthy that uses of the nonmotorized vehicle are also increased despite the poor presence of any nonmotorized friendly infrastructure and policies. We have to encourage more NMT mode by implementing some of the policies like educational campaigns, allocation of the fund to create more bicycle-oriented infrastructures. Apart from all the policies, the crucial point is to change the current mindset of all kind people in the society to promote NMT mode.

References

1. Aarts H, Verplanken B, Knippenberg AV (1997) Habit and information use in travel mode choices
2. Aarts H, Verplanken B, Van Knippenberg A (1998) Predicting behavior from actions in the past: repeated decision making or a matter of habit? *J Appl Soc Psychol* 28(15):1355–1374
3. Agartala Municipality corporation. <http://agartalacity.tripura.gov.in/>
4. Ajzen I (1987) Attitudes, traits, and actions: dispositional prediction of behavior in personality and social psychology. In: *Advances in experimental social psychology*, vol 20. Academic Press, pp 1–63
5. Ajzen I (1985) From intentions to actions: a theory of planned behavior. In: *Action control* (pp 11–39). Springer, Berlin, Heidelberg
6. Araghi Y (2017) Consumer heterogeneity, transport and the environment. *TRAIL*
7. Bagozzi RP (1980) *Causal models in marketing*. Wiley
8. Bamberg S, Schmidt P (1999) Regulating transport: behavioural changes in the field. *J Consum Policy* 22(4):479–509
9. Bamberg S, Ajzen I, Schmidt P (2003) Choice of travel mode in the theory of planned behavior: the roles of past behavior, habit, and reasoned action. *Basic Appl Soc Psychol* 25(3):175–187
10. Chatterjee K (2009) A comparative evaluation of large-scale personal travel planning projects in England. *Transp Policy* 16(6):293–305
11. Ding L, Zhang N (2016) Dynamics in mode choice decisions: a case study in Nanjing, China. *Procedia Eng* 137:31–40
12. Eristi B, Erdem C (2017) Development of a media literacy skills scale. *Contemp Educ Technol* 8(3):249–267

13. Fernández-Heredia Á, Jara-Díaz S, Monzón A (2016) Modelling bicycle use intention: the role of perceptions. *Transportation* 43(1):1–23
14. Gakenheimer R, Zegras C (2006) Drivers of travel demand in the developing world. A synthesis of eight case studies. World Business Council for Sustainable Development. www.wbcsd.org/web/publications/mobility/mobility-appendix.pdf. Accessed June
15. Gorsuch RL, Ortberg J (1983) Moral obligation and attitudes: their relation to behavioral intentions. *J Pers Soc Psychol* 44(5):1025
16. Kuppam A, Pendyala R, Rahman S (1999) Analysis of the role of traveler attitudes and perceptions in explaining mode-choice behavior. *Trans Res Rec J Transp Res Board* 1676:68–76
17. Ma JKG (1997) A dynamic analysis of person and household activity and travel patterns using data from the first two waves in the Puget Sound Transportation panel. *Transportation* 24(3):309–331
18. Morichi S, Acharya SR (2005) Sustainable transport for East Asian megacities. In: 6th annual conference of the East Asia society for transportation studies, Bangkok, Thailand
19. Pucher J, Korattyswaropam N, Mittal N, Ittyerah N (2005) Urban transport crisis in India. *Transp Policy* 12(3):185–198
20. Richard R, van der Pligt J, de Vries N (1996) Anticipated affect and behavioral choice. *Basic Appl Soc Psychol* 18(2):111–129
21. Richardson A (2003) Temporal variability of car use as an input to design of before and after surveys. *Transp Res Rec J Transp Res Board* 1855:112–120
22. Sarkar PP, Chunchu M (2016) Quantification and analysis of land-use effects on travel behavior in smaller indian cities: case study of Agartala. *J Urban Plann Dev* 142(4):04016009
23. Sarkar PP, Mallikarjuna C (2013) Effect of land use on travel behaviour: a case study of Agartala city. *Procedia-Soc Behav Sci* 104:533–542
24. Simma Anja, Axhausen K (2003) Commitments and modal usage: analysis of German and Dutch panels. *Trans Res Rec J Transp Res Board* 1854:22–31
25. Srinivasan K, Pradhan G, Naidu G (2007) Commute mode choice in a developing country: role of subjective factors and variations in responsiveness across captive, semicaptive, and choice segments. *Trans Res Rec J Transp Res Board* 2038:53–61
26. Sunkanapalli S, Pendyala R, Kuppam A (2000) Dynamic analysis of traveler attitudes and perceptions using panel data. *Trans Res Rec J Transp Res Board* 1718:52–60
27. Thøgersen J (2006) Understanding repetitive travel mode choices in a stable context: a panel study approach. *Transp Res Part A Policy Prac* 40(8):621–638
28. Verma M, Manoj M, Verma A (2016) Analysis of the influences of attitudinal factors on car ownership decisions among urban young adults in a developing country like India. *Transp Res Part F: Traffic Psych Behav* 42:90–103

Effect of Natural Rubber, Carbon Black, and Copper Slag as Construction Materials in Flexible Pavement: A Review



S. Asvitha Valli and Sreevalsa Kolathayar 

Abstract In this paper, the effect of natural rubber, carbon black, and copper slag in the construction of flexible pavement is discussed. Natural rubber is used as a construction material because of its abundant availability and for its high tensile strength and good vibration absorption properties. Copper slag is obtained as a by-product of copper production, which is available in ample in India. In the year 2017, the volume of copper produced in India is nearly 134,790 metric tons. So many researchers studied the effect of copper slag on pavement construction and observed convincing results in improving the mechanical properties of the mix. Carbon black is used as a bitumen modifier in the flexible pavement which improves the properties like tear strength, resilience, and conductivity. It is observed that with 10% carbon black the creep value is lowered. The copper slag, when used as fine aggregate in various mixes, proved the improvement of volumetric and mechanical property of the mixes. It is also found that the utilization of natural rubber, carbon black as bitumen modifier, and copper slag as a substitute for fine aggregate improves the properties of the pavement significantly.

Keywords Waste management · Natural rubber · Copper slag · Carbon black · Pavement

1 Introduction

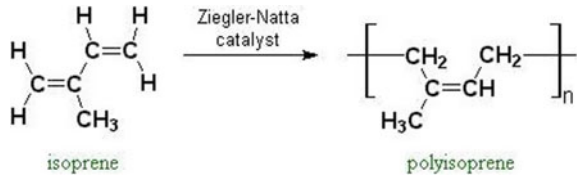
A pavement consists of superimposed layers of materials to transfer the vehicle load to the soil subgrade. The various layers in a flexible pavement are soil subgrade, subbase course, base course, and surface course. The subgrade serves as a foundation for the pavement. The subbase course functions as a structural support and also helps in

S. Asvitha Valli
Department of Civil Engineering, Francis Xavier Engineering College, Tirunelveli, India

S. Kolathayar (✉)
School of Civil Engineering, Vellore Institute of Technology, Vellore, India
e-mail: sreevalsakolathayar@gmail.com

© Springer Nature Singapore Pte Ltd. 2019
S. Pulugurtha et al. (eds.), *Advances in Transportation Engineering*,
Lecture Notes in Civil Engineering 34,
https://doi.org/10.1007/978-981-13-7162-2_6

Fig. 1 Ziegler–Natta polymerization



improving the drainage. The base course contributes to load distribution and surface drainage. This base course is generally made up of granular materials like crushed stone and crushed slag. The surface course should be made up of superior quality materials because of its direct contact with the traffic. The base course and subbase course are generally constructed using aggregates which are in greater demand in the market.

In recent years, studies have been done using the waste materials in the construction of pavements. This will lead to the usage of cost-effective construction material and also the effective disposal of the waste [1]. It is also evident from the previous researches that incorporation of copper slag, rubber, and carbon black improves the performance of the bituminous mix [2]. This bitumen modified with polymers or waste materials mainly focusses on the mechanical and physical properties of the rubberized mixture. It is found that rubberized bitumen are sensitive when exposed to heavy vehicle load and variation in temperature [4]. The use of copper slag as a partial replacement of fine aggregate in the mix proved a good interlocking property.

2 Natural Rubber

Natural rubber is an archetype of all elastomers. Rubber is obtained from the bark of Hevea tree in the form of latex. The rubber is extracted from the latex after treating it through several steps which include preservation, concentration, coagulation, dewatering, drying, cleaning, and blending. Depending on various factors like viscosity, oxidation resistance, and rate of cure, it is classified into various grades for marketing. Modified natural rubbers are available as epoxidized natural rubber, deproteinized natural rubber, and thermoplastic natural rubber.

Natural rubber is a quintessential polymer for engineering applications. Natural rubber chemically known as polyisoprene is diene polymer. These diene polymers have a carbon–carbon double bond in its backbone. This polyisoprene is obtained by Ziegler–Natta polymerization (Fig. 1).

2.1 Properties of Natural Rubber

- High tensile and tear strength.

- Resistance to fatigue.
- Insoluble in water, acetone, dilute acids, and alkalis.
- Absorb vibration.
- Elastic in nature.

The addition of carbon black, anti-degradants, softeners, and the proper vulcanization system will help in achieving the required properties. This polymer-modified bitumen is found to increase the quality of bitumen. This reduces the permanent deformations due to overload and is also unaffected by the changes in the atmospheric temperature.

2.2 *Natural Rubber–Bitumen Mixes*

Bitumen is manufactured from the distillation of crude oil during petroleum refining. The crucial characteristics of bitumen are adhesiveness, waterproof, thermoplastic, durable, modifiable, and recyclable as a construction material. It is found that 85% of the bitumen obtained is used as the binder in the construction of pavements [5]. In the early ages, rubber was mixed with bitumen to enhance the performance of the pavement. The rubber-modified bitumen was beneficial in extreme weather conditions, and the expansion and contraction due to the varying temperature were arrested by the elastic behavior of rubber [6]. Previous studies determined that the incorporation of rubber in bitumen proves the long-run performance of the pavement.

Due to the recent developments and lack of maintenance of pavements, the service life of pavements was decreased [7]. At a higher temperature in tropical areas, the bitumen runs similar to viscid liquid which proves the lack of viscoelastic and rheological properties in bitumen. This results in the deformation of the pavement surface [9]. On the other hand, at cold climate, the bitumen becomes inflexible and stiff resulting in the fatigue failure. So these leads to the inclusion of other materials like copper slag, carbon black in the pavement construction (Fig. 2) [10].

Deshmukh and Kshirsagar [3] performed an experimental study by varying the percentage of rubber by 0, 8, 10, 12, and 14% and observed that penetration value decreases as the percentage of rubber increases. This proves that the inclusion of rubber makes the bitumen mix harder. An increase in the softening point value with the increase in the rubber content is observed, which proved that rubber-modified is less vulnerable to temperature variation. Ductility value is found to be decreased with the increase in rubber content which proves that the addition of rubber makes the bitumen mix stiffer.

3 **Carbon Black**

Carbon black is a product of incomplete combustion. It is a commercial form of solid carbon. Carbon black typically contains 95% of pure carbon with minimal quanti-

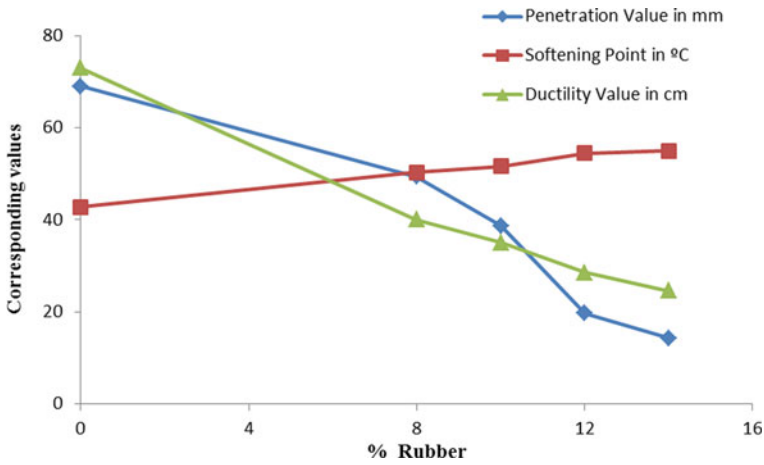


Fig. 2 Variation of experimental values with different percentages of rubber

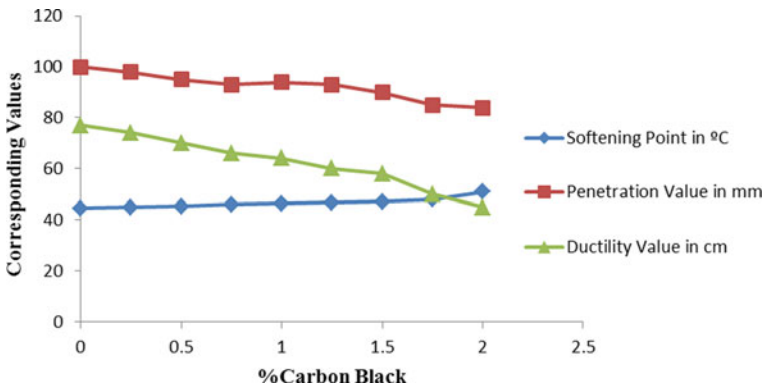


Fig. 3 Variation of experimental values with different percentages of carbon black

ties of hydrogen, nitrogen, and oxygen. It is used with other materials to improve their physical, electrical, and optical properties. Carbon black helps in increasing the properties like tear strength, resilience, and conductivity. It is used as a rubber reinforcing agent in the manufacturing of tires. This carbon black acts as a chemical strengthener in rubber. The carbon black is of two types like pyrolysis carbon black and petroleum carbon black. The pyrolysis carbon is economical compared to the petroleum carbon black. The pyrolysis carbon black is the second product of the tire pyrolysis industrial plant.

Experimental studies have been done by Saritha and Kiran Kumar [8] with different percentages of 0, 0.25, 0.5, 0.75, 1, 1.25, 1.5, 1.75, and 2% Carbon Black (CB) and observed a slight variation in the softening point, penetration, ductility values as shown in Fig. 3.

3.1 *Copper Slag as Aggregate*

The copper slag is added to the fine aggregate which improves the interlocking properties, volumetric, and mechanical properties of the bituminous mix. The density of the mix is increased by 16%, which shows the improvement in the interlocking property. The addition of 25% of CS shows favorable results in the Marshall quotient to the values closer than the conventional mix. The fatigue life of the bituminous mix is improved by the use of copper slag as a fine aggregate. This also increases the abrasion resistance of the pavement.

4 Conclusion

Thus the remains of natural rubber can be effectively used as the construction material for pavement. The penetration value obtained from experimental studies for natural rubber is in between 20 and 50 mm. This can be used in any climatic conditions. The softening point is between 50 and 55 °C; this can be used in warmer regions. The viscosity test proved that the resistance to flow increases with the increase in natural rubber. The incorporation of natural rubber thus improves the performance of the bitumen.

The asphalt binder does not have the electrical and thermal conductivity, but the addition of carbon black of different sources improved various properties like anti-aging, electrical, and thermal conductivity. This helps in improving the behavior of pavement at varying climatic conditions. The copper slag obtained from the extraction of copper can be used as a construction material because of its physical properties. This improves the interlocking property of the aggregate, thereby increasing the load transfer capacity of the pavement. Thus, the addition of natural rubber, carbon black, and copper slag in various proportions with the bituminous mix improves the behavior of flexible pavement.

References

1. Bejjenki (2015) Performance of bituminous mixes with modified binders 2(3):2–4
2. Cong P, Xu P, Chen S (2014) Effects of carbon black on the anti-aging, rheological and conductive properties of SBS/asphalt/carbon black composites. *Constr Build Mater* 52:306–313
3. Deshmukh NH, Kshirsagar DY (2017) Utilization of rubber waste in construction of flexible pavement. *Int J Adv Res Dev* 70–77
4. Feng Z et al (2016) Performance evaluation of bitumen modified with pyrolysis carbon black made from waste tyres. *Constr Build Mater* 111:495–501
5. Fini EH, Oldham D, Abu-Iebdeh T (2013) Bio-modified rubber: a sustainable alternative for use in asphalt pavements, pp 489–499
6. Kumar KR, Mahendran N (2014) Experimental studies on modified bituminous mixes using waste HDPE and crump rubber 4(4):587–597

7. Macadam DB (2005) Use of copper slag as construction material in bituminous pavements 64(December):997–1002
8. Saritha N, Kiran Kumar BV (2015) A study on use of carbon black powder in bituminous road construction. *Int J Eng Res Technol* 4(06)
9. Swetha V (2014) Effect of natural rubber on the properties of bitumen and bituminous mixes 5(10):9–21
10. Xiao F, Amirkhanian S, Juang CH (2007) Rutting resistance of rubberized asphalt concrete pavements containing reclaimed asphalt 19:475–483

Finite Element Modelling of Built-Up CFS Channel Columns Under Axial Load



Krishanu Roy, Tina Chui Huon Ting, Hieng Ho Lau and James B. P. Lim

Abstract A finite element model is described in this paper, which investigates the behaviour of CFS built-up channel columns, connected back-to-back with the help of intermediate web fasteners, subjected to axial load. Finite element package ABAQUS was used to develop the finite element models for built-up columns, which were verified against the test results reported by the authors. Non-linearities of materials and initial imperfections were included in the FEA model. Axial capacity, deformation patterns and load–displacement behaviour were reported from the FE analyses and validated against the test results, reported by the authors in another paper. Axial strengths obtained from the FEA modes were verified against the AISI and AS/NZS design strengths, for CFS built-up columns; obtained comparisons showed that AISI and AS/NZS standards were un-conservative for stub and short columns which failed by local buckling, whereas standards were over-safe for columns failed through overall buckling.

Keywords Cold-formed steel · Back-to-back sections · Built-up columns · Buckling · Fasteners

Notation

A' Total length of the web
 A_e Effective sectional area

K. Roy (✉) · J. B. P. Lim
Department of Civil and Environmental Engineering,
University of Auckland, Auckland, New Zealand
e-mail: kroy405@aucklanduni.ac.nz

T. C. H. Ting
Faculty of Engineering and Science, Curtin University Malaysia, Miri, Sarawak, Malaysia

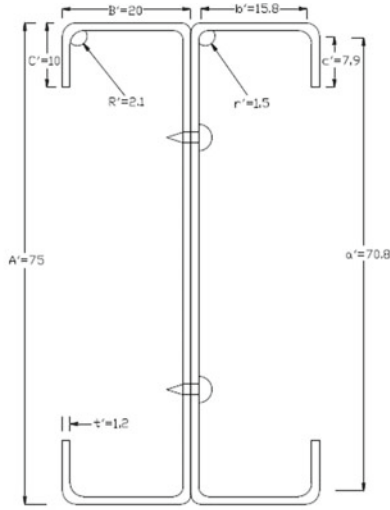
H. H. Lau
Faculty of Engineering, Computing and Science, Swinburne University of Technology, Sarawak
Campus, Kuching, Sarawak, Malaysia

B'	Total flange width
C'	Total lip width
CFS	Cold-formed steel
t	Section thickness
COV	Coefficient of variation
E	Young's modulus
F_n	Critical buckling stress
$(KL/r)_{ms}$	Modified slenderness
$(KL/r)_o$	Overall Slenderness
P_{AISI}	Axial capacity in accordance with American Iron and Steel Institute
P_{FEA}	Axial capacity determined from the finite element investigations
S	Longitudinal spacing between fasteners
λ_c	Non-dimensional slenderness ratio

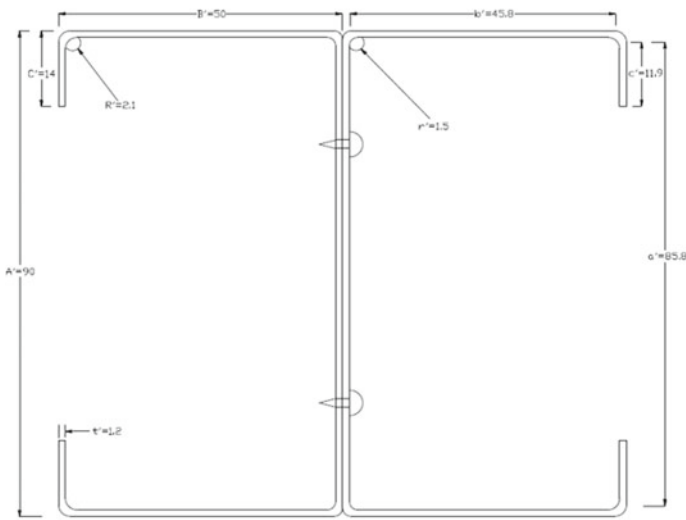
1 Introduction

The use of CFS built-up channels, connected back-to-back at the webs, is increasing (see Fig. 1), as compression members because of its superior strength-to-self weight ratios and economic design. Cold-formed steel members are easy to construct and also to compare hot-rolled steel members. CFS industry is looking for most effective cross sections of the structural members. However, for large span beam and column members, it is very effective to connect more than one section together to form a built-up section. These built-up sections can carry higher loads and can be used for larger spans, e.g. columns in warehouse or shopping malls, steel trusses, portal frames, space frames and wall frames. Current design guidance according to the American Iron and Steel Institute [1] and the Australian and New Zealand Standards (AS/NZS 4600: 2005) uses modified slenderness method to determine the axial capacity of CFS built-up channels. However, the applicability of the modified slenderness method has not been justified for CFS, unlike hot-rolled steel built-up columns.

Very few researches have been done to determine the axial strength of CFS built-up channel sections, as shown in Fig. 1. The effect of fastener spacing on the strength of built-up channels, connected back-to-back, was investigated by Ting et al. [14] which was followed by Roy et al. [6] to study the effect of thickness on the axial strength of built-up CFS channel sections, connected at the webs of two channels. CFS built-up battened columns were investigated by Dabaon et al. [3], and they have concluded that the AISI and AS/NZS and the eurocodes were un-conservative for columns undergoing local buckling but the standards predicted the failure load safely for those built-up columns failed through flexural buckling. Piyawat et al. [5] investigated welded back-to-back built-up columns. Zhang and Young [19] considered an opening in the CFS built-up columns, connected back-to-back (see Fig. 2). Whittle et al. [18] investigated the axial strengths of built-up columns which were welded toe-to-toe. Stone and LaBoube [16] considered stiffened flange and track back-to-back channel sections. Other works include that of Fratamio et al. [4] and Anbarasu



(a) BU75

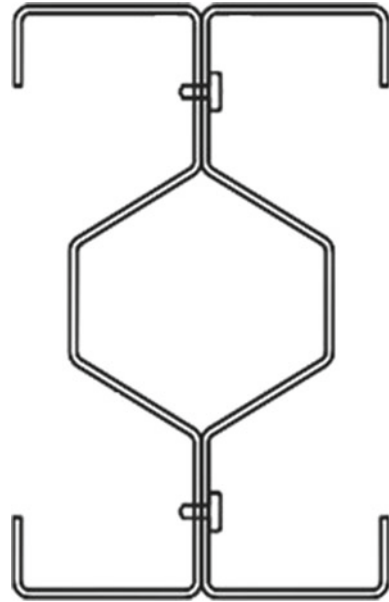


(b) BU90

Dimensions are in mm

Fig. 1 Cross-sectional details of the CFS built-up channel sections investigated herein

Fig. 2 Built-up CFS section investigated by Zhang and Young [19]



et al. [2] who considered CFS built-up columns, connected back-to-back, while CFS built-up columns, connected by intermediate screws and wood sheathed, were investigated experimentally by Fratamico et al. [4]. On the other hand, Roy et al. [15] investigated the effect of fastener spacing on axial capacity of built-up duplex stainless steel channels, connected back-to-back. Roy et al. [11–13] also studied experimentally and numerically, the axial capacity of built-up CFS channel sections, connected back-to-back with a gap between two channels and concluded that the current design guidelines by AISI and AS/NZS can be too conservative while predicting the axial capacity of such columns. Also, investigated by Roy et al. [7], the behaviour of built-up CFS un-lipped channel sections, connected back-to-back, subjected to compressive force. The cold-formed built-up stainless steel un-lipped channel sections under compression were investigated by Roy et al. [13]. On the other hand, face-to-face built-up CFS channels were tested under compression by Roy et al. [14]. Roy et al. [17] investigated the behaviour of built-up CFS columns connected back-to-back under axial load and compared the test results against the current design rules as per AISI and AS/NZS.

Sixty finite element results are presented in this paper for CFS built-up channels connected back-to-back under axial load. FE models considered non-linear material properties and initial imperfections. Explicit modelling of intermediate web fasteners has been described. The axial capacity and deformation patterns of CFS built-up columns are reported. FEA results agreed well when compared against the test results, conducted recently by authors [8–10]. FEA results compared against the AISI and AS/NZS strengths. AISI and AS/NZS standards were shown to be safe for all columns

failed through overall buckling; however, the AISI and AS/NZS were un-conservative for all stub and some short columns which failed by local buckling.

2 AISI and AS/NZS Design Guidelines

Finite element strengths were compared against the design strengths calculated in accordance with the AISI and AS/NZS. For built-up CFS columns, the axial strength is calculated according to AISI and AS/NZS as follows:

$$P_{\text{AISI}} = A_e F_n \quad (1)$$

The critical buckling stress (F_n) is determined as below:

$$\text{For } \lambda_c \leq 1.5: F_n = (0.658 \lambda_c^2) F_y \quad (2)$$

$$\text{For } \lambda_c > 1.5, F_n = \left(\frac{0.877}{\lambda_c^2} \right) F_y \quad (3)$$

The non-dimensional critical slenderness (λ_c) is calculated using Eq. 4:

$$\lambda_c = \sqrt{\frac{F_y}{F_e}} \quad (4)$$

Modified slenderness ratio was used for all calculations as per Eq. 5.

$$\left(\frac{KL}{r} \right)_{ms} = \sqrt{\left(\frac{KL}{r} \right)^2 + \left(\frac{s}{r_{yc}} \right)^2}; \quad \text{For which } \left(\frac{s}{r_{yc}} \right) \leq 0.5 \left(\frac{KL}{r} \right)_o \quad (5)$$

3 Summary of Experimental Tests

The non-linear FEA models, developed herein, were verified against the test results reported by the authors recently [8–10], (see Fig. 1). The built-up lipped channels were tested under compression for different column lengths starting from stub (length of 300 mm) to slender (length of 2000 mm) columns. Thickness of the CFS channels was 1.2 mm. Figures 1b and 2a show cross-sectional details of the built-up columns, investigated by Roy et al. [8–10], to be referred to as BU75 and BU90, respectively. The measured specimen dimensions are shown in Table 1a, b for BU75 and BU90, respectively. In total, 60 specimens were tested, covering four different column heights: 0.3, 0.5, 1 and 2 m. Types of the built-up section, fastener spacing, nominal specimen length and test specimen number were coded by the specimen

Fig. 3 Specimen labelling

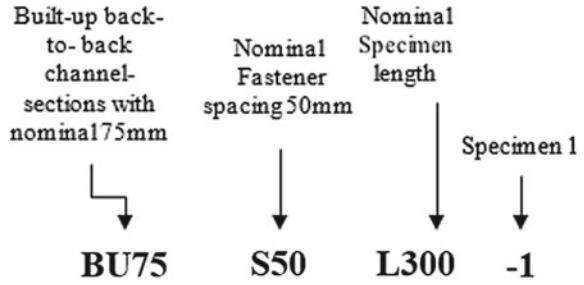
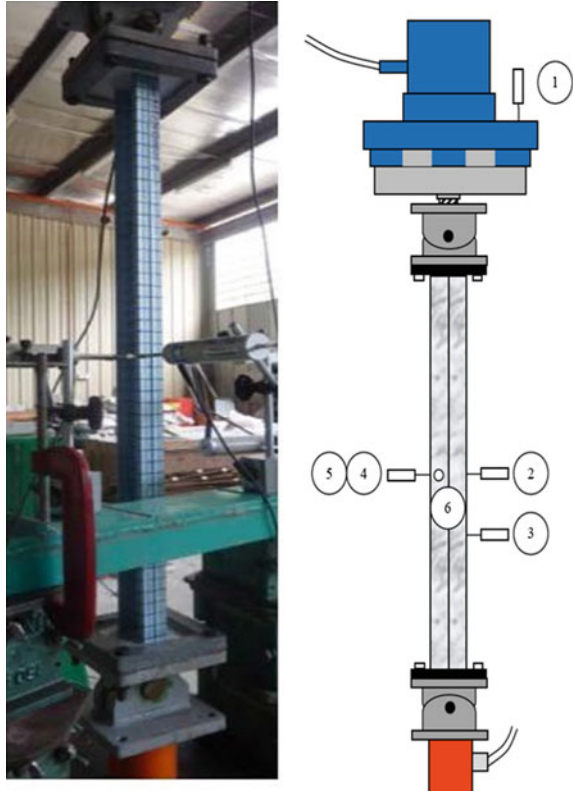


Fig. 4 Built-up column test setup (1-m-long column tests)



labelling. Figure 3 shows an example of the labelling used in the experimental programme.

In order to determine the material properties, i.e. the Young’s modulus and yield strength, tensile coupon tests were conducted. From the results of tensile coupon tests for longitudinal and transverse directional coupons, average values of the modulus of elasticity and yield stress were 207 N/mm^2 and 560 N/mm^2 , respectively.

All the built-up columns were loaded with the help of a Universal Testing Machine (UTM) (see Fig. 4). The capacity of the UTM was 600 kN. Prior to testing, an LVDT with 0.11 mm accuracy was used to measure initial geometric imperfections present

Table 1 Axial strength comparison from laboratory, finite element analyses and design standards

Specimen	Web	Flange	Lip	Length	Thickness	Spacing	Modified slen-dermess	Experimental results	AISI design strengths		FEA results	
	A'	B'	C'	L	t	S	(KL/r) m	P _{EXP}	P _{AISI}	P _{Exp/} P _{AISI}	P _{FEA}	P _{Exp/} P _{FEA}
	(mm)	(mm)	(mm)	(mm)	(mm)	(mm)	–	(kN)	(kN)	–	(kN)	–
<i>(a) BU75</i>												
<i>Stub</i>												
BU75S50L300-1	73.1	19.8	11.1	273	1.20	50.0	15.63	120.7	126.68	0.95	116.73	1.09
BU75S50L300-2	73.1	19.8	11.2	280	1.19	50.0	15.93	118.8	126.77	0.94	114.9	1.03
BU75S50L300-3	72.7	19.5	10.8	270	1.21	50.9	15.92	118.7	124.84	0.95	114.4	1.04
BU75S100L300-2	73.1	19.8	11.2	267	1.20	99.7	19.48	117.5	125.10	0.94	113.6	1.03
BU75S100L300-3	73.1	19.9	11.2	273	1.18	100.2	19.41	122.7	125.41	0.98	117.4	1.05
BU75S100L300-4	73.6	19.7	11.2	273	1.18	99.5	19.56	115.4	124.89	0.92	112.6	1.02
BU75S200L300-1	73.7	19.8	11.2	266.5	1.20	200.0	30.31	122.5	119.05	1.03	120.8	1.01
BU75S200L300-2	73.6	19.9	11.2	266	1.20	199.5	30.22	119.1	119.09	1.00	116.4	1.02
BU75S200L300-3	72.9	20.0	11.2	268	1.20	200.0	29.97	113.1	119.36	0.95	108.4	1.04
Mean										0.96		1.04
COV										0.04		0.02
<i>Short</i>												
BU75S100L500-1	73.6	19.8	11.2	655.0	1.21	100.0	69.11	83.0	78.881	1.05	79.5	1.04
BU75S100L500-3	73.6	19.7	11.2	680.0	1.20	100.5	72.16	74.1	78.376	0.95	78.4	0.95
BU75S200L500-1	73.5	19.5	11.3	653.0	1.18	195.0	73.36	86.2	79.992	1.08	80.3	1.07

(continued)

Table 1 (continued)

Specimen	Web	Flange	Lip	Length	Thickness	Spacing	Modified slen-derness	Experimental results	AISI design strengths		FEA results	
	A'	B'	C'	L	t	S	(KL/r) m	P _{EXP}	P _{AISI}	P _{Exp/} P _{AISI}	P _{FEA}	P _{Exp/} P _{FEA}
	(mm)	(mm)	(mm)	(mm)	(mm)	(mm)	–	(kN)	(kN)	–	(kN)	–
BU75S200L500-2	73.6	19.6	11.3	678.0	1.19	195.0	75.58	88.9	81.406	1.09	82.7	1.07
BU75S200L500-3	73.4	19.7	11.3	680.0	1.21	200.5	75.60	93.6	86.759	1.08	88.1	1.06
BU75S400L500-1	73.6	19.7	11.3	678.0	1.18	400.0	88.74	74.8	72.417	1.03	74.6	1.00
BU75S400L500-2	73.5	19.7	11.3	679.0	1.20	401.0	89.00	80.6	74.336	1.08	76.3	1.06
Mean										1.05		1.04
COV										0.05		0.05
<i>Intermediate</i>												
BU75S225L1000-1	75.3	20.2	10.4	1133	1.21	225.3	121.36	47.0	42.34	1.11	45.7	1.03
BU75S225L1000-2	75.7	19.9	10.4	1131	1.20	225.3	123.71	46.3	41.05	1.13	44.9	1.03
BU75S450L1000-1	75.8	19.9	10.4	1131	1.21	447.0	133.91	50.4	38.98	1.29	42.4	1.19
BU75S450L1000-2	75.6	19.9	10.4	1133	1.18	450.0	135.07	45.0	38.12	1.18	40.12	1.12
BU75S450L1000-3	75.9	19.8	10.3	1182	1.19	450.0	140.52	41.8	34.62	1.21	35.8	1.17
BU75S900L1000-1	76.0	19.9	10.3	1131	1.20	900.0	171.43	39.9	33.21	1.20	34.2	1.17
BU75S900L1000-2	76.3	19.8	9.1	1133	1.21	900.0	178.06	33.7	30.29	1.11	31.5	1.07
BU75S900L1000-3	75.9	19.8	10.3	1183	1.22	901.0	176.55	31.5	28.91	1.09	29.6	1.06
Mean										1.17		1.11
COV										0.07		0.07

(continued)

Table 1 (continued)

Specimen	Web	Flange	Lip	Length	Thickness	Spacing	Modified slen-derness	Experimental results	AISI design strengths		FEA results	
	A' (mm)	B' (mm)	C' (mm)	L (mm)	t (mm)	S (mm)	(KL/r) m	P _{EXP} (kN)	P _{AISI} (kN)	P _{Exp} /P _{AISI}	P _{FEA} (kN)	P _{FEA} /P _{FEA}
<i>Slender</i>												
BU75S475L2000-2	73.9	20.3	10.7	2184	1.20	474.5	231.2	10.9	10.27	1.03	10.6	1.03
BU75S475L2000-3	73.9	20.2	10.8	2183	1.20	462.0	231.61	10.8	10.22	1.03	10.5	1.03
BU75S950L2000-2	73.9	20.3	10.8	2184	1.18	949.5	255.17	8.8	8.43	1.02	8.6	1.02
BU75S950L2000-3	73.9	20.2	10.8	2184	1.17	950.0	256.21	8.6	8.36	1.01	8.5	1.01
BU75S1900L2000-2	73.9	20.3	10.9	2183	1.18	1900.0	334.82	7.6	7.34	1.03	7.4	1.03
BU75S1900L2000-3	73.9	20.4	10.7	2184	1.19	1901.0	333.86	7.5	7.31	1.01	7.4	1.01
Mean										1.02		1.02
COV										0.01		0.01
<i>(b) BU90</i>												
<i>Stub</i>												
BU90S50L300-1	91.3	49.8	14.6	277.0	1.20	50.0	7.95	172.5	179.7	0.96	162.7	1.06
BU90S50L300-2	91.8	49.7	14.5	272.0	1.19	49.8	7.89	171.6	182.6	0.94	160.4	1.07
BU90S50L300-3	92.9	49.4	14.5	261.0	1.21	50.0	7.93	170.6	179.6	0.95	160.9	1.06
BU90S100L300-1	90.8	49.7	14.6	262.0	1.20	99.9	9.45	166.2	178.7	0.93	152.5	1.09
BU90S100L300-2	90.6	49.5	14.6	268.0	1.18	100.0	9.42	165.8	176.4	0.94	156.4	1.06

(continued)

Table 1 (continued)

Specimen	Web	Flange	Lip	Length	Thickness	Spacing	Modified slen-derness	Experimental results	AISI design strengths		FEA results	
									P _{AISI}	P _{Exp} /P _{AISI}	P _{FEA}	P _{Exp} /P _{FEA}
	A'	B'	C'	L	t	S	$(KL/r)_m$	P _{EXP}	P _{AISI}	P _{Exp} /P _{AISI}	P _{FEA}	P _{Exp} /P _{FEA}
	(mm)	(mm)	(mm)	(mm)	(mm)	(mm)	–	(kN)	(kN)	–	(kN)	–
BU90S200L300-1	90.7	49.4	14.6	273.5	1.18	201.0	11.93	163.3	175.6	0.93	157.0	1.04
BU90S200L300-2	90.7	49.4	14.6	269.5	1.20	199.0	11.83	163.5	173.9	0.94	155.7	1.05
BU90S200L300-3	89.5	48.3	14.0	280.5	1.20	199.0	11.87	162.9	173.3	0.94	158.2	1.03
BU90S50L300-1	91.3	49.8	14.6	277.0	1.20	50.0	7.95	172.5	179.7	0.96	162.7	1.06
Mean												1.06
COV												0.02
<i>Short</i>												
BU90S100L500-1	90.6	49.5	14.6	656.0	1.21	100.5	35.42	160.4	149.9	1.04	152.8	1.05
BU90S100L500-2	90.6	49.4	14.6	678.0	1.20	100.5	34.25	158.1	152.0	1.08	153.5	1.03
BU90S200L500-1	90.4	49.3	14.7	653.0	1.18	199.5	38.52	152.2	140.9	1.09	142.2	1.07
BU90S200L500-2	90.4	49.3	14.7	678.0	1.19	199.5	39.41	150.9	138.4	1.10	142.4	1.06
BU90S200L500-3	90.4	49.3	14.6	680.0	1.21	200.5	40.20	149.2	135.6	1.06	143.5	1.04
BU90S400L500-1	90.6	49.4	14.7	678.0	1.18	400.0	50.20	132.4	124.9	1.06	127.3	1.04
BU90S400L500-2	90.4	49.4	14.7	678.0	1.20	399.0	49.41	134.5	126.9	1.07	128.1	1.05
Mean												1.05
COV												0.01

(continued)

Table 1 (continued)

Specimen	Web		Flange		Lip		Length		Thickness		Spacing		Modified slenderness		Experimental results		AISI design strengths			FEA results		
	A'	B'	C'	L	t	S	(KL/r) _m	P _{EXP}	P _{AISI}	P _{FEA}	P _{Exp} /P _{AISI}	P _{FEA}	P _{FEA} /P _{AISI}	P _{FEA}	P _{Exp} /P _{FEA}							
	(mm)	(mm)	(mm)	(mm)	(mm)	(mm)	(mm)	(kN)	(kN)	(kN)	(kN)	(kN)	(kN)	(kN)	(kN)							
<i>Intermediate</i>																						
BU90S225L1000-1	90.8	49.6	14.4	1182	1.21	225.0	60.42	102.6	92.43	100.6	1.11	100.6	1.02	100.6	1.02							
BU90S225L1000-2	90.6	49.6	14.3	1132	1.20	225.0	58.21	102.0	92.72	99.03	1.10	99.03	1.03	99.03	1.03							
BU90S450L1000-1	90.6	49.7	14.4	1130	1.21	450.0	64.21	96.51	86.18	90.20	1.12	90.20	1.07	90.20	1.07							
BU90S450L1000-2	90.4	49.7	14.4	1182	1.18	448.0	66.21	94.42	82.79	89.08	1.14	89.08	1.06	89.08	1.06							
BU90S450L1000-3	90.5	49.8	14.5	1180	1.19	452.0	65.29	93.33	82.54	87.22	1.13	87.22	1.07	87.22	1.07							
BU90S900L1000-1	90.5	49.6	14.4	1131	1.20	897.0	75.21	89.55	82.89	85.29	1.08	85.29	1.05	85.29	1.05							
BU90S900L1000-2	91.0	49.3	14.4	1182	1.21	899.0	77.21	87.58	80.31	82.62	1.09	82.62	1.06	82.62	1.06							
BU90S900L1000-3	90.1	49.2	14.5	1129	1.22	896.0	76.50	87.51	79.51	84.14	1.10	84.14	1.04	84.14	1.04							
Mean																						
COV																						
<i>Slender</i>																						
BU90S475L2000-1	90.6	49.5	14.5	2164	1.20	474.2	92.52	65.40	61.12	62.88	1.07	62.88	1.04	62.88	1.04							
BU90S475L2000-2	90.7	49.4	14.3	2172	1.20	466.6	94.42	66.01	61.63	62.87	1.07	62.87	1.05	62.87	1.05							
BU90S50L2000-1	90.5	49.5	14.6	2169	1.18	960.4	101.17	54.02	50.90	52.45	1.06	52.45	1.03	52.45	1.03							
BU90S50L2000-2	90.4	49.2	14.5	2148	1.17	949.3	103.21	45.62	43.41	44.73	1.05	44.73	1.02	44.73	1.02							

(continued)

Table 1 (continued)

Specimen	Web	Flange	Lip	Length	Thickness	Spacing	Modified slenderness	Experimental results	AISI design strengths		FEA results	
									P_{AISI}	P_{Exp}/P_{AISI}	P_{FEA}	P_{Exp}/P_{FEA}
	A'	B'	C'	L	t	S	$(KL/r)_m$	P_{EXP}	P_{AISI}	P_{FEA}	P_{FEA}	P_{FEA}
	(mm)	(mm)	(mm)	(mm)	(mm)	(mm)	–	(kN)	–	(kN)	–	–
BU90S1900L2000-1	90.5	49.3	14.6	2158	1.18	1902.4	115.2	48.04	44.80	48.53	0.99	0.99
BU90S1900L2000-2	90.9	49.7	14.2	2152	1.19	1906.7	116.42	43.21	41.14	43.21	1.00	1.00
Mean											1.06	1.02
COV											0.02	0.02

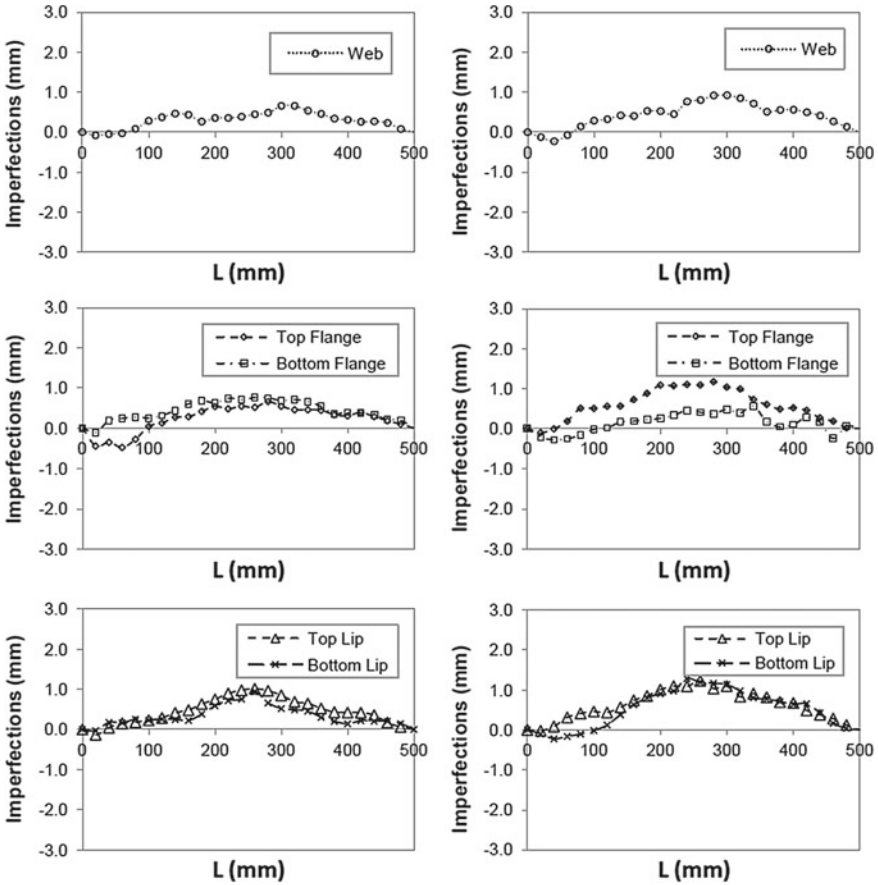


Fig. 5 Initial imperfections for BU90-S200-L300-1

in the channel sections. In Fig. 5, initial imperfections are plotted against the length of the built-up columns for BU90S200L300-1. These imperfections are included in FEA models described in this article. Further details of the experimental tests are available in [8–10].

4 Numerical Study

4.1 General

ABAQUS 6.14-2 was used to develop a finite element model for CFS built-up columns under axial load. Centre line dimensions were used for all FEA models.

Two types of finite element analysis were performed for buckling of built-up sections: Eigenvalue analysis and load–displacement analysis. Eigenvalues of the built-up columns were determined to model the geometric imperfections. A load–displacement non-linear analysis was, then, carried out using RIKS algorithm available in the ABAQUS library. The geometric imperfections and non-linear material properties were included in the FEA model. From this analysis, the failure loads, buckling modes and load–axial shortenings are determined. Specific modelling techniques are described in detail as below.

4.2 Geometry and Material Properties

The built-up channels were modelled considering the full geometry of the columns including web fasteners. Non-linear stress–strain relationships were specified in the finite element model to incorporate the material non-linearity. The non-linear elastic–plastic model was used for modelling the built-up columns in ABAQUS. Yield stress of 560 MPa and ultimate stress of 690 MPa, along with Young’s modulus of 207 GPa, were used in finite element modelling.

4.3 Type of Elements and Finite Element Meshing

S4R5 thick shell elements were used to model the built-up columns. S4R5 elements were four-noded quadrilateral thick shell element. Across the length and width, a mesh size of 5 mm × 5 mm was used for the convergence of the model. A number of elements were confirmed through a mesh sensitivity analysis. An FE mesh is shown in Fig. 6 for BU75-S100-L500-1.

4.4 Modelling of Boundaries and Loading Procedure

Pin–pinned boundaries were applied in all finite element models for built-up columns. Two rigid plates were used at top and bottom ends of the built-up columns to simulate the experimental test results. Pin–pin boundary condition was modelled by applying rotations and displacements to both the end plates through a reference point. The reference point was considered as the CG of the cross section of built-up channels. The reference point was used to apply the load through the upper end plates. Fasteners between two back-to-back channels were modelled using MPC beam connector elements available in the ABAQUS library (see Fig. 7). MPC beam connector elements were assigned a stress of 62.10 MPa to incorporate the stiffness of the fasteners.

4.5 Contact Modelling

“*Surface to surface*” contact was defined as the interaction of the webs of two channels connected back-to-back. The web of one channel was modelled as slave surface, while the web of other channel section was considered as master surface. There was no penetration between the two contact surfaces.

4.6 Geometric Imperfections in FEA Models

Initial imperfections were considered in the FE modelling. Superimpositions of local and global buckling modes were considered for accurate FE analysis. For all built-up columns, eigenvalue analyses were performed. For local buckling, very small channel thickness was considered; however, for global buckling, large channel thickness was used in finite element models. For local and global buckling modes, lowest eigenmode was used in ABAQUS. The imperfections used in the modelling of built-up channels were calibrated to the values measured from experiments by Roy et al. [8–10]. Besides, local imperfection of 0.5% of channel thickness was included in all finite element models as recommended by Roy et al. [7]. In Fig. 8, the contours of local and overall buckling are shown for BU75-S100-L500-1.

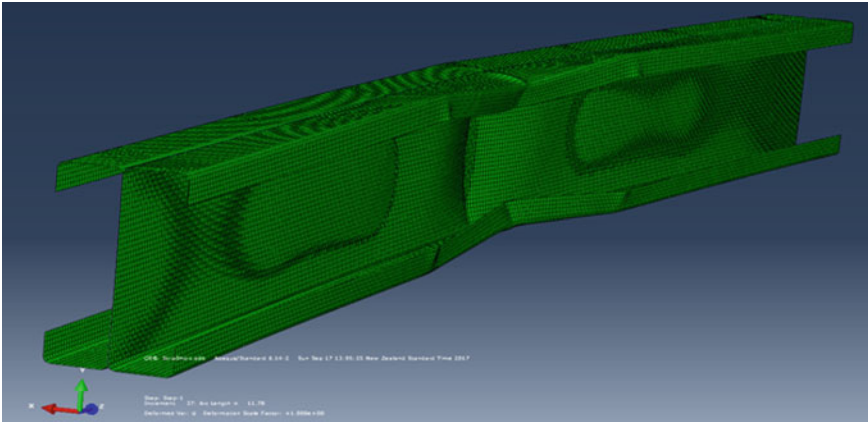


Fig. 6 FE mesh at failure BU75-S100-L500-1

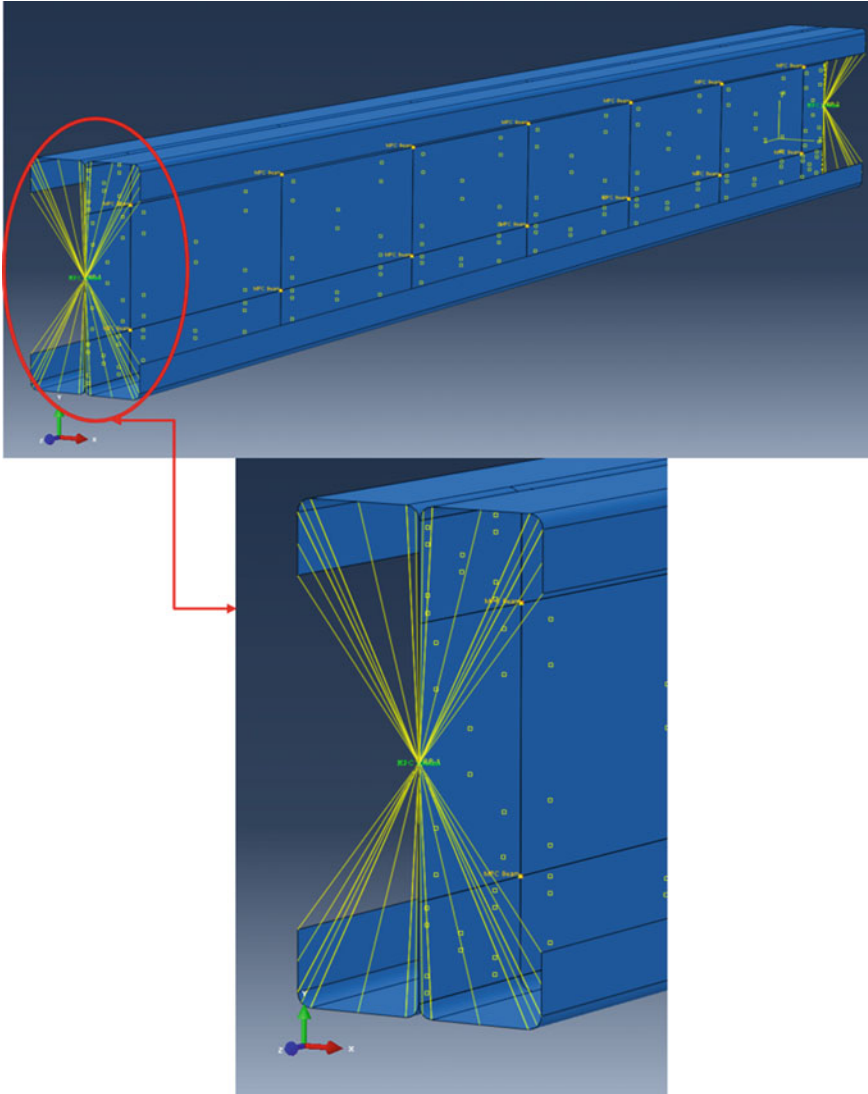


Fig. 7 Boundary condition applied to the FE model (BU75-S100-L500-1)

4.7 FEA Model Validation

Results from the FEA models were verified against the test results available in the literature for built-up CFS columns, connected back-to-back under axial load. Figure 8 shows the failure modes of stub, short and intermediate columns obtained from exper-

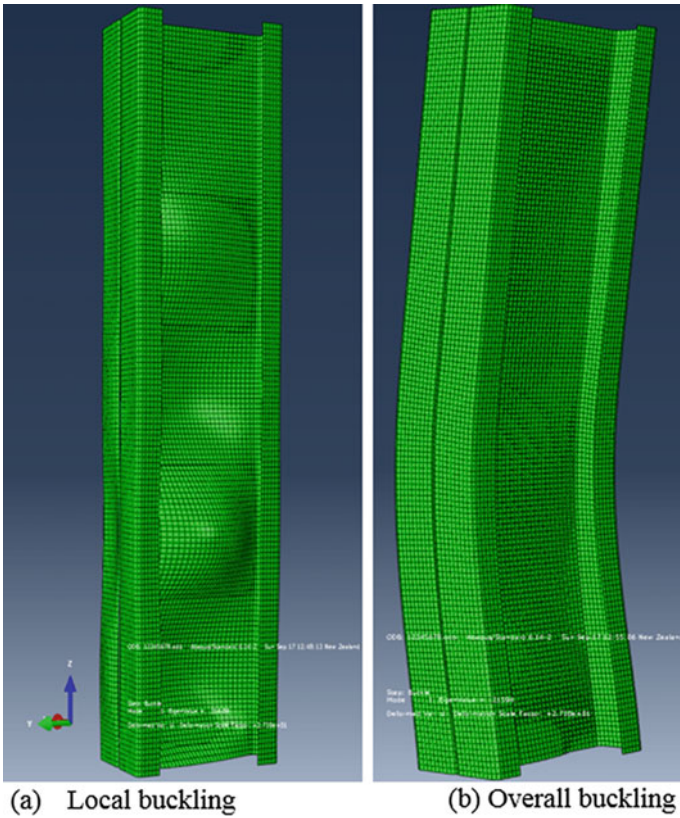


Fig. 8 Initial imperfection contours (BU75-S100-L500-1)

imental tests conducted by Roy et al. [8–10]. Also, in Fig. 9, test and FEA strengths are compared for BU75-S50-L300-1. As can be seen, the tests and FE results show good comparison in terms of both failure load and deformed shapes.

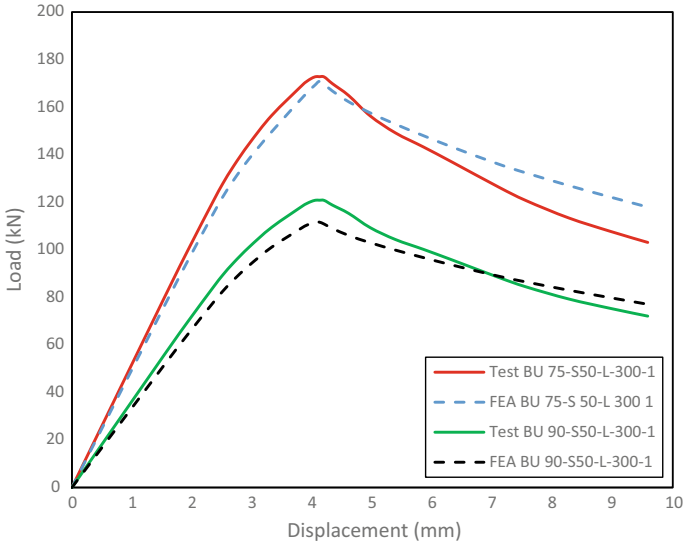


Fig. 9 Comparison of numerical and test results

Table 1a, b summarises the failure load obtained from the tests [8–10], which were compared against the FEA results for BU75 and BU90, respectively. It is shown that the mean of P_{EXP}/P_{FEA} is 1.04, with a COV of 0.02 for stub column of BU75 series and P_{EXP}/P_{FEA} is 1.06, with a COV of 0.02 for stub column of BU90 series.

5 Comparison of FEA Results Against the Design Strengths

Table 1a, b shows the comparison of FEA strengths against the AISI and AS/NZS strengths for BU75 and BU90, respectively. In Table 1a, b, it is shown that the AISI and AS/NZS strengths were higher than FEA strengths by around 10% for all stub columns. For reference, experimental strengths are also included in Table 1a, b for BU75 and BU90, respectively. However, AISI and AS/NZS standard safely predicted the axial capacity of the built-up columns which failed through global or overall buckling.

Figure 11a, b plotted the FEA and design strengths for BU75 and BU90, respectively, against the modified slenderness. Experimental strengths from [8–10] were also plotted in Fig. 11a, b for comparison. It is clear that the FEA strengths are very close to test strengths. From Fig. 10, it can be seen that when the modified slenderness ratio was less than 30, most of the built-up columns failed through local buckling while most of the built-up columns failed through global buckling when the modified slenderness was greater than 55. Comparison of AISI and AS/NZS strengths and FEA strengths are plotted in Fig. 12a, b for BU75 and BU90, respectively.

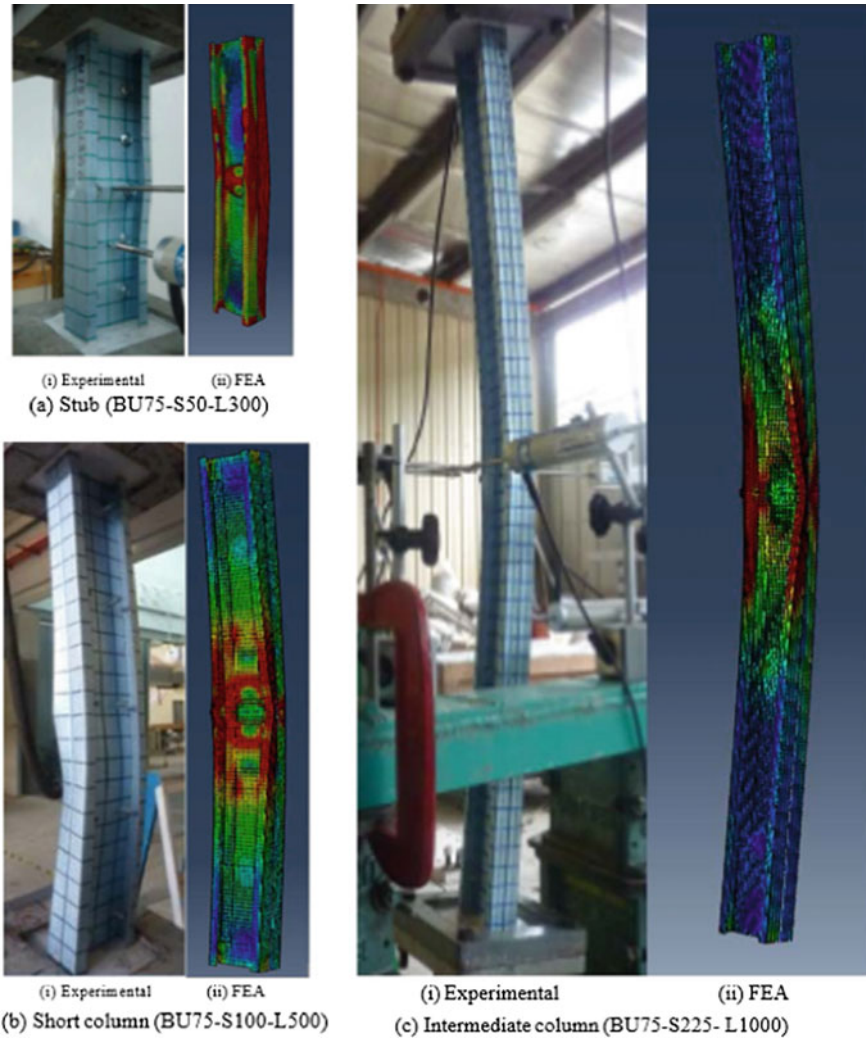


Fig. 10 Built-up sections at failure

6 Conclusions

This paper has presented the results of 60 non-linear FEA analyses on CFS built-up columns, connected back-to-back, subjected to axial load. Finite element model includes explicit modelling of web fasteners, material non-linearity and geometric imperfections. Failure loads and buckling modes for different lengths of built-up columns are discussed. FEA models were validated against the experimental test results which showed good agreement.

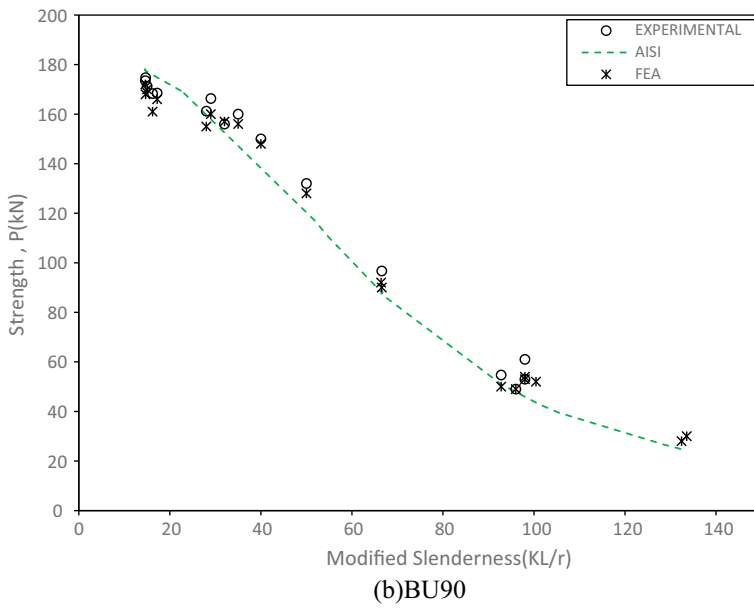
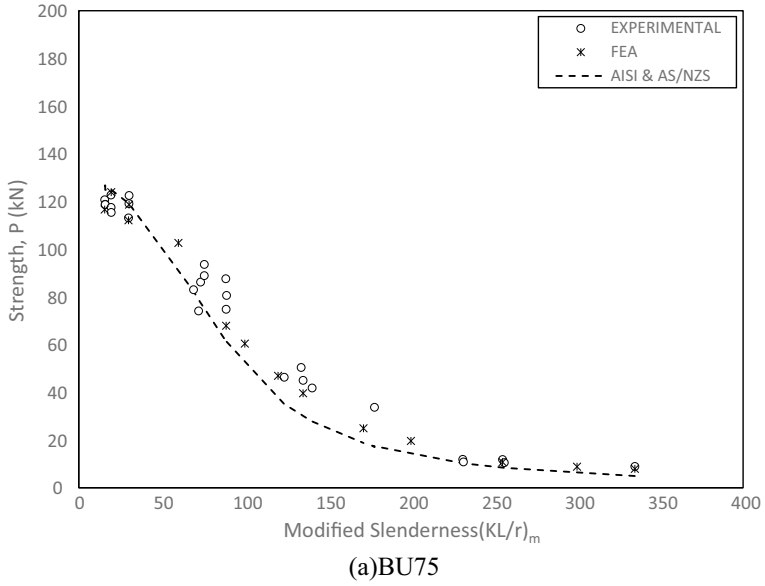


Fig. 11 Fig. 8: Plot of strength against the modified slenderness

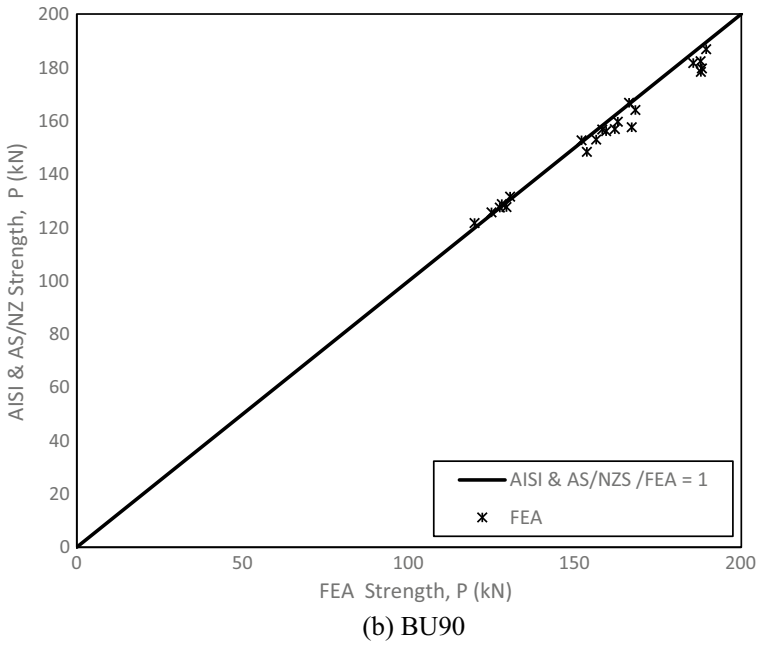
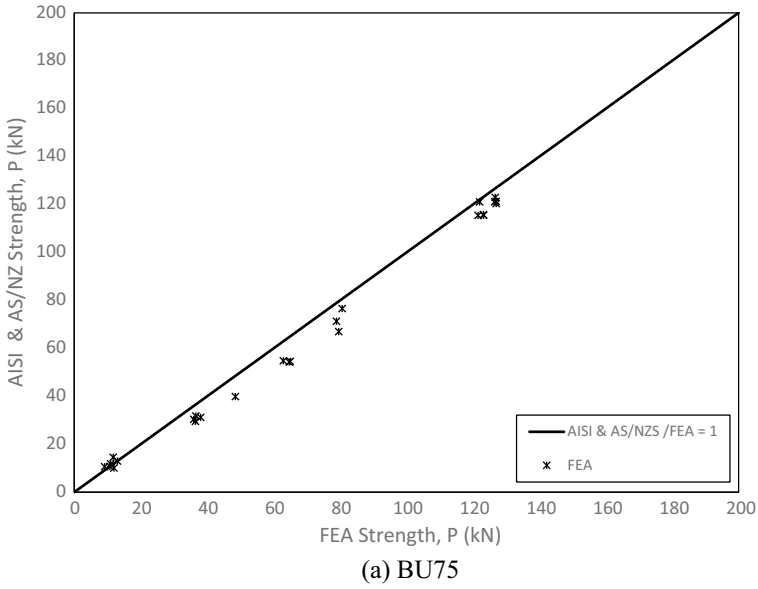


Fig. 12 FEA strength against the AISI and AS/NZ strengths

The validated FEA models were used to check the accuracy of current design guidelines. The column strengths from the FEA were compared against the AISI and AS/NZS strengths. AISI and AS/NZS strengths were safe by around 15%, when compared to the FEA results for 0.5, 1 and 2 m columns; however, for 0.3 m columns AISI and AS/NZS, they were un-conservative by around 10%.

The first author is currently investigating the effect of different cross sections and arrangement of screws for CFS built-up columns under eccentric load to develop better design methods that will incorporate more accurate estimations of column cross sections and screw spacing for different end conditions.

References

1. American Iron and Steel Institute (2012) North American specification for the design of cold-formed Steel Structural Members. NAS S100
2. Anbarasu M, Bharath KP, Sukumar S (2014) Study on the capacity of cold-formes steel built-up battened colums under axial compression. *Lat Am J Solids Struct* 11(12):1375–2271
3. Dabaon M, Ellobody E, Ramzy K (2015) Nonlinear behavior of built-up cold-formed steel section battened columns. *J Constr Steel Res* 110:16–28
4. Fratamico DC, Schafer BW (2014) Numerical studies on the composite action and buckling behavior of built-up cold-formed steel columns. In: 22nd international specialty conference on cold-formed steel structures, St. Louis, MO
5. Piyawat K, Ramseyer C, Kang Thomas H-K (2013) Development of an axial load capacity equation for doubly symmetric built-up cold-formed sections. *J Struct Engi Am Soc Civil Eng* 139(12):04013008–13
6. Roy K, Lau HH, Lim JBP (2018) Effect of fastener spacing on axial strength of back-to-back built-up cold-formed stainless steel un-lipped channels. *Steel Compos Struct Int J*
7. Roy K, Mohammadjani C, Lim JBP (2018) Experimental and numerical investigation into the behaviour of face-to-face built-up cold-formed steel channel sections under compression. *Thin-Walled Struct* (in press)
8. Roy K, Ting TCH, Lau HH, Lim JB (2018) Nonlinear behaviour of back-to-back gapped built-up cold-formed steel channel sections under compression. *J Constr Steel Res* 147:257–276
9. Roy K, Ting TCH, Lau HH, Lim JBP (2018) Effect of thickness on the behaviour of axially loaded back-to-back cold-formed steel built-up channel sections—experimental and numerical investigation. *Structures*. <https://doi.org/10.1016/j.istruc.2018.09.009>
10. Roy K, Ting TCH, Lau HH, Lim JB (2018) Nonlinear behavior of axially loaded back-to-back built-up cold-formed steel un-lipped channel sections. *Steel Compos Struct Int J* 28(2):233–250
11. Roy K, Ting TCH, Lau HH, Lim JBP (2018) Compression tests on back-to-back gapped built-up cold-formed steel channel sections. In: 2018 Proceedings of the international conference on engineering research and practice for steel construction, ICSC, Hong Kong, China
12. Roy K, Ting TCH, Lau HH, Lim JBP (2018) Effect of screw spacing into the behaviour of back-to-back cold-formed duplex stainless steel built-up channel sections under compression. In: 2018 Proceedings of the international conference on engineering research and practice for steel construction, ICSC, Hong Kong, China
13. Roy K, Ting TCH, Lau HH, Lim JBP (2018) Experimental investigation into the behaviour of back-to-back gapped built-up cold-formed steel channel sections under compression. In: Wei-Wen Yu international specialty conference on cold-formed steel structures, St. Louis, Missouri, USA, 7–8 Nov 2018
14. Roy K, Ting TCH, Lau, HH, Lim JBP (2018) Experimental investigation into the behaviour of CFS built-up channels subjected to axial compression. In: International conference on the

- trends and recent advances in civil engineering-TRACE-2018, Noida, Uttar Pradesh, India, 23rd to 24th Aug 2018
15. Standards Australia (2005) Cold-formed steel structures. AS/NZS 4600:2005, Standards Australia/Standards New Zealand
 16. Stone TA, LaBoube RA (2005) Behaviour of cold-formed steel built-up I-sections. *Thin-Walled Struct* 43(12):1805–1817
 17. Ting TCH, Roy K, Lau HH, Lim JBP (2018) Effect of screw spacing on behavior of axially loaded back-to-back cold-formed steel built-up channel sections. *Adv Struct Eng* 21(3):474–487
 18. Whittle J, Ramseyer C (2009) Buckling capacities of axially loaded, cold-formed, built-up channels. *Thin-Walled Struct* 47(2):190–201
 19. Zhang JH, Young B (2012) Compression tests of coldformed steel I-shaped open sections with edge and web stiffeners. *Thin-Walled Struct* 52:1–11

Experimental Investigation into the Behaviour of CFS Built-Up Channels Subjected to Axial Compression



Krishanu Roy, Tina Chui Huon Ting, Hieng Ho Lau and James B. P. Lim

Abstract Cold-formed steel (CFS) structural elements are emerging as the preferred solution for many commercial and industrial buildings in the construction industry; thus, the use of built-up CFS channel sections is inevitable. Available design rules, for such back-to-back built-up sections, prescribe modified slenderness approach as mentioned in the AISI and AS/NZS. In the literature, very few results are available for such built-up sections. Sixty experimental tests are reported in this paper, which were conducted on CFS built-up channel sections, connected back-to-back by intermediate fasteners. Tests were conducted for different values of slenderness from short-to-long columns. Results from these built-up column tests are discussed in the context of load–axial shortening relationship, buckling modes and deformed shapes. Experimental results are compared with the AISI and AS/NZS design strengths. Comparison shows that the design strength is approximately 15% more conservative as a whole; however, it overestimates the capacity of built-up columns governed by local buckling failure.

Keyword CFS · Back-to-back channels · Built-up channels · Buckling · Fasteners

Notation

A' Total web width
 A_e Effective cross-sectional area

K. Roy (✉) · J. B. P. Lim
Department of Civil and Environmental Engineering,
University of Auckland, Auckland, New Zealand
e-mail: kroy405@aucklanduni.ac.nz

T. C. H. Ting
Faculty of Engineering and Science, Curtin University Malaysia, Miri, Sarawak, Malaysia

H. H. Lau
Faculty of Engineering, Computing and Science, Swinburne University
of Technology Sarawak Campus, Kuching, Sarawak, Malaysia

© Springer Nature Singapore Pte Ltd. 2019
S. Pulugurtha et al. (eds.), *Advances in Transportation Engineering*,
Lecture Notes in Civil Engineering 34,
https://doi.org/10.1007/978-981-13-7162-2_8

B'	Total flange width
C'	Total lip width
t	Section thickness
COV	Coefficient of variation
E	Young's modulus
F_n	Critical buckling stress
S	Longitudinal spacing between fasteners
λ_c	Non-dimensional slenderness ratio

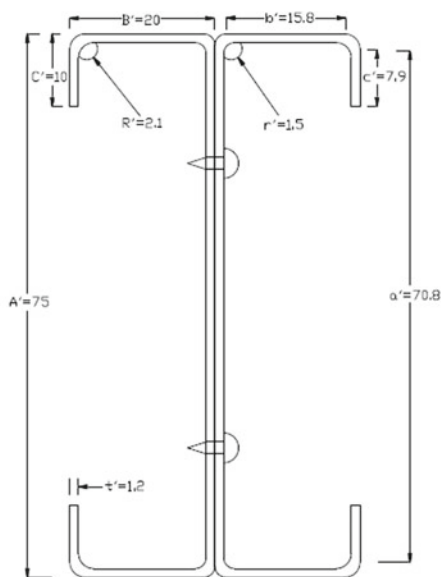
1 Introduction

The increasing needs for innovation to cater for construction needs have led to the development of cold-formed steel (CFS) industry. CFS is very much used due to benefits such as ease of construction, and its high strength to weight ratio, which allows economical and effective design of structural members. One of the innovations is the CFS built-up channels connected back-to-back at the webs (see Fig. 1). It is very effective to use built-up I-section for large span beam and column members. These built-up sections can carry higher loads and can be used for larger spans, e.g. columns in warehouse or shopping malls, steel trusses, portal frames, space frames and wall frames. Current design standards use the modified slenderness approach to estimate the axial capacity of CFS built-up columns based on the design guidelines from the American Iron and Steel Institute [1] and the Australian and New Zealand Standards (AS/NZS 4600:2005) [21]. However, the effectiveness of the modified slenderness approach has not been justified for CFS, unlike hot-rolled steel built-up columns.

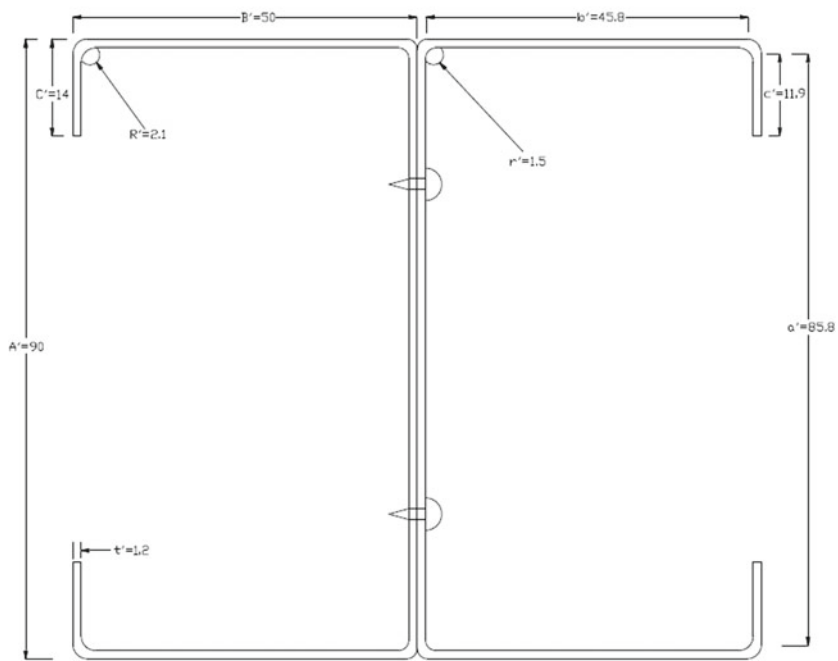
Very few literature are available on determining the compressive capacity of CFS built-up channel sections with the configuration in Fig. 1. The authors studied the effect of different fastener spacings in [23], and the influence of thickness in [11] on the capacity of CFS built-up back-to-back channel columns connected at the webs of two channels.

Previous research involves various forms of built-up sections. Piyawat et al. [7] studied on back-to-back built-up columns connected by welds. Zhang and Young [25] researched on CFS built-up columns connected back-to-back with an opening at the web (see Fig. 2). There was also investigation on the axially loaded welded built-up sections connected at the toes done by Whittle and Ramseyer [24]. Other works on back-to-back built-up columns include [2, 5], while CFS built-up columns connected by intermediate screws and wood sheathed were investigated experimentally by Fratamico et al. [6].

Due to limited studies, research on other forms of built-up section serves as important references as well. Dabaon et al. [4] studied on CFS built-up battened columns. They found that the design standards, which include AISI and AS/NZS and the Eurocodes, are un-conservative for columns governed by local buckling failure but are conservative for columns governed by flexural buckling failure. Roy et al. [10,



(a) BU75

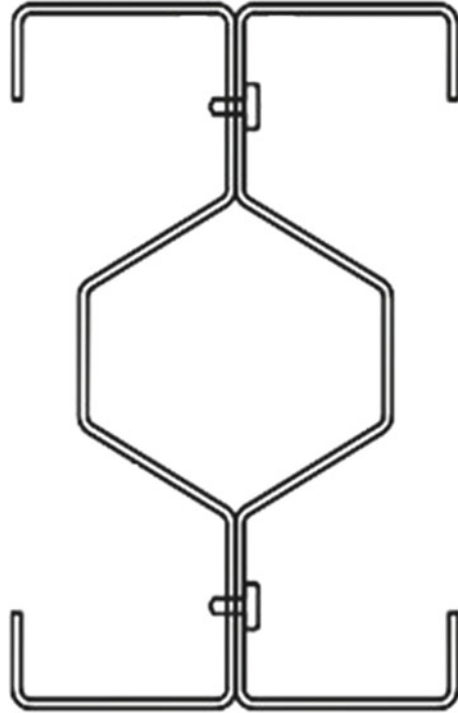


(a) BU90

*Dimensions are in mm

Fig. 1 Dimensions of the investigated CFS built-up channel sections

Fig. 2 Built-up CFS section investigated by Young and Zhang [22]



[13, 18] also studied, experimentally and numerically, the axial capacity of back-to-back gapped built-up cold-formed steel-lipped channel sections and concluded that the current design guidelines by AISI and AS/NZS can be too conservative in predicting the axial capacity of such columns. Also, investigated by Roy et al. [12], the behaviour of built-up CFS un-lipped channel sections, connected back-to-back, subjected to compressive force. The cold-formed built-up stainless steel sections under compression were considered by Roy et al. [9, 14, 15, 20]. Axial load capacity of cold-formed steel sections was investigated by Ramseyer [8]. On the other hand, built-up CFS channels connected face-to-face were tested under compression by Roy et al. [16, 17].

This paper presents 60 experimental test results conducted on axially loaded back-to-back built-up CFS channels. Material properties and initial imperfections were determined for all test specimens. The test results are analysed in terms of failure loads, deformed shapes and load–deflection behaviour for two types of cross section, BU75 and BU90, at various lengths of 0.3–2 m. When the experimental strengths were compared against the AISI and AS/NZS, design guidelines are generally safe for columns governed by overall buckling failure, however, are unsafe for built-up channels governed mainly by local buckling failure. A finite element model is presented for these built-up columns by the authors in another paper [19].

2 Current Design Rules as Per AISI and AS/NZS

The theoretical results of the built-up columns investigated were calculated based on the relevant clauses in the American Iron and Steel Institute specifications and the Australia/New Zealand standard. These calculated strengths were later used for comparison with the test strengths. The axial strength for built-up CFS columns is calculated according to the equations from AISI and AS/NZS as follows:

$$P_{AISI} = A_e F_n \quad (1)$$

The critical buckling stress (F_n) is determined as below:

$$\text{For } \lambda_c \leq 1.5 \quad F_n = (0.658 \lambda_c^2) F_y \quad (2)$$

$$\text{For } \lambda_c > 1.5 \quad F_n = \left(\frac{0.877}{\lambda_c^2} \right) F_y \quad (3)$$

The non-dimensional critical slenderness (λ_c) is calculated using Eq. 4:

$$\lambda_c = \sqrt{\frac{F_y}{F_e}} \quad (4)$$

Modified slenderness ratio was used for all calculations as per Eq. 5.

$$\left(\frac{KL}{r} \right)_{ms} = \sqrt{\left(\frac{KL}{r} \right)_o^2 + \left(\frac{s}{r_{yc}} \right)^2}; \quad \text{For which } \left(\frac{s}{r_{yc}} \right) \leq 0.5 \left(\frac{KL}{r} \right)_o \quad (5)$$

3 Experimental Investigations

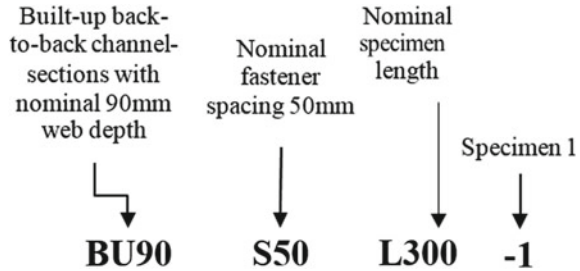
3.1 Test Specimens

The column specimens consist of channel sections of C75 and C90 as shown in Fig. 1. Built-up column specimen dimension is also shown in Table 1. In total, 60 built-up columns were tested, with four different column heights from 0.3 to 2 m. All the columns were loaded under axial compression and under pin-ended boundary conditions on both ends of the columns, except the stub column (0.3 m), which was loaded under fixed ended boundary conditions. As shown in Table 1, the following fastener spacings were considered in the test programme.

Table 1 Fastener spacing

Column height (m)	Screw spacing (m)		
	Five locations	Three screw locations	Two screw locations
0.3	0.050	0.100	0.200
0.5	0.100	0.200	0.400
1.0	0.225	0.450	0.900
2.0	0.475	0.950	1.900

Fig. 3 Specimen labelling



3.2 Determination of Material Properties

The material properties, i.e. the modulus of elasticity and yield stress, were determined using tensile coupon tests in accordance with the British Standard for Testing and Materials [3]. The coupons were cut from both longitudinal and transverse directions with width and gauge length in accordance with the testing standards at 12.5 mm and 50 mm, respectively. A test machine MTS was used to conduct the tensile coupon tests. Load was applied through displacement control. An extensometer of 50 mm gauge length was used to record the strain values. Two strain gauges were also used to measure the strain values. The tensile coupon tests for longitudinal and transverse coupons yield an averaged result of 207 MPa for modulus of elasticity and 560 MPa for yield stress.

3.3 Labelling

Types of the built-up section, fastener spacing, nominal specimen length and test specimen number were coded by the specimen labelling. For example, specimen coding for BU90-S50-L300-1 is shown in Fig. 3. The specimen label shows that the depth of the channel (i.e. the width of the web) is 90 mm as denoted by BU90. BU stands for built-up section. Fastener spacing is denoted by S (50 mm), and the length of the built-up column is 300 mm, as denoted by L. At the end of the label, the number 1 is used to express the specimen number as 1.

3.4 Test Setup and Loading Procedure

All the built-up columns were loaded with the help of a Universal Testing Machine (UTM) (see Fig. 4). The capacity of the UTM was 600 kN. A constant loading rate (below 25 kg/cm²/s) was maintained during the load application. Six LVDTs were used for short, intermediate and slender built-up column tests, while three LVDTs were used for stub columns. Figure 4 illustrates the locations of the LVDTs, with one LVDT measuring the longitudinal direction for axial shortening, while all other LVDTs measure the transverse direction for lateral displacement of the built-up columns. The failure load was recorded by an external load cell in between the bottom of the specimen and the base plate.

3.5 Initial Imperfection Measurement

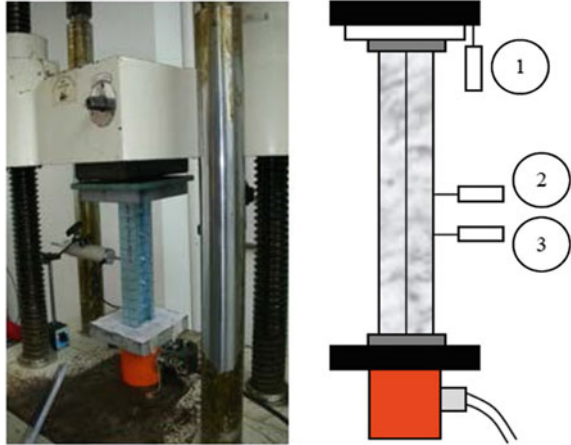
Initial imperfections are caused in cold-formed steel sections because of fabrication error and transportation problem. It is very important to include those geometric imperfections in finite element models to validate the results of experimental tests. An imperfection measurement setup is shown in Fig. 5a. The imperfection measurement was conducted on all test specimens using an LVDT of 0.001 mm precision at an interval of 20 mm. LVDT positions for imperfection measurements are shown in Fig. 5b. In Fig. 5c, initial imperfections are plotted against the length of the built-up columns for BU90S200L300-1. It was found that the maximum imperfections for the test specimens were 0.2 mm for 0.3 m specimen, 0.2 mm for 0.5 m specimen, 0.4 mm for 1 m specimen and 0.6 mm for 2 m specimen. These values can be used as imperfections input for the finite element models to yield a better axial capacity prediction for the test specimens [16].

3.6 Results from Experimental Tests

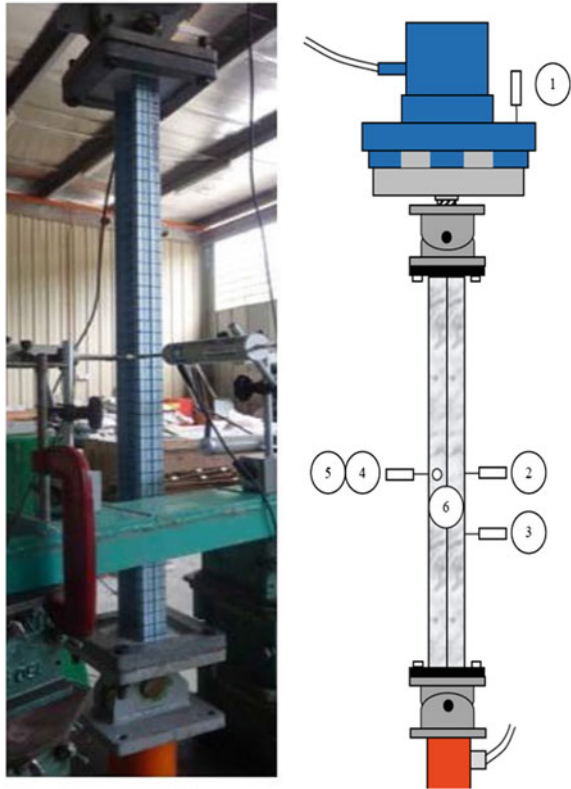
Table 2 summarises the dimensions of the built-up specimens tested and the respective experimental failure loads (P_{EXP}). In order to compare the experimental results to the design strength, AISI and AS/NZS strengths are also included in Table 2a for BU75 and Table 2b for BU90. The modified slenderness's of all test specimens are calculated and shown in Table 2. Comparison of design and test strengths shows that columns governed by global buckling failure are conservatively predicted by the design standard; however, columns governed by local buckling failure (i.e. stub columns) are un-conservatively predicted by the design standard.

Graph of load versus axial shortening for BU75S50L300-1 is shown in Fig. 6. The graph shows a linear relationship between the load and axial shortening up to 70% (85 kN) of the failure load (120.7 kN) for BU75S50L300-1. Plastic behaviour

Fig. 4 Built-up column test setup



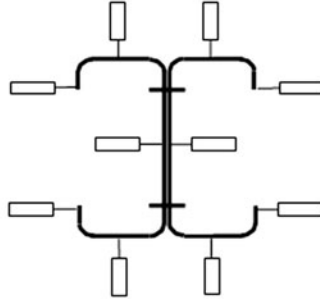
(a) 0.3 m high built-up column test



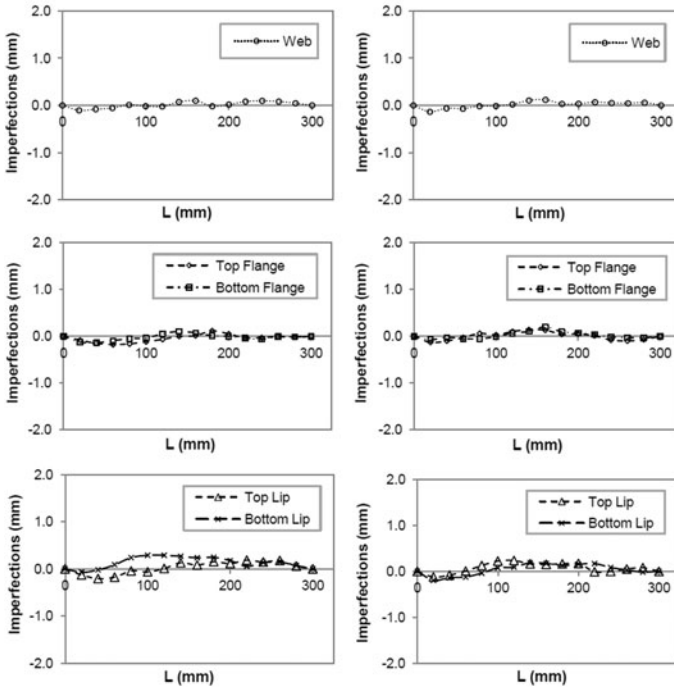
(b) 1 m high built-up column test



(a) Photo of the imperfection measurement setup



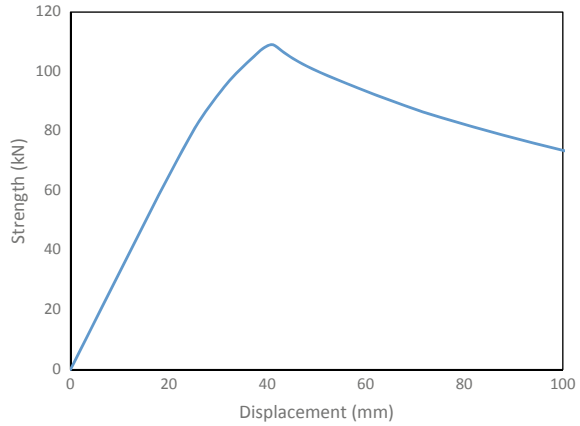
(b) Position of LVDTs for imperfection measurement



(c) Initial imperfections for BU90-S200-L300-1

Fig. 5 Details of imperfection measurements

Fig. 6 Typical experimental test results for stub column of BU 75 series with five screws



was observed for BU75S50L300-1, when the load was increased beyond 85 kN and the non-linear behaviour continued up to the failure.

It was observed that at different slenderness, the columns are governed by different failure modes. It was also noticed that the behaviour of the built-up columns is significantly influenced by the change in screw spacing except for stub columns. The stub columns from both BU75 and BU90 were governed by local buckling failure. This happens even when the screw spacing was decreased from 5 to 3. No distortional buckling was observed. Although two channels in a built-up section buckled separately between the screws (see Fig. 7a), both BU75S200L300 and BU90S200L300

Table 2 Experimental test results

Specimen	Web	Flange	Lip	Length	Thickness	Spacing	Modified slenderness	Test results	AISI and AS/NZS design strengths	
	A'	B'	C'	L	t	S	$(KL/r)_m$	P _{EXP}	P _{AISI}	P _{Exp} /P _{AISI}
	(mm)	(mm)	(mm)	(mm)	(mm)	(mm)	–	(kN)	(kN)	–
<i>(a) BU75</i>										
<i>Stub</i>										
BU75S50L300-1	73.1	19.8	11.1	273.0	1.20	50.0	15.63	120.7	126.68	0.95
BU75S50L300-2	73.1	19.8	11.2	280.1	1.21	50.0	15.93	118.8	126.77	0.94
BU75S50L300-3	72.7	19.5	10.8	270.0	1.20	50.9	15.92	118.7	124.84	0.95
BU75S100L300-2	73.1	19.8	11.2	267.2	1.18	99.7	19.48	117.5	125.1	0.94
BU75S100L300-3	73.1	19.9	11.2	273.0	1.19	100.2	19.41	122.7	125.41	0.98
BU75S100L300-4	73.6	19.7	11.2	273.3	1.20	99.5	19.56	115.4	124.89	0.92
BU75S200L300-1	73.7	19.8	11.2	266.4	1.21	200.0	30.31	122.5	119.05	1.03
BU75S200L300-2	73.6	19.9	11.2	266.5	1.20	199.5	30.22	119.1	119.09	1.00
BU75S200L300-3	72.9	20.0	11.2	268.4	1.20	200.0	29.97	113.1	119.36	0.95
Mean										0.96
COV										0.04

(continued)

Table 2 (continued)

Specimen	Web	Flange	Lip	Length	Thickness	Spacing	Modified slenderness	Test results	AISI and AS/NZS design strengths	
	A'	B'	C'	L	t	S	(KL/r) _m	P _{EXP}	P _{AISI}	P _{EXP} /P _{AISI}
	(mm)	(mm)	(mm)	(mm)	(mm)	(mm)	–	(kN)	(kN)	–
<i>Short</i>										
BU75S100L500-1	73.6	19.8	11.2	655.0	1.20	100.0	69.11	83.0	78.881	1.05
BU75S100L500-3	73.6	19.7	11.2	680.0	1.21	100.5	72.16	74.1	78.376	0.95
BU75S200L500-1	73.5	19.5	11.3	653.0	1.20	195.0	73.36	86.2	79.992	1.08
BU75S200L500-2	73.6	19.6	11.3	678.0	1.18	195.0	75.58	88.9	81.406	1.09
BU75S200L500-3	73.4	19.7	11.3	680.0	1.19	200.5	75.61	93.6	86.759	1.08
BU75S400L500-1	73.6	19.7	11.3	678.0	1.20	400.0	88.74	74.8	72.417	1.03
BU75S400L500-2	73.5	19.7	11.3	679.0	1.22	401.0	89.00	80.6	74.336	1.08
Mean										1.05
COV										0.05
<i>Intermediate</i>										
BU75S225L1000-1	75.3	20.2	10.4	1133.1	1.20	225.3	121.36	47.0	42.34	1.11
BU75S225L1000-2	75.7	19.9	10.4	1131.2	1.20	225.3	123.71	46.3	41.05	1.13
BU75S450L1000-1	75.8	19.9	10.4	1131.6	1.21	447.0	133.91	50.4	38.98	1.29
BU75S450L1000-2	75.6	19.9	10.4	1133.4	1.20	450.0	135.07	45.0	38.12	1.18
BU75S450L1000-3	75.9	19.8	10.3	1182.2	1.18	450.0	140.52	41.8	34.62	1.21
BU75S900L1000-1	76	19.9	10.3	1131.3	1.19	900.0	171.43	39.9	33.21	1.20
BU75S900L1000-2	76.3	19.8	9.1	1133.4	1.20	900.0	178.06	33.7	30.29	1.11
BU75S900L1000-3	75.9	19.8	10.3	1183.3	1.22	901.0	176.55	31.5	28.91	1.09
Mean										1.17
COV										0.07
<i>Slender</i>										
BU75S475L2000-2	73.9	20.3	10.7	2184.4	1.20	474.5	231.20	10.9	10.27	1.03
BU75S475L2000-3	73.6	20.2	10.8	2183.6	1.20	462	231.61	10.8	10.22	1.03
BU75S950L2000-2	73.5	20.3	10.8	2184.2	1.18	949.5	255.17	8.8	8.43	1.02
BU75S950L2000-3	73.4	20.2	10.8	2184.4	1.17	950.0	256.21	8.6	8.36	1.01
BU75S1900L2000-2	73.1	20.3	10.9	2183.2	1.18	1900.0	334.82	7.6	7.34	1.03
BU75S1900L2000-3	73.7	20.4	10.7	2184.2	1.19	1901.0	333.86	7.5	7.31	1.01
Mean										1.02
COV										0.01
<i>(b) BU90</i>										
<i>Stub</i>										
BU90S50L300-1	91.3	49.8	14.6	277.0	1.20	50.0	7.95	172.5	179.7	0.96
BU90S50L300-2	91.8	49.7	14.5	272.0	1.19	49.8	7.89	171.6	182.6	0.94
BU90S50L300-3	92.9	49.4	14.5	261.0	1.21	50.0	7.93	170.6	179.6	0.95
BU90S100L300-1	90.8	49.7	14.6	262.0	1.20	99.9	9.45	166.2	178.7	0.93
BU90S100L300-2	90.6	49.5	14.6	268.0	1.18	100.0	9.42	165.8	176.4	0.94
BU90S200L300-1	90.7	49.4	14.6	273.5	1.18	201.0	11.93	163.3	175.6	0.93

(continued)

Table 2 (continued)

Specimen	Web	Flange	Lip	Length	Thickness	Spacing	Modified slenderness	Test results	AISI and AS/NZS design strengths	
	A'	B'	C'	L	t	S	$(KL/r)_m$	P _{EXP}	P _{AISI}	P _{EXP} /P _{AISI}
	(mm)	(mm)	(mm)	(mm)	(mm)	(mm)	–	(kN)	(kN)	–
BU90S200L300-2	90.7	49.4	14.6	269.5	1.20	199.0	11.83	163.5	173.9	0.94
BU90S200L300-3	89.5	48.3	14	280.5	1.20	199.0	11.87	162.9	173.3	0.94
BU90S50L300-1	91.3	49.8	14.6	277.0	1.20	50.0	7.95	172.5	179.7	0.96
Mean										0.94
COV										0.01
<i>Short</i>										
BU90S100L500-1	90.6	49.5	14.6	656	1.21	100.5	35.42	160.4	149.9	1.04
BU90S100L500-2	90.6	49.4	14.6	678	1.20	100.5	34.25	158.1	152.0	1.08
BU90S200L500-1	90.4	49.3	14.7	653	1.18	199.5	38.52	152.2	140.9	1.09
BU90S200L500-2	90.4	49.3	14.7	678	1.19	199.5	39.41	150.9	138.4	1.10
BU90S200L500-3	90.4	49.3	14.6	680	1.21	200.5	40.20	149.2	135.6	1.06
BU90S400L500-1	90.6	49.4	14.7	678	1.18	400.0	50.20	132.4	124.9	1.06
BU90S400L500-2	90.4	49.4	14.7	678	1.20	399.0	49.41	134.5	126.9	1.07
Mean										1.07
COV										0.02
<i>Intermediate</i>										
BU90S225L1000-1	90.8	49.6	14.4	1182	1.21	225.0	60.42	102.6	92.43	1.11
BU90S225L1000-2	90.6	49.6	14.3	1132	1.20	225.0	58.21	102.0	92.72	1.10
BU90S450L1000-1	90.6	49.7	14.4	1130	1.21	450.0	64.21	96.51	86.18	1.12
BU90S450L1000-2	90.4	49.7	14.4	1182	1.18	448.0	66.21	94.42	82.79	1.14
BU90S450L1000-3	90.5	49.8	14.5	1180	1.19	452.0	65.29	93.33	82.54	1.13
BU90S900L1000-1	90.5	49.6	14.4	1131	1.20	897.0	75.21	89.55	82.89	1.08
BU90S900L1000-2	91.0	49.3	14.4	1182	1.21	899.0	77.21	87.58	80.31	1.09
BU90S900L1000-3	90.1	49.2	14.5	1129	1.22	896.0	76.50	87.51	79.51	1.10
Mean										1.11
COV										0.07
<i>Slender</i>										
BU90S475L2000-1	90.6	49.5	14.5	2164	1.20	474.2	92.52	65.4	61.12	1.07
BU90S475L2000-2	90.7	49.4	14.3	2172	1.20	466.6	94.42	66.01	61.63	1.07
BU90S950L2000-1	90.5	49.5	14.6	2169	1.18	960.4	101.17	54.02	50.90	1.06
BU90S950L2000-2	90.4	49.2	14.5	2148	1.17	949.3	103.21	45.62	43.41	1.05
BU90S1900L2000-1	90.5	49.3	14.6	2158	1.18	1902.4	115.20	48.04	44.8	1.07
BU90S1900L2000-2	90.9	49.7	14.2	2152	1.19	1906.7	116.42	43.21	41.14	1.05
Mean										1.06
COV										0.02

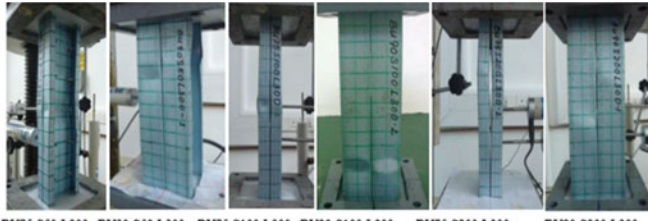
test specimens had two fasteners each. Due to less number of fasteners, the back-to-back channels pry apart at the mid-height of the built-up column. For short column of BU75 series, local buckling was the pre-dominant mode of failure at the start of the test; however, at the end of the test global buckling was observed for BU75 columns having two fasteners (see Fig. 7b). For intermediate columns of both test series, mostly overall buckling was seen (see Fig. 7c). However, some columns of BU90-L1000 failed through flexural–torsional buckling. Most of the slender columns were dominated by overall buckling failure, showing a large lateral deformation at the middle of the columns (see Fig. 7d). Some failure modes of slender columns of BU90 series were governed by local–global buckling interactions. Once the columns reached failure load, the built-up specimens showed local deformation on the compression side at the mid-height.

4 Comparison with Design Standards

The experimental and theoretical results for BU75 and BU90 are tabulated in Table 2(a) and 2(b), respectively. The theoretical results are calculated using the design steps documented in AISI and AS/NZS, which involves the modified slenderness approach. Comparison of the experimental and theoretical results shows that the design standard is on average 12% more conservative in predicting the capacity of columns governed by overall buckling failure; however, prediction for stub columns governed by local buckling failure was approximately 10% un-conservative.

Table 2a, b also shows that the influence of fastener spacing is negligible in stub and slender columns; however, the effect is significant for short and intermediate columns. Fastener spacing is influential on slender columns because the test specimens failed in global buckling. For short and intermediate columns, the increment of twice the screw spacing reduced the axial strength by approximately 5–10% and 10–15%, respectively.

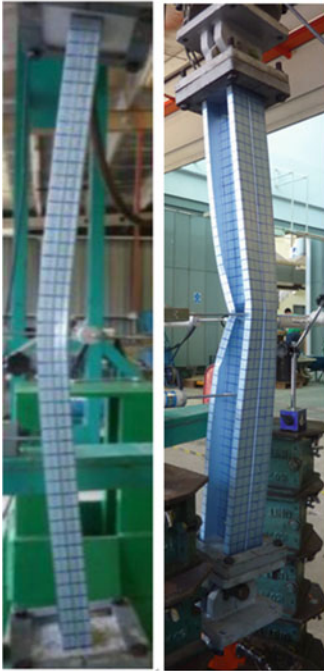
Graph of design strength versus modified slenderness ratio was plotted on BU75 in Fig. 8a and BU90 on Fig. 8b. Figure 8a shows that at modified slenderness ratio of less than 32, local buckling failure is dominant, while, at modified slenderness ratio of greater than 53, global buckling failure is dominant. Similar trend is observed in the BU90 series in Fig. 8b. Local buckling failure was noticed when the modified slenderness is less than 29, and global buckling failure was observed when the modified slenderness ratio was greater than 48. The behaviour of the slender columns was as anticipated, whereby there was minimal increase in axial strength when the number of screws increases. Generally, the design standards are conservative when overall buckling governed the failure mode of the columns but un-conservative by approximately 10% when local buckling dominated the column's failure mode.



BU75-S50-L300 BU90-S50-L300 BU75-S100-L300 BU90-S100-L300 BU75-S200-L300 BU90-S200-L300
(a) Stub column



BU75-S200-L500 BU90-S200-L500
(b) Short column



BU75-S225-L1000 BU90-S225-L1000
(c) Intermediate column



BU75-S950-L2000 BU90-S950-L2000
(d) Slender column

Fig. 7 Built-up columns at failure

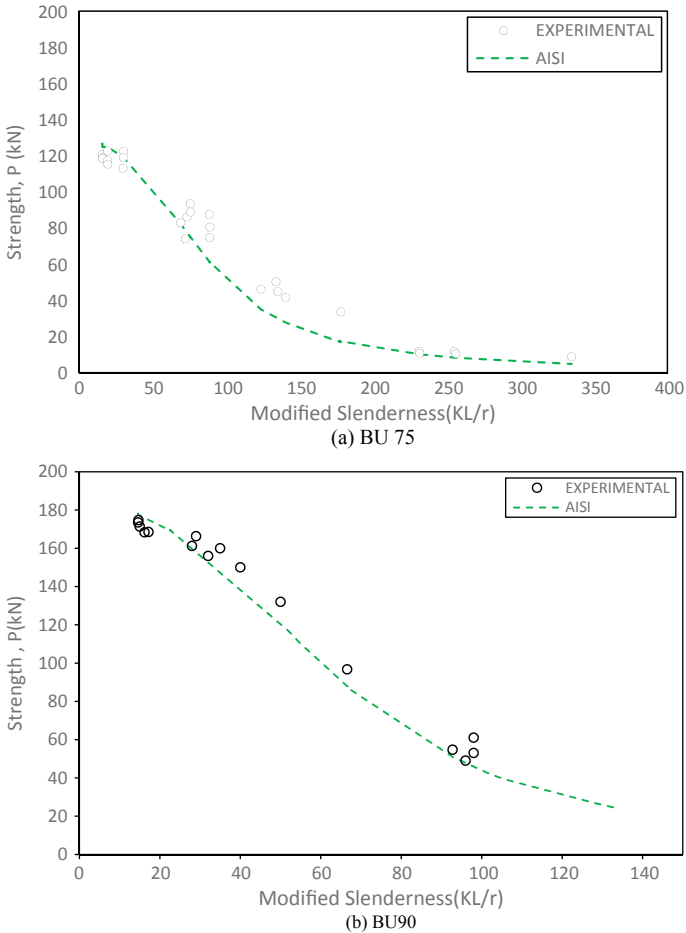


Fig. 8 Plot of axial strength against the modified slenderness

5 Conclusions

This paper presented a total of 60 experimental tests on axially loaded back-to-back built-up CFS channel sections for investigation. The material properties and geometric imperfections for all specimens were measured. Two cross sections, BU75 and BU90, at varying lengths from 0.3 to 2 m were involved in the investigation. The failure modes and load carrying capacities at failure were compared and analysed. Comparison of test results and design strength from AISI and AS/NZS shows that the column capacity predicted by the design standards is conservative for specimens with overall buckling failure but un-conservative for specimens with local buckling failure.

Ongoing work will aim to develop better design methods, for different types of CFS built-up columns, with improved approximations of the column cross sections and end conditions. The authors are following this work to further develop a numerical model to study the different parameters affecting the strength of back-to-back built-up CFS columns including explicit modelling of web fasteners.

References

1. American Iron and Steel Institute (2012) North American specification for the design of cold-formed steel structural members, NAS S100
2. Anbarasu M, Bharath KP, Sukumar S (2014) Study on the capacity of cold-formes steel built-up battened colums under axial compression. *Latin Am J Solids Struct* 11(12):1375–2271
3. BS EN (2001) Tensile testing of metallic materials method of test at ambient temperature, British Standards Institution
4. Dabaon M, Ellobody E, Ramzy K (2015) Nonlinear behavior of built-up cold-formed steel section battened columns. *J Constr Steel Res* 110:16–28
5. Fratamico DC, Schafer BW (2014) Numerical studies on the composite action and buckling behavior of built-up cold-formed steel columns. In: 22nd international specialty conference on cold-formed steel structures, St. Louis, MO
6. Fratamico DC, Torabian S, Rasmussen KJR, Schafer BW (2016) Experimental studies on the composite action in wood-sheathed and screw-fastened built-up cold-formed steel columns. In: Proceedings of the annual stability conference structural stability research council, Orlando, FL
7. Piyawat K, Ramseyer C, Kang Thomas H-K (2013) Development of an axial load capacity equation for doubly symmetric built-up cold-formed sections. *J Struct Eng Am Soc Civil Eng* 139(12):04013008–13
8. Ramseyer CCE (2006) Axial load capacity of cold-formed steel sections, PhD dissertation, University of Oklahoma, Norman, USA
9. Roy K, Lim JBP (2018) Numerical investigation into the buckling behaviour of face-to-face built-up cold-formed stainless steel channel sections under axial compression. *Structures* (revised)
10. Roy K, Ting TCH, Lau HH, Lim JB (2018) Nonlinear behaviour of back-to-back gapped built-up cold-formed steel channel sections under compression. *J Constr Steel Res* 147:257–276
11. Roy K, Ting TCH, Lau HH, Lim JB (2018) Effect of thickness on the behaviour of axially loaded back-to-back cold-formed steel built-up channel sections—experimental and numerical investigation. *Structures* 16:327–346
12. Roy K, Ting TCH, Lau HH, Lim JB (2018) Nonlinear behavior of axially loaded back-to-back built-up cold-formed steel un-lipped channel sections. *Steel Compos Struct Int J* 28(2):233–250
13. Roy K, Ting TCH, Lau HH, Lim JBP (2018) Compression tests on back-to-back gapped built-up cold-formed steel channel sections. In: Proceedings of the international conference on engineering research and practice for steel construction 2018 (ICSC 2018), Hong Kong, China
14. Roy K, Lau HH, Lim JBP (2018) Finite element modelling of back-to-back built-up cold-formed stainless-steel lipped channels under axial compression. *Steel Compos Struct Int J*, under review
15. Roy K, Ting TCH, Lau HH, Lim JBP (2018) Effect of screw spacing into the behaviour of back-to-back cold-formed duplex stainless steel built-up channel sections under compression. In: Proceedings of the international conference on engineering research and practice for steel construction 2018 (ICSC 2018), Hong Kong, China
16. Roy K, Mohammadjani C, Lim JB (2018) Experimental and numerical investigation into the behaviour of face-to-face built-up cold-formed steel channel sections under compression. *Thin-Walled Struct* 134:291–309

17. Roy K, Ting TCH, Lau HH, Lim JBP (2018) Experimental and numerical investigations on axial capacity of CFS built-up box sections. *J Constr Steel Res* (revised)
18. Roy K, Ting TCH, Lau HH, Lim JBP (2018) Experimental investigation into the behaviour of back-to-back gapped built-up cold-formed steel channel sections under compression. In: Wei-Wen Yu international specialty conference on cold-formed steel structures 2018, 7–8 November, 2018, St. Louis, Missouri, USA
19. Roy K, Ting TCH, Lau HH, Lim JBP (2018) Finite element modelling of built-up CFS channel columns under axial load. In: International conference on the 'Trends and recent advances in civil engineering-TRACE-2018', 23rd to 24th August, 2018, Noida, Uttar Pradesh, India
20. Roy K, Lau HH, Lim JBP (2019) Numerical investigations on the axial capacity of back-to-back gapped built-up cold-formed stainless steel channels. *Adv Struct Eng* (revised)
21. Standards Australia (2005) Cold-formed steel structures, AS/NZS 4600:2005, Standards Australia/ Standards New Zealand
22. Stone TA, LaBoube RA (2005) Behaviour of cold-formed steel built-up I-sections. *Thin-Walled Struct* 43(12):1805–1817
23. Ting TCH, Roy K, Lau HH, Lim JBP (2018) Effect of screw spacing on behavior of axially loaded back-to-back cold-formed steel built-up channel sections. *Adv Struct Eng* 21(3):474–487
24. Whittle J, Ramseyer C (2009) Buckling capacities of axially loaded, cold-formed, built-up channels. *Thin-walled Struct* 47(2):190–201
25. Zhang JH, Young B (2012) Compression tests of cold-formed steel I-shaped open sections with edge and web stiffeners. *Thin-Walled Struct* 52:1–11

Development of Speed Prediction Model for Mixed Traffic Conditions: Case Study of Urban Streets



Satyajit Mondal, Vijai Kumar Arya and Ankit Gupta

Abstract A microlevel analysis of vehicular speed is done to develop model between two mean speeds of vehicles such as time mean speed (TMS) and space mean speed (SMS) under mixed traffic stream. Traffic volume and speeds were collected on a mid-block section of an urban arterial to analyze different stream parameters. Vehicular composition along with the individual speed characteristics of each vehicle class was extracted from the collected field data. Models are framed between the speed characteristics of vehicles estimated from the field. A comparative analysis is also done with the existing traditional model to check the applicability of the suggested model. The result shows that the suggested models are reliable in forecasting vehicular speeds with higher accuracy.

Keywords Mid-block · Mixed traffic stream · Space mean speed (SMS) · Time mean speed (TMS) · Urban street

1 Introduction

Speed is one of the prime constraints in traffic and transportation engineering. In roadway, it plays an essential role in determining the capacity of roadway through traffic flow characteristics. Vehicular speed is also associated with the several roadway and traffic parameters such as geometric elements of the road, enhancement of vehicular and pedestrian's safety using several traffic control measures, consumption of fuel, and interrelated vehicle operating cost (VOC) for financial assessment of

S. Mondal · V. K. Arya · A. Gupta (✉)
Department of Civil Engineering, Indian Institute of Technology (BHU),
Varanasi 221005, UP, India
e-mail: anki_ce11@yahoo.co.in

S. Mondal
e-mail: satyajit07iest@gmail.com

V. K. Arya
e-mail: vkaryabd56@gmail.com

© Springer Nature Singapore Pte Ltd. 2019
S. Pulugurtha et al. (eds.), *Advances in Transportation Engineering*,
Lecture Notes in Civil Engineering 34,
https://doi.org/10.1007/978-981-13-7162-2_9

roadway projects [1]. The vehicular speed in traffic engineering is usually represented in two forms that are time mean speed (TMS) and space mean speed (SMS). Time mean speed is basically arithmetic mean of the vehicular speed traversing through the section or a point on a roadway. It is also denoted as the average spot speed of the vehicles. The speed of each vehicle class passing through the selected section is collected using laser gun and corresponding the arithmetically average of the speed is known as TMS as shown in Eq. 1.

$$v_t = \frac{1}{n} \sum_{i=1}^n v_i \quad (1)$$

where v_t is the TMS (km/h); v_i represents spot speed of the i th vehicle (km/h); n stands for a number of vehicles crossing the section in a specified time period.

Space mean speed is a statistical component and can be expressed as a mean speed of vehicle based on the average time spent of all vehicles to cross the segment. Therefore, the average travel time is weighted upon the length of the segment for each vehicle class to define SMS as shown in Eq. 2.

$$U_s = \frac{d}{\frac{1}{n} \sum_{i=0}^n t_i} \quad (2)$$

where U_s is the SMS (km/h); d signifies the length of the segment (km); t_i indicates the time required to cross the segment by an i th vehicle (hours); n stands for a number of vehicles crossing the section in a specified time period.

Being a microscopic parameter, speed has a significant impact on roadway and traffic elements especially the speed-flow analysis of a roadway section [2]. In developed countries, where the same type of vehicle is traveling with the same speed range has less effect on speed variance. Therefore, shorter consideration of roadway length gives the less erroneous result of SMS, whereas, in developing country like India, where a mixed traffic stream exists gives less accurate result in shorter roadway length consideration due to extensive range of static and dynamic characteristics of vehicles. Also, the existing methods of SMS estimation are too laborious and tedious for mixed traffic stream. Therefore, the present study put an effort to analyze and develop models between TMS and SMS based on collected speed data using laser technologies and vehicles travel time.

Many studies have been conducted to study the relationships between TMS and SMS over the years [5, 6, 8]. The conventional and most popular model which explains the relationship between TMS and SMS is given by Wardrop [9] shown in Eq. 3.

$$U_t = U_s + \frac{\sigma^2}{U_s} \quad (3)$$

where $\sigma^2 =$ Variance in SMS.

Highway capacity manual [4] has proposed a linear relationship between these two types of speed shown in Eq. 4.

$$S_R = 1.026 * S_T - 3.042 \quad (4)$$

Rakha and Zhang [7] emphasized that it is comparatively challenging to collect SMS data compared to TMS data. Accordingly, they proposed a relationship between these two speed parameters which assisted SMS from TMS result shown below:

$$U_s \approx U_t - \frac{\sigma^2}{U_t} \quad (5)$$

where $\sigma^2 =$ Variance of TMS.

They found that estimated SMS from the proposed model gives a less erroneous result with the higher statistical significance of R^2 value of 0.99. They also suggested that the distance used as a trap length should be such that the vehicle's length could be ignored while computing the vehicle speed.

Han et al. [3] have estimated the value of the expectation operator $E(v_i^2)$ using TMS values which were then incorporated to compute SMS of vehicles using the following equation:

$$\text{SMS} = \frac{3 \times \text{TMS} + \sqrt{9 \times \text{TMS}^2 - 8 \times E(v_i^2)}}{4} \quad (6)$$

2 Motivation

Considering all the conventional models, it can be observed that the variance of speed plays a vital role in the estimation of speeds. The difference in speeds for homogeneous traffic is relatively less in comparison with the variation in the speeds of mixed traffic within a defined period. Therefore, the application of these models might not yield realistic results under mixed traffic prevailing on Indian roads. Hence, there is a need for assessing the validity of these conventional models for mixed traffic and to propose an appropriate model which is suitable exclusively for mixed traffic conditions. Given these aspects, the objective of our study was formulated mainly to model SMS and TMS considering mixed conditions.

3 Data Collection and Extraction

Traffic survey conducted on VIP road in Kolkata city (India) and road stretch was selected such that there is no merging or diverging of vehicles in the given stretch. Also, there was no traffic signal or speed breaker on the stretch. Segment length

was chosen such that the vehicle dimension does not contribute significantly to the calculation of SMS. A camera was mounted on a high rise stand for capturing the vehicular movements both in peak and off-peak hours of the mixed traffic stream.

TMS data: Spot speed data were collected using a laser gun.

SMS data: Space mean speeds were calculated from the recorded video.

Different types of vehicles are considered for the study, and these vehicles are categorized as

1. Small cars (sc),
2. Big cars (bc),
3. Two wheelers (2W),
4. Buses,
5. Auto rickshaws (3W), and
6. Light Commercial Vehicles (LCV).

The hourly volume and composition of vehicles over the study stretch are shown in Figs. 1 and 2, respectively. A significant number of each vehicle type were observed traveling through the selected section in one hour shown in Fig. 2.

The Space Mean Speed (SMS) of the individual vehicle was measured by taking into account their entry and exit time, that is, the time required for a vehicle to cross the trap length of 60 m. The SMS is calculated by dividing the trap length with the time needed to traverse the segment, whereas the Time Mean Speed (TMS) data were collected using the laser-based instrument. The collected speed data were taken from the device and converted the speed into the frequency tables. The collected speed data are analyzed to estimate the operating speed for the traffic stream as well as for the individual vehicle category by plotting the cumulative frequency distribution

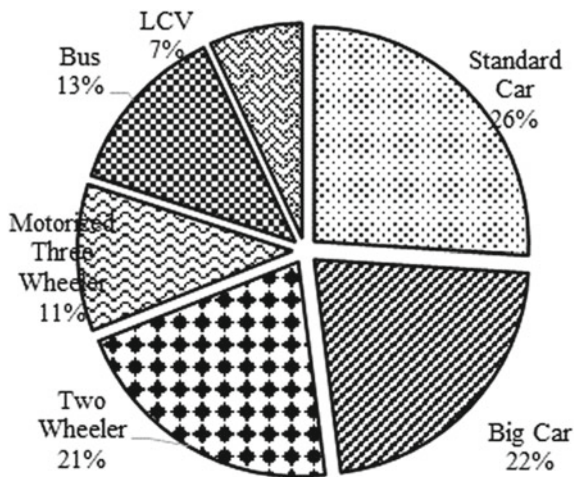


Fig. 1 Compositional share of vehicle type over the section

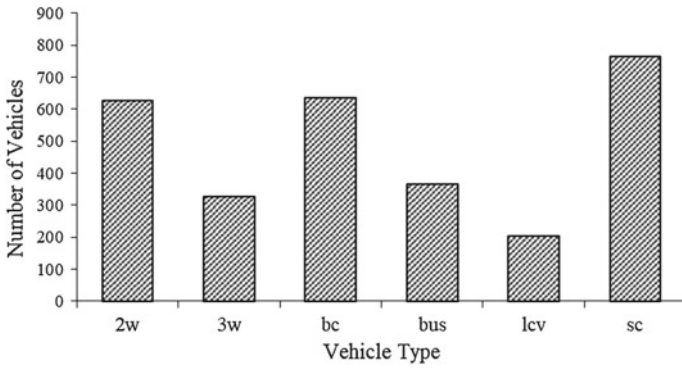


Fig. 2 Hourly traffic volume

with respect to the speed. The 85th percentile speed is considered as operating speed presented in Fig. 3 and Fig. 4, respectively.

Also, the variances in TMS and SMS for the individual vehicle are estimated and presented in Fig. 5.

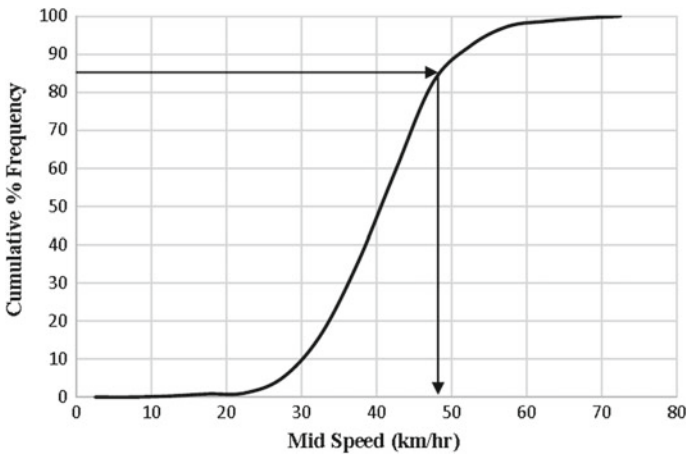


Fig. 3 Cumulative percentage frequency distribution of spot speed

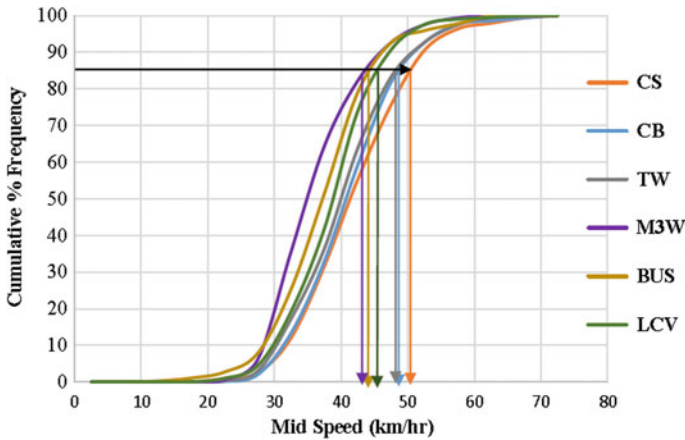


Fig. 4 Cumulative percentage frequency distribution of spot speed for individual vehicle categories

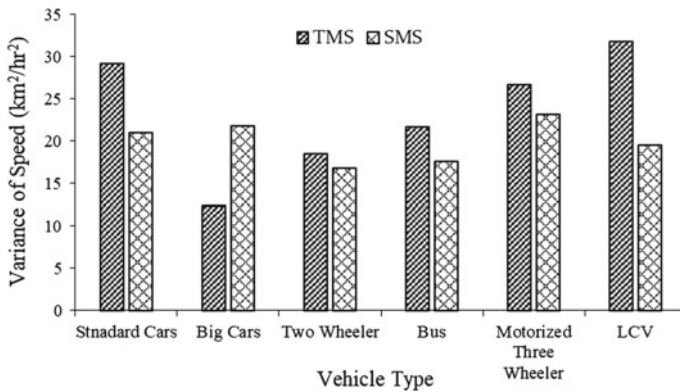


Fig. 5 Variance in TMS and SMS for each vehicle type

4 Model Development

4.1 Conventional Model

All the vehicle’s speed data collected through the videographic technique and laser-based instrument are processed to comprehend the characteristics of vehicle speeds through the correlation between the observed TMS and SMS. The R^2 value indicates that the observed SMS and TMS values do not have a strong correlation. As per the objective of the present study, TMS was assessed using the Wardrop equation. A correlation plot is drawn using observed and estimated TMS values shown in Fig. 6 with the help of Wardrop equation. The figure shows a poor estimation of TMS obtained using the conventional model.

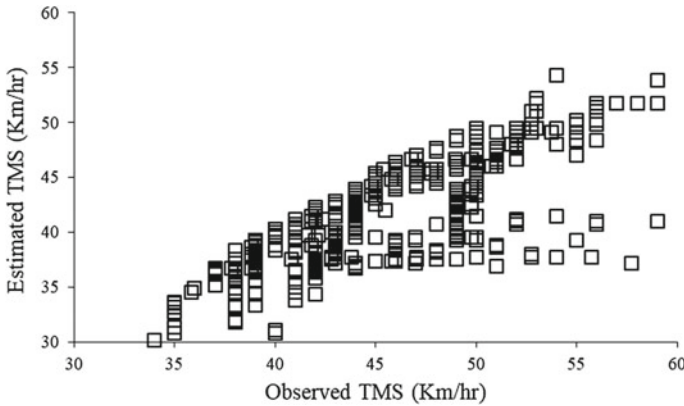


Fig. 6 Correlation between observed and estimated TMS

The less significance of the conventional model may be recognized because of higher variance in vehicle speeds due to the non-lane-based mixed traffic stream on Indian roads. Hence, it becomes imperious to modify the existing model to fit it with the non-lane-based Indian mixed traffic stream with sufficient accuracy.

4.2 TMS Model

Wardrop [9] considered the variances in vehicle’s speed to formulate a model which is primarily represented for lane-based homogeneous traffic conditions. As per the model description, TMS and SMS would give the same value under zero variance conditions, and TMS would always be more than or equal to SMS under any prevailing traffic condition. In homogeneous traffic conditions, the same type of vehicle is traveling through the section with less varying vehicles characteristics (vehicle static and dynamic parameters) results in the same amount of variance of speeds. Therefore, the influence of such parameters gives a lower value in variance of speeds for homogeneous traffic conditions. However, these parameters have a significant impact in providing a high variation in vehicular speeds under mixed traffic conditions.

Therefore, the predicted TMS values for mixed traffic conditions may be estimated by modifying the existing model using appropriate multiplication factors which can overcome the under-prediction problem. Furthermore, TMS should always be more than or equal to SMS under any traffic conditions. Taking into this account, various speed prediction models are framed based on linear and nonlinear practices. The suggested models in prediction of TMS are shown in Eqs. 7 and 8.

$$\text{Model 1 } U_t = a \times U_s + b \times \frac{\sigma^2}{U_s} \tag{7}$$

Table 1 Statistical result of the model parameters

	a	b	RMSE	R ²	Sample size
Wardrop	1	1	4.77	0.84	700
Model 1	1.077	1.541	3.27	0.93	700
Model 2	1.012	0.392	3.63	0.95	700

$$\text{Model 2 } U_t = (U_s)^a + \left(\frac{\sigma^2}{U_s}\right)^b \tag{8}$$

where a and b denote the model parameters.

These models are calibrated, and the corresponding coefficient values of the parameters are estimated using regression analysis. Table 1 shows the statistical results for both the models.

Table 1 shows that both the models have produced good statistical validity with lower values RMSE. The lower standard error represents the higher accuracy of the suggested models.

The suggested models are validated using another sample of 100 vehicles, and corresponding RMSE is determined using observed and estimated speed values. The suggested models are again compared with the Wardrop model [9] to determine their suitability for Indian mixed traffic conditions, shown in Table 2.

The table shows that both the models give more accurate results than the Wardrop model, where model 1 is more significant compared to model 2 in terms of RMSE. Figures 7 and 8 show the goodness of fit between observed and actual speed values obtained using both the models.

It can be observed from the above figures that projected speed values from model 1 are much closer to the diagonal line (45°) related to model 2 and can be used to predict the speed values of vehicles for Indian mixed traffic stream.

Table 2 Validation result of the suggested models

	Validation RMSE	Sample size
Wardrop	4.733	100
Model 1	2.945	100
Model 2	3.943	100

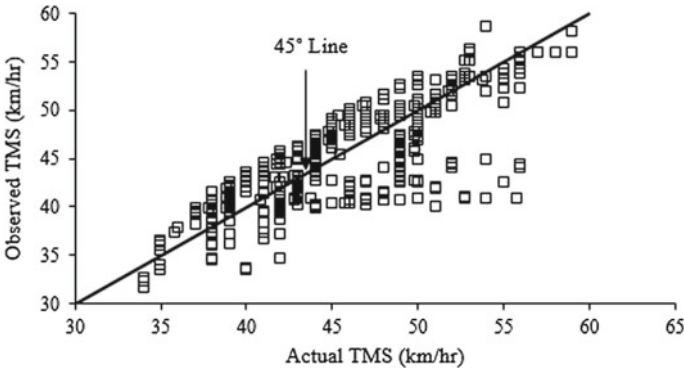


Fig. 7 Goodness of fit between observed and actual TMS for model 1

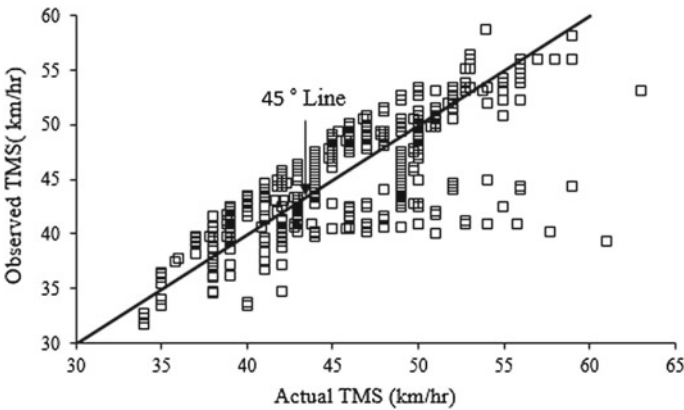


Fig. 8 Goodness of fit between observed and actual TMS for model 2

5 Conclusions

The present study focuses toward the analysis of the speed of vehicles, i.e., TMS and SMS on urban arterials under non-lane-based mixed traffic stream. The existing conventional and popular Wardrop [9] model is mainly developed for lane-based homogeneous traffic conditions and least suitable for a heterogeneous traffic stream. Vehicle speed data were collected from an urban mid-block section using video photographic technique and laser-based instrument. Required data were extracted from the collected field data to analyze and develop model between TMS and SMS. Two different models are developed using observed field data using regression technique. Comparative analysis is also done between the established models and conventional Wardrop model. Results show that model 1 gives the more significant result to predict the speed values as compared to model 2 and can be used to predict the speed values of vehicles for Indian mixed traffic stream.

References

1. Coifman B, Dhoorjaty S, Lee Z (2003) Estimating median velocity instead of mean velocity at single loop detectors. *Transp Res Part C* 11:211–222
2. Hall FL, Persaud BN (1989) Evaluation of speed estimates made from single-detector data from freeway traffic management systems. *Transportation research record*, vol 1232, Transportation Research Board, National Research Council. Washington, DC
3. Han J, Polak WJ, Barria J, Krishnan R (2010) On the estimation of space-mean-speed from inductive loop detector data. *Transp Plann Technol* 33(1):91–104
4. HCM (2000) Highway capacity manual. Transportation Research Board, National Research Council, Washington, DC
5. Li B (2009) On the recursive estimation of vehicular speed using data from a single inductance loop detector: a Bayesian approach. *Transp Res Part B* 43:391–402
6. Mikhalkin B, Payne H, Isaksen L (1972) Estimation of speed from presence detectors. *Highw Res Rec* 388:73–83
7. Rakha H, Zhang W (2005) Estimating traffic stream space-mean speed and reliability from dual and single loop detectors. *J Transp Res Board* 1925:38–47
8. Wang Y, Nihan LN (2003) Can single-loop detectors do the work of dual-loop detectors? *J Transp Eng* 129(2):169–176
9. Wardrop JG (1952) Some theoretical aspects of road traffic research. *Proc Inst Civil Eng* 1–2:325–378

Safety Assessment at Unsignalized Intersections Using Post-Encroachment Time's Threshold—A Sustainable Solution for Developing Countries



Madhumita Paul

Abstract India, a country with the highest number of road crashes and resulting injuries/deaths, has several issues associated with crash data for traditional safety analysis. For adequate and faster safety evaluation, traffic conflict technique using several proximal indicators is in practice worldwide. Among all indicators, Post-Encroachment Time (PET) is the most popular one for its easier measurement. However, accurate identification of critical conflicts based on PET threshold is still a gray area. For this purpose, four unsignalized intersections have been selected from the NCR India. This study is focused on identifying critical conflicts on the concept of perception-reaction time for emergency situations and adopted PET threshold of 1 s. This value of emergency perception-reaction is recommended by AASHTO (2001) for hazardous situations. Among various crossing situations, the maximum proportion of critical conflicts is found when through-moving vehicles are Two Wheelers (2W) followed by Light Commercial Vehicles (LCV). The appropriateness of the proposed method is verified by using 5 years' crash data for right-turn right angle and right-turn head-on collisions and finding a statistically significant relationship between these right-turn-related crashes and critical crossing conflicts. This study can be utilized as an effective tool to evaluate the safety at various traffic facilities where the collection of detailed crash data is a serious issue.

Keywords Unsignalized intersection · Proximal safety indicator · Post-encroachment time · Critical conflicts

1 Introduction

Road traffic crash is increasing at a rapid pace across the globe, and presently it is one of the leading causes of death. In developing countries like India, vehicle population and construction of good road networks are increasing rapidly. However,

M. Paul (✉)

Department of Civil Engineering, IIT Roorkee, Roorkee, Uttarakhand, India
e-mail: paul.madhu05@gmail.com

© Springer Nature Singapore Pte Ltd. 2019
S. Pulugurtha et al. (eds.), *Advances in Transportation Engineering*,
Lecture Notes in Civil Engineering 34,
https://doi.org/10.1007/978-981-13-7162-2_10

117

the lack of enforcement and policies are unable to deal with increasing traffic and have contributed to the significant increase in traffic crashes. Road crashes have earned India a dubious distinction.

The situation is worst at intersections locations. Within transportation system, an intersection is an operationally complex location where large numbers of conflict points are created, thus rendering it one of the most crash-prone locations. According to the latest ministry report, in India, about 37.8% of motor vehicle crashes occurred at intersections [1]. Most of the severe crashes and fatalities are found to occur more at unsignalized intersections that accounted for around 85% of crashes [1]. This is because, in India, most of the unsignalized intersections are uncontrolled, i.e., no signals or pavement markings are available to control the traffic. Additionally, traffic signs associated with the priority rules such as the stop and yield signs are not provided to a particular movement at these intersections. Even if any movement is prioritized with signs, many drivers do not follow those due to the nonexistence of enforcement. The priorities are basically established by the situations drivers perceive [2, 3]. At many instances, vehicles from all the directions attempt crossing and turning at the same time which increases the probability of crashes. The traffic rule in India is to keep left, and hence the maneuver of left-turning traffic is not a serious issue at intersection locations. On the other hand, the right-turning traffic of major/minor road has to wait for suitable gaps between through-traffic traveling along the major road to cross the road. If high traffic volume exists on the major road, drivers turning right from the major/minor road onto the minor/major road have to wait long for the adequate gaps. Due to that longer waiting time, many right turners lose their patience and demonstrate a tendency to cross over the intersection by accepting smaller gaps which may be dangerous [4]. While right turners are supposed to reduce their speed in order to take a turn, higher speed is observed for both right turnings and through traffic which increases the chances of severe collisions. Accordingly, critical conflict situations occur at frequent intervals between right turners and through traffic, which often lead to unsafe crossing situations and result in probable collisions.

Under such circumstances, drivers get engaged in many unsafe activities such as the sudden application of brakes, abrupt lane changes or not following lane discipline, etc. Therefore, traffic maneuvers at such intersections are highly complex and potentially very unsafe which have a direct influence on the higher crash rate observed at uncontrolled intersections. Due to all of the abovementioned facts, intersection safety becomes a serious public health issue which cannot always be solved merely by providing or making changes in signs and signals. Therefore, it is important to conduct rigorous and reliable safety analysis which will help to reduce the crash rate at uncontrolled intersection locations and enhance the road traffic safety significantly.

Traditionally, road safety evaluation has been performed using different statistical techniques based on historical crash data. There are several drawbacks associated with these types of analysis such as random and rare nature of accidents, underreporting of different types of accidents, improper documentation of accidents types, and their precise locations by the law enforcement officers. These observational errors negatively affect the accuracy and reliability of safety analysis. Over the past few

decades, researchers have identified traffic conflict as the best surrogate measure as it occurs more frequently than crashes and represents the nearness to the collision [5–9]. This indirect safety measure, traffic conflict technique, was originally developed by Perkins and Harris [10]. Traffic conflict analysis using proximal safety indicators has received widespread attention across the globe. The key benefit of these indicators is that they represent the temporal and spatial proximity characteristics of unsafe interaction and near accident [11]. Proximal safety indicators such as time to collision (TTC), time-exposed TTC, time-integrated TTC, deceleration rate (DR), proportion of stopping distance (PSD), etc. have been proposed by various researchers to assess the safety of a traffic facility using traffic conflict technique. However, these indicators are not easily measurable from the video recordings. One indicator which is most commonly used to identify the crossing conflicts between two road users is post-encroachment time (PET). It refers to the time interval between two instances when the first vehicle leaves a conflict point and the second vehicle enters into it. PET has all the essential properties of surrogate safety measure.

Similar to other surrogate measures, PET is estimated from observable non-crash events and indicates the resulting event of conflicts between vehicles, how closely a collision has been avoided. In fact, PET is a less resource-demanding indicator as it does not involve an estimation of vehicular speed and distance from the common conflict point as in the case of TTC [12]. To identify conflict as a critical one, a threshold value of PET is used which indicates that identified critical conflicts can be resulting in collision. However, in previous studies, it is observed that several threshold values of PET ranging from 1 to 6.5 s have been historically used [13–15]. The selection of these threshold values to determine a critical conflict situation has been carried out in several ways, such as using the SSAM's default threshold values, the perception-reaction time, or even arbitrarily. American Association of State Highway and Transportation Officials (AASHTO) Greenbook [16] provides the driver perception-reaction time of 1 s for hazardous situations. Therefore, the present study aims to identify critical conflicts in crossing situation using PET threshold as 1 s. For this purpose, four unsignalized intersections located at National Capital Region (NCR) locations are selected, and critical conflicts are identified. The appropriateness of the proposed method is verified from a relationship between observed critical conflicts and five years' crash data for right-turn right angle and right-turn head-on collisions.

2 Literature Review

Several studies talked about the importance of the threshold values associated with proximal indicators. Chin and Quek [17] mentioned that a PET threshold value of 1.0 was considered as critical. Svensson [18] talked about the importance of threshold identification for the conflict measure to know about the safety problems that are to be investigated. Gettman et al. [19] stated that PET thresholds depend on the type of roads, vehicles as well as involved road users in a particular traffic conflict situation.

An FHWA report [12] first talked about Surrogate Safety Assessment Model (SSAM) to identify conflicts among all vehicular interactions. It proposed default threshold values for two surrogate measures, TTC and PET as 1.5 s and 3 s, respectively. Sonchitruska and Tarko [20] studied crossing conflicts leading to right angle collisions at signalized intersections. They modeled the behavior of PET in their proposed extreme value theory approach and found a promising relationship between conflicts and historical crash data at a PET threshold of 6.5 s. Archer and Young [13] observed that proximal measures of safety through observation or video analysis are useful to assess safety at specific locations by their threshold values so that appropriate countermeasures could be implemented. The maximum threshold value for the PET safety indicator was set to 1.5 s. Caliendo and Guida [14] selected SSAM's default thresholds for TTC and PET, 1.5 s and 5 s, respectively, as reported in FHWA study, 2008 [19]. Shekhar Babu and Vedagiri [20] observed crossing conflicts at an uncontrolled intersection using PET. A threshold value of 2.5 s was considered which is the perception-reaction time for stopping sight distance recommended by Indian Roads Congress. Peesapati et al. [21] determined PET threshold as 1 s from the correlation between conflicts and crashes. Zheng et al. [22] mentioned that the selection of a proper threshold is a big challenge on the use of traffic conflict counts. In brief, it is observed that several threshold values of PET ranging from 1 to 6.5 s have been historically used. The selection of these threshold values to determine a critical conflict situation has been carried out in several ways, such as using the SSAM's default threshold values, the perception-reaction time for a comfortable driving situation or even arbitrarily. Adaptation of any such value can influence all the components of a safety-based study, including evaluation tasks, determination of crash causation, and countermeasure analysis. Additionally, there is no basis to support the practice of a default, predetermined or arbitrary threshold without any proper justification. Contrarily, the present study carried out the safety analyses by a PET threshold of 1 s which is a recommended value by AASHTO for the unexpected driving situation or hazardous situation.

3 Methodology

PET is a quantitative measure to identify the conflict situation. This is calculated as a time difference between the passages of two road users with a common spatial point or area of potential collision [11]. For the present study, critical conflicts are identified based on a threshold value of PET, which can assess the probability of collision. A PET value of 1 s is taken as a threshold to determine the critical conflicts. AASHTO [15] proposed this value as the perception-reaction time of drivers for stopping sight distance at the unexpected situation. It was also mentioned in AASHTO that at any hazardous situation, 90% of drivers' perception-reaction time is 1 s as traffic conflict situation is also defined as an unexpected condition on the road confronted by drivers; in the present study, the PET threshold is considered as 1 s. Any conflict with PET value less than 1 s is identified.

3.1 Site Selection and Data Collection

To evaluate the effectiveness of the new indicator for the assessment of safety performance at unsignalized intersections, study sites have been selected from the National Capital Region (NCR), India. Primarily, several unsignalized intersections are identified considering different geometric configurations and traffic conditions such as (i) they are geometrically alike, (ii) there is high traffic demand at each site to capture large number of conflict data within a limited time period, (iii) motorists travel at their desired speed, (iv) there is no influence of on-street parking and bus stops within the functional area of intersection, and (v) there are very limited pedestrian and cyclists activities. Later, by associating these configurations, intersections are further shortlisted based on their crash history. Accordingly, 5 years (2011–2015) crash data for the selected sites are collected from concerned police stations. From the crash database, for each crash, a variety of information is obtained, e.g., date, time, precise location (distance and direction from the intersection), types of the crash (head-on, read end, right angle, right-turn head-on, sideswipe, etc.), and severity of collision (property damage only to fatality). As the present study focuses on crossing conflicts, only the sites with a higher number of right-turn related crashes (i.e., right-turn right angle and right-turn head-on crashes) are selected. By considering all of these factors, four unsignalized intersections located on four different intercity highways are finally selected for further analyses. Out of these four sites, two are three-legged intersections, whereas other two are four-legged ones. All the intersections are at-grade intersections and have major and minor roads. The details of the intersection locations along with crash data of selected crash types are given in Table 1.

As per objective of the study, the data collection is focused on the conflicts between two cross-traffics approaching from major as well as minor roads. It is already mentioned in the site selection section that selected intersections are located on intercity highways. No distinct peak or off-peak hours are observed for these kinds of highways. Therefore, data are collected using videography technique for a particular daytime (from 10 A.M. to 1 P.M.) on weekdays under good visibility conditions. For this purpose, a high-definition video camera is set up at an elevated point to obtain the clear view of the study location. Using this technique, two types of data are collected from the field, namely, traffic operational data and conflict data. A snapshot of video recording is shown in Fig. 1.

At all the study sites, three types of crossing maneuver are observed between (i) right turners from the major/minor roads and through-moving vehicles on the major roads, (ii) right-turning vehicles from the major road and right turners from the minor road, and (iii) two through-moving vehicles along the minor and major roads particularly for four-legged intersections. Among all traffic movements, crossing maneuvers between right turners from the major/minor roads and through-moving vehicles on the major roads are observed to be more in numbers and therefore included in this study. It is interesting to note that the crash record of similar types, i.e., right-

Table 1 Description of selected intersections

Name of sites	Case	Type of intersection	Traffic movement of major road on the side of the median	Lane width (m)	Number of total right-turn-related crashes (5 years)
Airport-NHAI-AIFF intersection at Dwarka	S-1	3-legged	2-lane 1-way	3.5	12
Faridabad-Gurgaon-Sikenderpur intersection at Gurgaon	S-2	3-legged	2-lane 1-way	3.5	15
Bahadurgarh intersection at Delhi	S-3	4-legged	2-lane 1-way	3.5	9
Dwarka-Kargil intersection	S-4	4-legged	2-lane 1-way	3.5	10



Fig. 1 A snapshot of study site 1 (S-1)

turn related crashes are found to be more at the selected study sites. Different traffic movements which are considered for the estimation of PET and subsequent analyses are shown in Fig. 2.

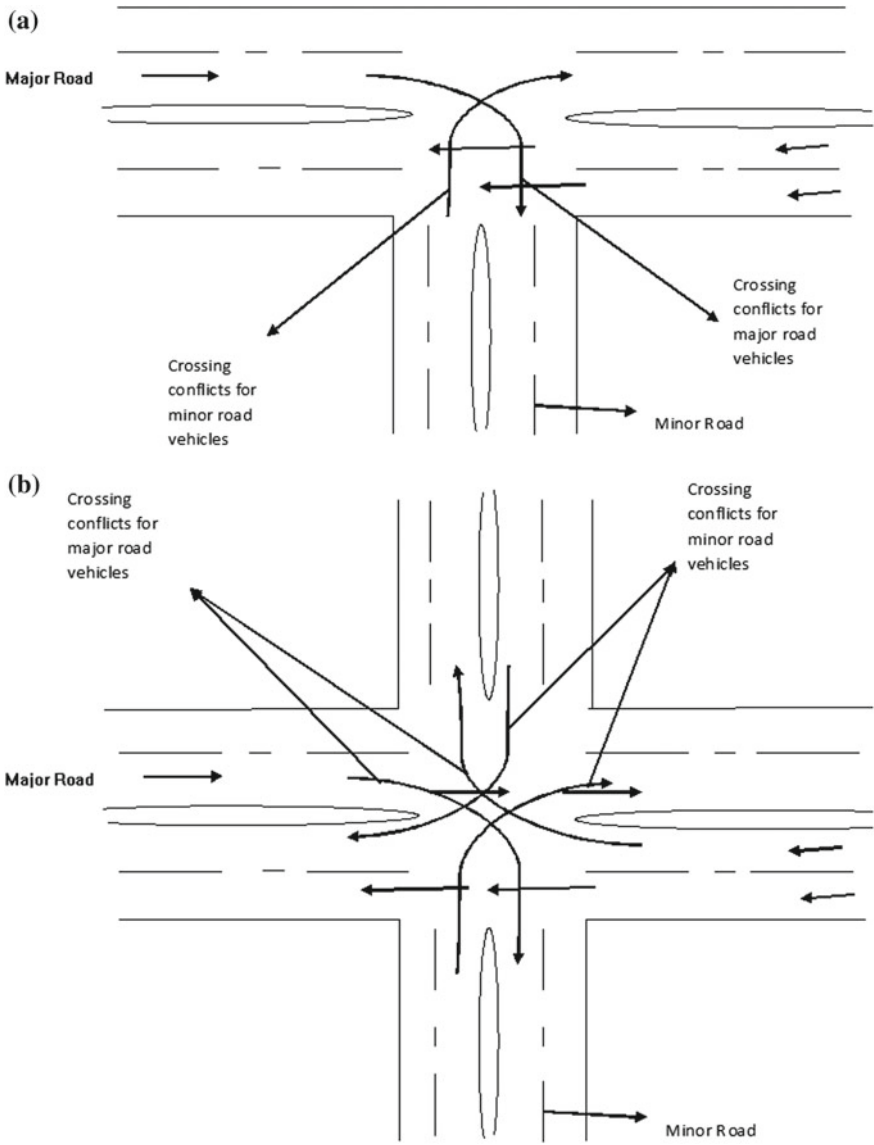


Fig. 2 Crossing conflicts between right turners and through-moving vehicles **a** for three-legged intersections (S-1, S-2), **b** for four-legged intersections (S-3, S-4)

3.2 Data Extraction

Once the field survey is over, several data are extracted from the recorded video as per the requirement of the study. Necessary information such as hourly traffic volume, PET, the number of vehicles involved in the conflict situations along with

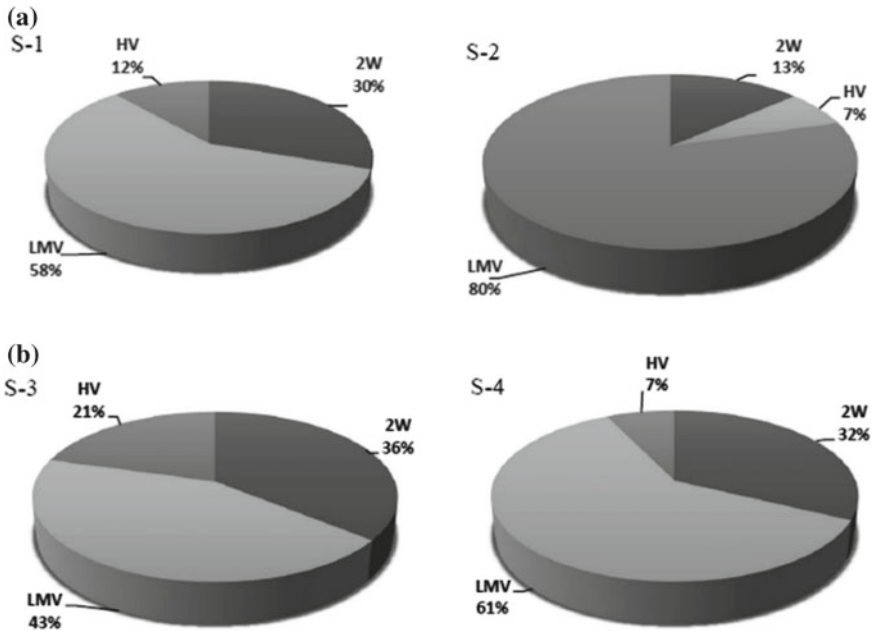


Fig. 3 Composition of vehicles **a** for three-legged intersections (S-1, S-2), **b** for four-legged intersections (S-3, S-4)

their categories, etc. are extracted. In order to have the conflict data, the conflict area of each intersection is divided into an equal number of square grids. The dimension of grids is selected as per the standard size of vehicles (i.e., 2.5 m × 2.5 m). This grid is prepared using Autodesk Maya 3D and then overlaid on the videos using a video editing software, Corel Video Studio Pro X6. Recorded videos are played on a large television screen at a frame rate of 25 frames per second and two time events t_1 and t_2 are noted down to calculate the PET values. t_1 is the time at which a right-turning vehicle exits a particular grid of conflict zone, and t_2 represents the time when the front of through vehicle just enters the respective grid. The difference between these two time events t_2 and t_1 gives the PET value. The hourly traffic volume of the study sites ranged from 1868 to 3778 veh/h. Three different vehicle categories are observed in the study sites, viz., Two Wheelers (2W), Light Motor Vehicle (LMV), and Heavy Vehicle (HV). LMV includes three wheeler, car, big car, and van, whereas HV represents bus, truck, and tractor-trailer. The compositions of total vehicles comprising of both right turners and conflicting through vehicles involved in the observed conflicts are shown in Fig. 3a and b, respectively.

Figure 3a, b shows that, among all the vehicle categories, LMV constitutes dominant share ranging from 43 to 80% of total traffic at all the sites. The percentage of 2W is found to be the second highest followed by HV.

4 Results and Discussion

From the video data, PET values between various right turning and through movements are estimated for all the study sites. Subsequently, the frequency distribution of calculated PET and empirical analysis of these PET values are then carried out.

4.1 Frequency Distribution of Observed PET

The frequency distributions of calculated PET values for the three-legged as well as four-legged intersections are presented in Fig. 4a and b, respectively.

It can be observed from Fig. 4 that at all the study sites the maximum numbers of PET values are distributed from 0.5 to 2 s.

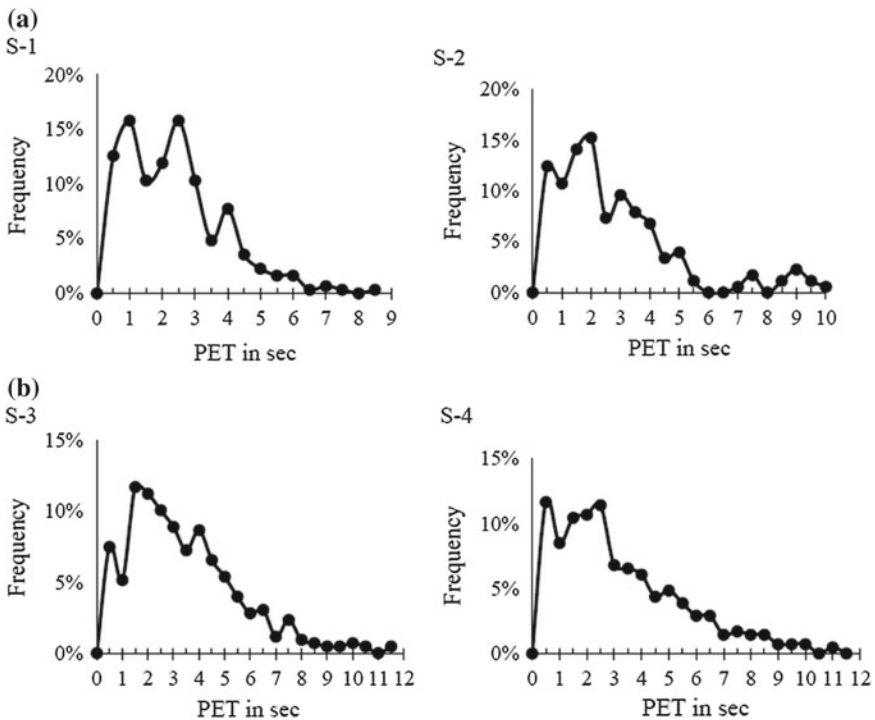


Fig. 4 Distribution of PET **a** for three-legged intersections (S-1, S-2), **b** for four-legged intersections (S-3, S-4)

4.2 Characteristics of PET

An empirical analysis has been carried out to determine the characteristics of PET between right turners and through vehicles. For this purpose, several parameters are estimated, namely, the number of total conflicts as well as critical conflicts observed at each site, the average, minimum, and maximum values of PET, presented in Table 2.

From the recorded data, a total of 1138 conflicts is observed. The minimum PET values are found to be ranging from 0.09 to 0.20 s and for maximum PET values, the range lies between 8.5 and 11 s. The average PET values for all the sites range from 2.08 to 2.87 s, which are very low in numbers. From this observation, it can be stated that non-prioritized vehicles adopted higher risk right-turning maneuvers in front of right-of-way vehicles instead of yielding for through vehicles along the major road. It is observed that four-legged intersections are having a lower value of average PET in comparison with three-legged ones. This observation is due to the greater number of small PET values observed at three-legged sites implying higher risk taken by the right turners. Table 2 shows that the percentage of critical conflicts based on 1 s PET threshold is also found to be more at study sites S-3 and S-4 (four-legged intersections) than S-1 and S-2, which are three-legged intersections. This is because S-3 and S-4 are four-legged intersections and due to the absence of priority rules, drivers of all four legs have equal opportunity to enter the intersection at the same time, either from the major as well as the minor road. This makes the situation critical, and a higher proportion of low PET values are observed than PET threshold. Hence, based on the PET threshold value, it can be inferred that the four-legged intersections are more hazardous locations than three-legged sites. It can also be said that the probability of resulting collisions is also more at these three-legged sites.

Table 2 Characteristics of PET

Study site	S-1	S-2	S-3	S-4
No. of total observed conflicts	263	283	317	301
Minimum PET (s)	0.20	0.16	0.09	0.16
Maximum PET (s)	11	9.0	10	8.5
Average PET (s)	2.74	2.87	2.08	2.42
No. of critical conflicts (i.e., PET values less than 1 s)	58 (22.05%)	61 (21.55%)	80 (25.23%)	76 (25.24%)

4.3 Distributions of Critical Conflicts for Each Through-Moving Vehicle Category with All Right-Turning Traffic

For in-depth information, the effect of each through-moving vehicle category on critical conflicts has been determined. Critical conflicts are further distributed with respect to the observed vehicle categories (i.e., 2W, LMV, and HV) traveling on the major roads. Subsequently, a number of critical conflicts as well as its percentage over the total number of observed conflicts are identified and illustrated for each site in Table 3.

From Table 3, for all the study sites, the percentage of critical conflicts is found to be more for through-moving 2W and LMV compared to HV. It indicates that right-turning vehicles accept smaller gap between the fast-moving through vehicles (2W and LMV), and the conflicts associated with these categories are found to be more critical. Same findings are also observed in the study of Pirdavani et al. [4]. It is thus because 2W is having the smallest size among all the vehicles traveling at the study sites, thus provoking the drivers of other vehicles to take a right turn by disobeying the priority rules. Resultantly, the temporal difference between the end of the encroachment of right turners and the entry of the through-moving 2W at a conflict zone becomes very less, which in turn increases the percentage of critical conflicts. Additionally, at four-legged intersections (S-3 and S-4), the percentage of 2W is observed to be higher than that of the remaining sites (as evident from Fig. 3), which also increases the proportion of critical conflicts at S-3 and S-4. Hence, from the conflict analysis based on PET threshold, it can be ascertained that more critical conflicts are observed when the through-moving vehicles are 2W.

Table 3 Distributions of critical conflicts for each through-moving vehicle category with all right turners

Case	No. of total conflicts	Through-moving vehicle categories					
		2W		LMV		HV	
		No. of critical conflicts	% of critical conflicts (%)	No. of critical conflicts	% of critical conflicts (%)	No. of critical conflicts	% of critical conflicts (%)
S-1	263	41	15.58	32	12.61	5	1.90
S-2	283	45	15.90	36	12.72	2	0.70
S-3	317	52	16.4	47	14.82	9	2.83
S-4	301	56	18.60	51	16.94	6	1.99

4.4 Relationship Between Right-Turn-Related Crashes and Critical Crossing Conflicts

Historically, the validity of the application of proximal indicator is being investigated by checking the correlation between conflicts and actual crash records [23]. The present study primarily used right-turn-related crashes for the final selection of study sites. It is also employed to evaluate the appropriateness of the study attempt. Consequently, a crash–conflict relationship is developed for the selected intersections which represent how observed critical conflicts between right-turning traffic and through-moving vehicles are correlated with the right-turn right angle and right-turn head-on collisions. A nonparametric test is performed to determine whether a statistically significant relationship exists or not between the groups, crash, and critical conflict. As the sample sizes of both the groups are small and they are not normally distributed, therefore, a two-sample Mann–Whitney U test is performed for statistical hypothesis testing. The equations to calculate the test statistics (U values) are, this study used, presented in Eqs. (1) and (2)

$$U_{1(crash)} = n_1n_2 + \frac{n_1(n_1 + 1)}{2} - W_1 \tag{1}$$

$$U_{2(critical\ conflict)} = n_1n_2 + \frac{n_2(n_2 + 1)}{2} - W_2 \tag{2}$$

where n_1, n_2 = sample size, i.e., the number of study locations from where the crash and critical conflict data are collected, W_1, W_2 = the observed sum of ranks for samples of the crashes and critical conflicts. W_1 and W_2 are calculated by combining all the samples from both groups (crash and critical conflict) to one group and then providing ranks to the samples with a numerical number of 1 for the smallest observation. The results of the statistical analysis carried out between the selected crash types and critical conflicts are given in Table 4.

Table 4 Statistical analysis between right-turn-related crash and critical crossing conflict

Parameters	Crash	Critical Conflict
Observation numbers	46	382
Sample size (No. of selected locations)	$n_1 = 4$	$n_2 = 4$
Ranks of samples for four locations	(3, 4, 1, 2)	(7, 8, 5, 6)
Summation of ranks (W)	$W_1 = 10$	$W_2 = 26$
Mann–Whitney U value	$U_1 = 16$	$U_2 = 0$
U_0	0	
p -value	0.0143 (two-tailed)	
R^2	0.68	

Table 4 shows that at $n_1 = 4$ and $n_2 = 4$, the minimum value of U_0 as the test statistics is found for critical conflict, i.e., $U_0 = U_2 = 0$. For a two-tailed test at the 0.05 significance level, p -value for Mann–Whitney U statistic for the small sample is determined, and it is found to be 0.0143 which is less alpha value. Therefore, it can be implied that the relationship between the crash and critical conflicts is statistically significant as given in Table 4. From the test results and goodness of fit, a promising relationship is found between actual crash data and observed critical conflicts. Literature also showed a statistically significant relationship between traffic conflict and crashes by types [14, 21]. This relationship indicates that PET threshold value of 1 s is fit to identify the critical conflict at crossing situation of unsignalized intersections.

5 Conclusions

Traditional safety analysis based on historical crash data has several limitations regarding adequacy and timeliness. Additionally, in developing countries like India, crash data are highly underreported. Only crashes which are severe in nature, i.e., major injuries and fatal crashes, are reported. Apart from these issues, crashes are not reported precisely (types of crashes, location, and other necessary information). Therefore, safety evaluation based on police-reported historical crash data only could lead to erroneous outcomes. By keeping these in mind, the present study utilizes traffic conflict technique to evaluate the safety performance at unsignalized intersections using proximal safety indicator, PET. Employing PET as an indicator provides a useful observation about the safety state of selected study sites. A threshold value of PET is widely used in many studies to distinguish the conflict as serious and non-serious ones. However, historically, PET thresholds have been selected arbitrarily or based on predetermined threshold values. At Indian-unsignalized intersections, priorities are established by the situations drivers perceive, and thus vehicles from all the directions attempt crossing and turning at the same time. Therefore, without proper justification, considering any value as a PET threshold for safety evaluation can be misleading. In this study, the threshold is taken as 1 s, i.e., the reaction time of a driver for unexpected traffic condition based on the assumption that below this time driver could not perceive the situation properly, which may be unsafe and lead to a collision. This value of perception-reaction time for hazardous situations is recommended by AASHTO [15].

The average PET values at these sites are found to be ranging between 2.08 and 2.87 s indicating higher risk-taking crossing behavior of the non-prioritized traffic. The percentage of critical conflicts is observed more at four-legged intersections compared to three-legged ones. This is because, at four-legged intersections, due to the absence of priority rules, drivers of all four legs have equal opportunity to enter the intersection at the same time, either from the major as well as the minor road. The percentage of critical conflicts is found to be more when conflicts occur between all right turners and through-moving vehicle categories of 2W and LMV.

It is thus because 2W is having the smallest size of all the vehicles traveling at the study sites, thus provoking the drivers of other vehicles to take a right turn by disobeying the priority rules. As a result, the temporal difference between the end of the encroachment of right turners and the entry of the through-moving 2W at a conflict zone becomes very less, which in turn increases the percentage of critical conflicts. Moreover, it is observed that at four-legged intersections the percentage of 2W is observed to be higher than that of the remaining sites, which also increases the proportion of critical conflicts. For validation of the proposed method, a statistical analysis is conducted between the observed right-turn-related crashes and critical crossing conflicts identified using PET threshold of 1 s and a statistically significant relationship is observed between them.

Overall, the proposed method is proved to be effective for safety assessment at unsignalized intersections particularly for right-turn related crashes which are the most severe crashes among all crash types [24–26]. This new method is capable of assisting traffic engineers and safety experts proactively with the selection of appropriate traffic calming and management measures to improve the safety at unsignalized intersections. The insights are thus helpful for the safety improvements at unsignalized intersections in an indiscipline traffic environment. The present study can be further extended by collecting conflict data for the whole day. Safety evaluation can also be carried out by considering other types of crashes (e.g., rear end) and using different proximal indicators.

Acknowledgements The video data used in this paper is collected as a part of a research project on “Development of Indian Highway Capacity Manual (INDO-HCM),” sponsored by CSIR-Central Road Research Institute (CRR), New Delhi, India. The financial assistance provided by the sponsoring agency for traffic studies is gratefully acknowledged.

References

1. MoRTH (2018) Road accidents in India., Ministry of Road Transport and Highways. Government of India, New Delhi
2. Ashalatha R, Chandra S (2011) Service delay analysis at TWSC intersections through simulation. *KSCE J Civ Eng* 15(2):413–425
3. Patil G, Pawar D (2014) Temporal and spatial gap acceptance for minor road at uncontrolled intersections in India. *Transp Res Rec* 2461:129–136
4. Pirdavani A, Brijs T, Bellemans T, Wets G (2010) Evaluation of traffic safety at un-signalized intersections using microsimulation: a utilization of proximal safety indicators. *Adv Transp Stud* 22(22):43–50
5. Glauz WD, Migletz DJ (1980) Application of traffic conflict analysis at intersections. Transportation Research Board, Washington D.C., USA., No. HS-028 882
6. Cooper PJ (1984) Experience with traffic conflicts in Canada with emphasis on “post encroachment time” techniques. International calibration study of traffic conflict techniques. Springer, Heidelberg, pp 75–96
7. Hyden C (1987) The development of a method for traffic safety evaluation: the Swedish traffic conflicts technique. *Bull Lund Inst Technol* 70
8. Parker Jr MR, Zegeer CV (1989) Traffic conflict techniques for safety and operations: observers manual, no FHWA-IP-88-027

9. Chin HC, Quek ST, Cheu RL (1992) Quantitative examination of traffic conflicts. *Transp Res Rec* 1376:67–74
10. Perkins SR, Harris JI (1967) Criteria for traffic conflict characteristics. Warren, MI, General Motors Corporation, Report GMR 632
11. Archer J (2005) Indicators for traffic safety assessment and prediction and their application in micro- simulation modelling: a study of urban and suburban intersections. Doctoral Dissertation, Department of Infrastructure, Division for Transport and Logistic, Centre for Transport Research, Royal Institute of Technology, Stockholm, Sweden
12. Gettman D, Head L (2003) Surrogate safety measures from traffic simulation models. *Transp Res Rec* 1840:104–115
13. Archer J, Young W (2010) The measurement and modelling of proximal safety measures. *Proc Inst Civ Eng Transp* 163(4):191–201
14. Caliendo C, Guida M (2012) Microsimulation approach for predicting crashes at unsignalized intersections using traffic conflicts. *ASCE J Transp Eng* 138(12):1453–1467
15. AASHTO (2001) A policy on geometric design of highways and streets, 6th edn. American Association of State Highways and Transportation Officials, Washington, DC
16. Hyden C (1996) Traffic safety work with video-processing. Technical report, Transportation Department, University Kaiserslautern
17. Chin HC, Quek ST (1997) Measurement of traffic conflicts. *Saf Sci* 26(3):169–185
18. Svensson A (1998) A method for analysing the traffic process in a safety perspective. Doctoral Dissertation, Department of Traffic Planning and Engineering, Lund University, Lund, Sweden
19. Gettman D, Pu L, Sayed T, Shelby SG (2008) Surrogate safety assessment model and validation: FHWA—HRT-08-051
20. Shekhar Babu S, Vedagiri P (2012) Safety evaluation of an uncontrolled intersection using surrogate safety measures. *Proc Urban Mob India (UMI)*, Institute of Urban Transport (India)
21. Peesapati L, Hunter M, Rodgers M (2013) Evaluation of post encroachment time as surrogate for opposing left-turn crashes. *Transp Res Rec* 2386:42–51
22. Zheng L, Ismail K, Meng X (2014) Traffic conflict techniques for road safety analysis: open questions and some insights. *Can J Civ Eng* 41(7):633–641
23. Mahmud SS, Ferreira L, Hoque M S, Tavassoli A (2017) Application of proximal surrogate indicators for safety evaluation: A review of recent developments and research needs. *IATSS Res* 1–11
24. Wolshon, B (2004) Toolbox on intersection safety and design. Chapter 1—Geometric design. Institute of Transportation Engineers, U.S Dept. of Transportation
25. Abdel-Aty M, Keller J (2005) Exploring the overall and specific crash severity levels at signalized intersections. *Acc Anal Prev* 37(3):417–425
26. McCarthy J, Bared, Zhang W, Doctor M (2013) Public roads—design at the crossroads, no: FHWA-HRT-13-005, US Dept. of Transportation, Federal Highway Administration, Washington, DC, vol 77, no 1

Effect of Stratification on Underground Opening: A Numerical Approach



Mudassir Ali Khan , Mohd. Rehan Sadique  and Mohammad Zaid 

Abstract Due to the increase in urbanization and requirement of rapid transportation and storage purpose, the demand for various underground structures has been exponentially increased. Underground structures like tunnel, subways, and storage tank have been constructed to fulfill the requirement of the urban society. In the present paper, two-dimensional finite element analysis has been performed using finite element program, ABAQUS. The settlement and the effective stresses in the tunnel liner due to the stratification of soil have been analyzed. The geostatic stress of soil has been calculated to fix the initial condition of site which is used for simulating the other phase of construction. It has been found that stratification has not much affected the stresses on the liner. Maximum value of stresses has been observed at the Springer level and crown level. However, the vertical displacement has been reduced by 27% when the silty sand (SM) layer moves closer to the crown of opening. Lateral displacement has not much affected by the stratification. However, the maximum value of lateral displacement was reported near mid-axis of opening in each case.

Keywords Transportation · Urbanization · Underground · Structure · Finite element method · Springer level

1 Introduction

For the better facilities and employment purpose, most of the people have been migrating to the metro cities which lead to increase in urbanization. Various surveys have been done to predict the population of the metro cities for providing the required infrastructure and facilities. A report of UN-Habitat (2008) has shown that 50% of

M. Ali Khan (✉) · Mohd. R. Sadique · M. Zaid
Department of Civil Engineering, AMU Aligarh, Aligarh 202002, India
e-mail: mudassir290@gmail.com

Mohd. R. Sadique
e-mail: rehan.sadique@gmail.com

© Springer Nature Singapore Pte Ltd. 2019
S. Pulugurtha et al. (eds.), *Advances in Transportation Engineering*,
Lecture Notes in Civil Engineering 34,
https://doi.org/10.1007/978-981-13-7162-2_11

the world's population now lives in cities and the rate of urbanization is such that this proportion will reach 70% up to 2050 [10]. Despite this huge pressure, the protection of natural spaces and provision of good facilities remains a major challenge in the effort to limit horizontal urban drift. The influence of these two constraints, i.e., huge pressure and property economics, leads mechanically to the vertical development of urban area [3].

Owing to advancement of the technology, various methods have been developed for the excavation of underground opening. Mechanized tunneling like (NATM) has proved well-established tunnel construction technique to excavate tunnels in complex ground conditions as well as in vulnerable built-up areas. NATM has characterized by a repeated sequence of these individual steps: The pressure of the TBM through hydraulic jacks that has concurrent with the excavation of the soil at the face by the cutter head and the installation of a tunnel lining with synchronous tail void grouting.

2 Previous Studies

Several parameters have been found responsible for the deformation and the stresses in the lining of the tunnel such as depth of the tunnel, types of soil, liner material, diameter of tunnel, surcharge loading (e.g., building and seismic loading, stratification of soil, etc.). Very few researches have been found which deal with the layering effect on liner. Nunes and Meguid [11] had evaluated the effects of overlying sandy layers above a tunnel excavated in soft ground. They had concluded that the bending stresses reduce up to 70% when the stiff layer (sand) was closer to the tunnel as compared to the case of homogeneous clay. The volume loss (the ratio of the difference between excavated soil volume and tunnel volume over excavated soil volume) in stratified soil had influence on the deformation and stresses of underground opening as reported by Mazek and Almannaei [10]. They observed that 1.5–4.5% of volume loss influences the stresses and displacement in underground opening. Similarly, Katebi et al. [7] had performed a finite element analysis and observed the existence of surface buildings in layered soil under 2D plane-strained condition. It was observed that bending moment increases 20% when depth of tunnel varied up to 2 times the tunnel diameter as compared to the greenfield condition. Zhang et al. [14] had also investigated the influence of the layered soils in terms of their relative stiffness and thickness of layer on the lining behavior. It had been observed that, for two-layered soil conditions, the increase of the relative stiffness of the overlying sandy layer leads approximately to 45% reduction of the bending moment and 50% reduction of the convergence and for a three-layered soil condition, the increase of the relative thickness of the sandwiched clay layer leads to an increase of approximately 90% of both the moment and the convergence. The soil structure interaction played the important role to improve the computed surface settlement trough for Shanghai soft clay in layered soil. Soil structure interaction has modified the result for estimating the horizontal and vertical displacement. The Horizontal displacement had increased by 21% in layered soil when considering the soil structure interaction as compared

to greenfield condition studied by the Bian et al. [4]. Effect of seismic wave on liner in stratified soil had been studied by several researchers (e.g., [1, 2, 5, 9]).

2.1 Geometric Modeling

The tunnel has been considered as a circular shape with diameter of 8 m and to be constructed at a depth of 18.3 m below the ground surface. Stresses and displacement have been measured on the tunnel invert, springing zone, and crown level by numerical approach. Length and height of soil domain have been chosen in such a way that it simulates the actual behavior of the tunnel in the field condition. Boundaries are adopted at 7.5 d from center of the tunnel from various sensitivity analyses as shown in Fig. 1, where d is the diameter of the tunnel equal to 8 m. At the lateral boundaries, displacements perpendicular to boundaries have restrained, whereas fix support has been applied to the bottom boundary.

2.2 Constitutive Material Modeling

Tunneling in the soft soil has proved difficult task due to volume loss (e.g., shield loss, tail void loss, lining losses, uncertainty in soil behavior, etc.). To understand the response of liner in stratified soil, two types of soil have been chosen in this study as shown in Fig. 3. Soil domain has been modeled by using Mohr–Coulomb’s constitutive model with nonassociative flow rule, and liner has discretized by elasticity model in finite element program. In this study, shield tunneling has simulated by considering the suitable stiffness of liner material as shown in Table 2. Physical and

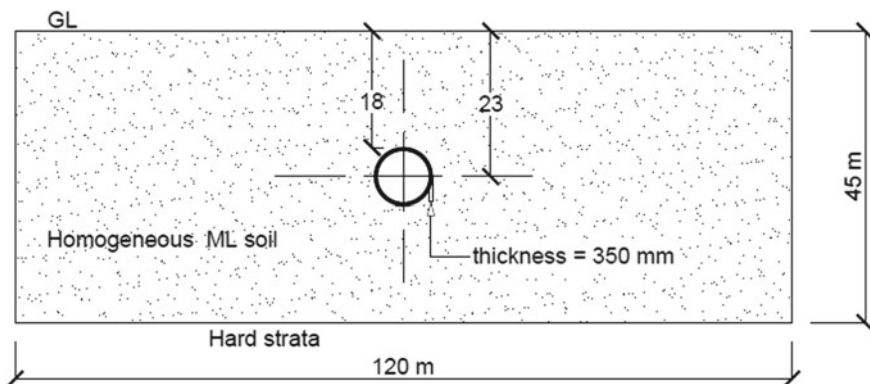


Fig. 1 Geometric features of the present study

mechanical properties of soil and lining material have been taken from the research paper of Katebi et al. [7].

3 Numerical Modeling

Although empirical–experimental method has been developed to analyze the forces and deformation in tunnel liner, they have limited application due to various assumptions to calculate the required output in a particular problem. The advancement of technology has developed various numerical techniques of analysis in all fields of engineering on the basis of DEM, FEM, LEM, FDM, etc. to expedite the computational process. Several different approaches have been developed to represent the soil structure within a constitutive modeling framework, but Mohr–Coulomb’s plasticity is one of the most popular methods widely used for modeling the soil domain in the finite element program.

In this study, it has been assumed that the behavior of the tunnel liner is linear elastic and that of the ground is governed by an elastic–perfectly plastic constitutive relation. In this study, numerical simulations have been performed by means of ABAQUS a finite difference element solver. Tunnels have often 3D model (e.g., [8, 12]) but it need extra computational resources, hence 2D modeling has been preferred as many researchers (e.g., [6, 13]) have simulated the same. Soil domain and liner material have been discretized by a four-node bilinear plain strain quadrilateral, reduced integration, and hourglass control (CPE4R). Mesh type and size have been selected by several sensitivity analyses which not influenced the result. Mesh consists of 21,161 quad-type elements uniformly spaced in soil domain and 92 elements in liner material. For avoiding the distortion of element, local seed has also been adopted as shown in Fig. 2. Numerical analysis has been simulating in the following three steps.

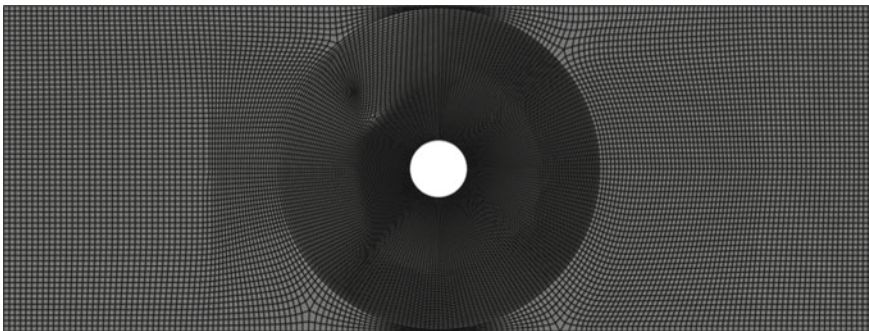


Fig. 2 The mesh density of the proposed study

3.1 Geostatic Step

Initial stresses in soil before excavation have been calculated in this step. In Abaqus continuum geostatic step has an advantage to show the zero displacement. The elements that are within the excavation of the tunnel are active, and the elements of the liner are not active (i.e., the tunnel has not been excavated yet).

3.2 Excavation

Excavation has been simulated by the stiffness reduction method in which soil element of excavation area was deactivated and the elements of the liner were activated. Compatibility of deformations between the liner and the ground is ensured by requiring the nodes of the elements of the ground in contact using general surface-to-surface contact.

3.3 Effect of Stratification

Effect of stratification has been simulated by considering the two-layer soil whose properties have been mentioned in Table 1. For comparison purpose, single layer of low plastic silt (ML) has treated as ideal condition. Depth of stiff layer of sand (SM) has been varied from top to bottom as shown in Fig. 3.

In the present study, it has been simulated that minimum stresses and deformation occur at which condition to minimize the effect surcharge on the secondary support. For this purpose, two-layer system condition has been adopted. To observe the effect of SM layer on liner, a different depth has been chosen which has been shown in Table 2.

Table 1 Properties of the soil and liner material opted in the present study [7]

Type of material	Dry density (kg/m ³)	Wet density (kg/m ³)	Permeability (m/s)	Elastic modulus Pa	Poisson ratio (ν)	Cohesion (pa)	Internal friction	Dilation angle
Silty sand (SM)	1625	2000	1E-08	40E06	0.3	7000	34	3
Low plastic silt (ML)	1680	2035	5E-09	25E06	0.35	17,000	25	0
R.C.C. liner	2500	–	–	25.2E09	0.2	–	–	–

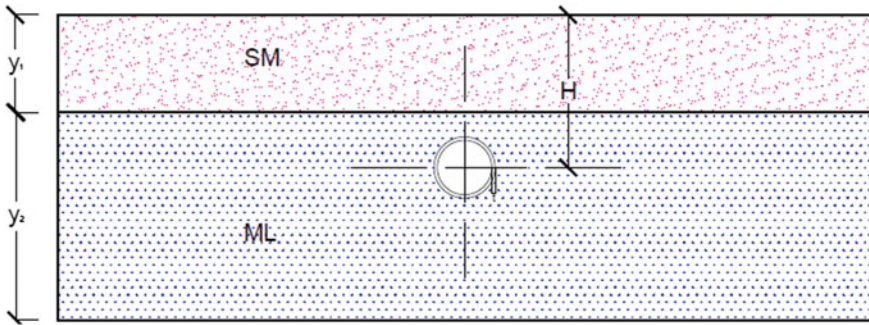


Fig. 3 Variation of silty sand in the proposed study

Table 2 Variation of silty sand (SM) along depth

S. no	Depth of SM from top, y_1 (m)	Depth of ML, y_2 (m)	Remark
1	0	45	Fully plastic silt
2	10.7	34.3	Both SM and ML
3	18.33	26.67	SM up to crown
4	22.5	22.5	SM up to spring
5	28.9	16.1	SM below invert
6	45	0	Fully SM

4 Results and Discussion

Numerical analysis has been carried out to observe the effect of stratification of soil around the opening using ABAQUS/Standard program. The observation has been made on underground structure excavated in low plastic soil in terms of displacement and stresses; further, its response has compared with underground opening in two-layered soil. More than 30 plain strain models have been simulated to study the response of stratification on the liner at different depths mentioned in Table 2.

4.1 Geostatic Step

In this step, it was observed that displacement in the vertical and horizontal direction is almost zero because tunnel had not excavated as shown in Fig. 4a. Radial stresses along the circumferential path have also been calculated to understand the initial stress in the liner. It has been found that maximum geostatic stresses occur at the crown. It provides the initial value of stresses in liner and soil needed for calculating the increase or decrease in stresses at various phases of construction.

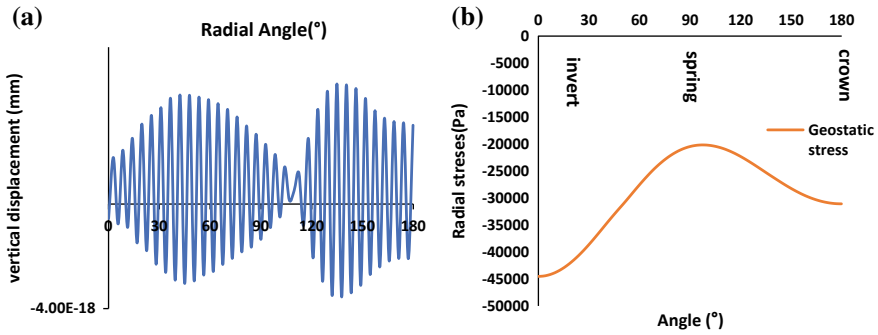


Fig. 4 Variation of vertical displacement (a) and radial stress (b) with radial angle in geostatic step

4.2 Effect of Stratification

Stratification has been simulated by choosing two types of soil ML followed by SM as shown in Fig. 3. Homogeneous ML layer has been considered as ideal condition for all the simulations. It has been observed that horizontal displacement does not get influenced by the stratification. Affected area of soil in horizontal direction has been shown in Fig. 5 due to tunneling in the silty soil. Radial stresses and tangential stresses have been simulated at different depths of the SM from top surface shown in Table 2. It has been observed that stiff layer (SM) closer to liner reduces the liner stresses effectively. The response of stratification on the liner stresses has been shown in Figs. 6, 7, and 8.

It has been observed that the horizontal displacement has maximum value on the springer zone or center of tunnel axis which has been shown in Fig. 5. It provides the base to fix the lateral boundaries in simulation. Radial and tangential stresses have also been plotted for various depths of silty soil. It has been found that the maximum value of radial stresses occurs at springer level and has not much affected

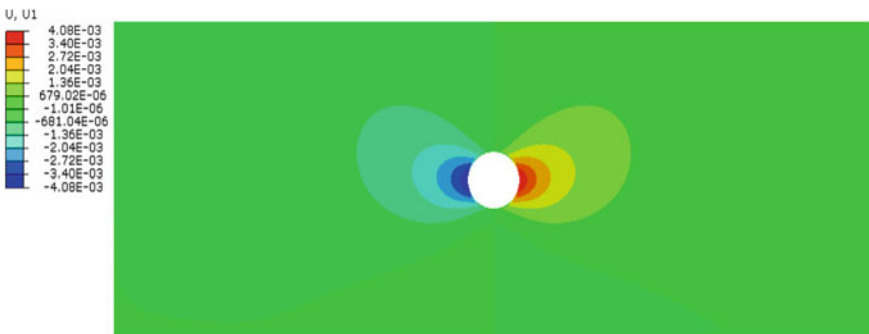


Fig. 5 Contour of the lateral displacement of low plastic silty soil (ML)



Fig. 6 Contour of tangential stresses in low plastic soil (ML)

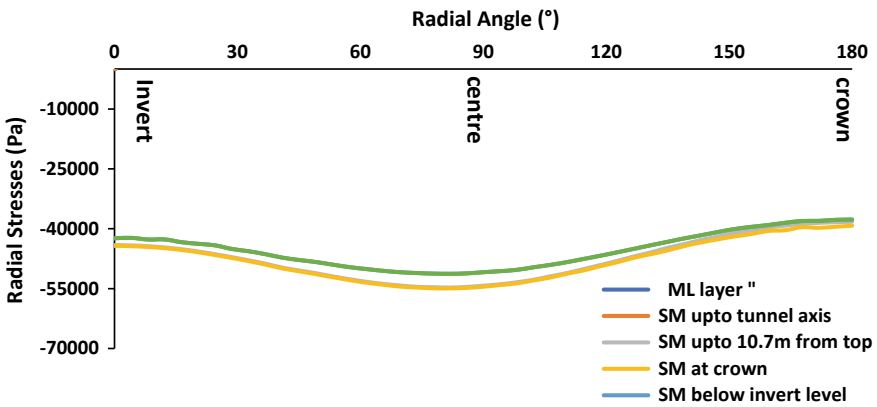


Fig. 7 Effect of stratification on radial stresses in tunnel liner

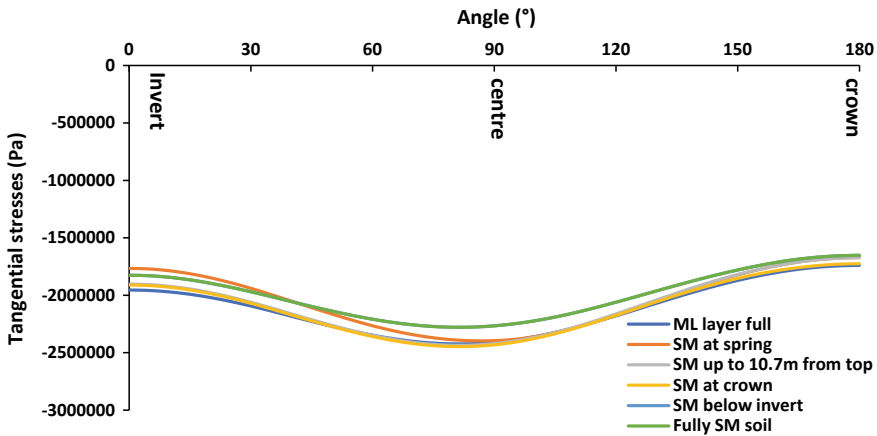


Fig. 8 Layering effect on tangential stresses at the liner

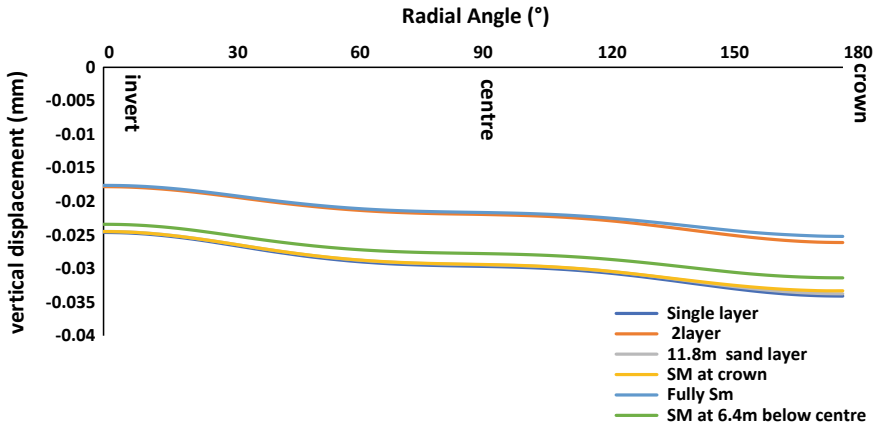


Fig. 9 Effect of stratification on the vertical displacement

by the stratification of soil. Tangential stresses have found maximum value at springer level and decrease about 10–12% when stiff layer moves toward the crown. Vertical displacement has been found to reduce 27% when the silty soil (SM) passes from springer line as shown in Fig. 9. Vertical settlement of liner is the important parameter which could not neglect while adopting the rational and economic design of the liner. Figure 9 also depicts the Maximum value of vertical settlement occurs at crown in homogeneous silty clay soil which reduces to 25 mm when silty sand was present up to the center of tunnel axis.

5 Conclusion

Numerical analysis has been carried out using finite element package Abaqus. Material behavior of soil has been incorporated through well-known Mohr–Columb’s constitutive model. Effect of stratification has been simulated, and it has been found that consideration of soil stratification will lead to economic and rational design of the liner in soft soil.

- Soil has been modeled using Mohr–Columb’s plasticity with nonassociative flow rule in 2D plain strain numerical model.
- It has been observed that vertical displacement decreased by 27% as compared to low plastic silty (ML) soil.
- Radial stresses in the liner have not been affected by the stratification as stresses reduce only 5–6% when SM layer moves toward the liner.
- Tangential stresses have been found maximum at springer level and decrease by the 10–12% when SM layer is closer to the crown.

- Horizontal displacement has not much affected by the stratification but has maximum value at spring level which helps to decide the lateral boundaries of soil domain.
- From the above study, it has been recommended that excavation should be done in above type of soil condition with little care to reduce the volume loss.

Acknowledgements Authors are highly thankful to University Grant Commission (India) for their support in carrying out this study through the UGC-Start Up Grant.

References

1. Asheghabadi AS, Matinmanesh H (2011) Finite element seismic analysis of cylindrical tunnel in sandy soils with consideration of soil-tunnel interaction. *Procedia Eng Elsevier* 14:3162–3169. <https://doi.org/10.1016/j.proeng.2011.07.399>
2. Azadi M (2011) The seismic behaviour of urban tunnels in soft saturated soils. *Procedia Eng Elsevier* 14:3069–3075. <https://doi.org/10.1016/j.proeng.2011.07.386>
3. Attard G, Rossier Y, Winiarski T, Eisenlohr L (2017) Urban underground development confronted by the challenges of groundwater resources: guidelines dedicated to the construction of underground structures in urban aquifers. *Land Use Policy* 64:461–469
4. Bian X, Hong ZS, Ding JW (2016) Evaluating the effect of soil structure on the ground response during shield tunnelling in Shanghai soft clay. *Tunn Undergr Space Technol* 58:120–132. <https://doi.org/10.1016/j.tust.2016.05.003>
5. Gomes RC, Gouveia F, Torcato D, Santos J (2015) Seismic response of shallow circular tunnels in two-layered ground. *Oil Dyn Earthq Eng* 5:37–43. <https://doi.org/10.1016/j.soildyn.2015.03.012>
6. Hashash YMA, Park D, Yao JIC (2005) Ovaling deformations of circular tunnel under seismic loading, an update on seismic design and analysis of underground structures. *Tunn Undergr Space Technol* 20:435–441
7. Katebi H, Rezaei AH, Hajialilue BM (2013) The influence of surface buildings and ground stratification on lining loads applying the finite element method. *Electron J Geotech Eng* 18(1):1845–1861
8. Kramer GJ, Sederat H, Kozak A, Liu A, Chai J (2007) Seismic response of precast tunnel lining. In: *Proceedings of the rapid excavation and tunnelling conference*, pp 1225–1242
9. Motaal AA, Mohamed F, El-Nahhas (2013) Mutual seismic interaction between tunnels and the surrounding granular soil. *HBRC J* 10:265–278. <https://doi.org/10.1016/j.hbrj.2013.12.006>
10. Mazek SA, Almannaei HA (2013) Finite element model of Cairo metro tunnel-Line 3 performance. *Shams Eng J* 4:709–716. <https://doi.org/10.1016/j.asej.2013.04.002>
11. Nunes MA, Meguid MA (2009) A study on the effects of overlying soil strata on the stresses developing in a tunnel lining. *Tunn Undergr Space Technol* 24:716–722. <https://doi.org/10.1016/j.tust.2009.04.002>
12. Nagggar HE, Hinchberger SD (2012) Approximate evaluation of stresses in degraded tunnel linings. *Soil Dynamic's Earthq Eng* 43:45–57
13. Pakbaz MC, Yareevand A (2005) 2-D analysis of circular tunnel against earthquake loading. *Tunn Undergr Space Technol* 20:411–417
14. Zhang D, Huang H, Hub Q, Jiang F (2015) Influence of multi-layered soil formation on shield tunnel lining. *Tunn Undergr Space Technol* 47:123–135. <https://doi.org/10.1016/j.tust.2014.12.011>